

THE ROLE OF MITOFUSIN PROTEINS IN MITOCHONDRIAL FUSION
AND DISEASE

Thesis by
Scott A. Detmer

In Partial Fulfillment of the Requirements
for the Degree of
Doctor of Philosophy

California institute of Technology

Pasadena, California

2007

(Defended March 1, 2007)

© 2007

Scott Detmer

All Rights Reserved

Acknowledgements

First, I thank my advisor, David Chan. David's ideas are usually very creative or logical, often both, and I have enjoyed being part of his lab. I will try to approach experimental design and analysis with the level of acuity and rigor that David has brought to our discussions. Also, to my committee members: Pamela Bjorkman, Ray Deshaies, and Scott Fraser—thank you for pragmatism in goal setting, practical experimental advice, and encouragement.

Erik Griffin, Hsiuchen Chen, Takumi Koshiba, Yan Zhang, Priscilla Tee, Zhiyin Song, Tara Suntoké, Toby Rosen, Lloyd Lytle, Tadato Ban, and Sungmin Park-Lee, you have all made the Chan lab a great place to work. I am also grateful to Christine Vande Velde from Don Cleveland's lab at UCSD for her skills and enthusiasm relating to mitochondria and motor neurons.

I have been lucky to have really incredible classmates and friends at Caltech—Stijn Cassenaer, Dan Gold, Davin Malasarn, Erik Griffin, Dave Buchbinder—it has been grand. Also, to the many people in biology who have always been very warm and helpful, thank you—especially to Liz Ayala, Diane Solis, Gwen Williams, Marta Murphy, and Carole Worra.

My family has been supportive throughout my schooling, even after they stopped asking when I would be done. Mom and Dad, Dave and Debbie, Dan and Jesse, thank you for the encouragement and diversions over the last thirty years. And more recently, Kris and Steve, Eleanor and Stan, Roselle and Joe, thank you for the same.

Finally, to Robin. You have absolutely been the highlight of grad school and marrying you has been the best thing to come of it. Your support, patience, love, advice, and occasional needling—especially at the end—have been all that I needed. Many adventures to come, not the least of which begins in May...

Abstract

We have investigated the role of mitofusin proteins in mitochondrial fusion and Charcot-Marie-Tooth disease Type 2A (CMT2A). Mitofusins (Mfn1 and Mfn2) are required for mammalian mitochondrial fusion. In structure-function analysis, we have identified loss-of-function mutations in mitofusin GTPase and heptad-repeat domains that disrupt homotypic and heterotypic domain interactions. Mutations in Mfn2 cause CMT2A, a progressive peripheral neuropathy. We have functionally characterized Mfn2 disease mutations and find that wild-type Mfn1, but not Mfn2, can efficiently complement nonfunctional CMT2A alleles to restore mitochondrial fusion. This finding demonstrates the importance of Mfn1-Mfn2 heterooligomers and suggests that Mfn1 expression is important in determining the cell-type specificity of CMT2A. To study the consequences of an Mfn2 CMT2A allele *in vivo*, we generated transgenic mice that express Mfn2 T105M in motor neurons. These animals demonstrate gait impairments due to distal muscle loss, axonopathy and altered mitochondrial morphology and distribution in motor neurons. In a second approach, we have generated CMT2A knock-in mice by replacing the endogenous genomic Mfn2 with Mfn2 alleles L76P or R94Q. Preliminary characterizations suggest that heterozygous animals have no disease symptoms, but homozygous Mfn2 R94Q animals are severely affected. Together, these mouse models provide means to assess the pathology of Mfn2 CMT2A alleles and the role of mitochondrial dynamics *in vivo*.

Table of Contents

Acknowledgements	iii
Abstract	v
Table of Contents	vi
List of Figures and Tables	x
Chapter 1: New Functions for Mitochondrial Dynamics	1
Introduction	2
Mitochondria as dynamic organelles	3
Control of mitochondrial shape by fusion and fission	3
Control of mitochondrial distribution by active transport	4
Dynamic internal structure	5
Mechanisms of mitochondrial dynamics	6
Mediators of fusion	6
Mediators of fission	9
Other regulators of morphology	10
Proteins required for mitochondrial transport	10
Proteins mediating inner membrane morphology	11
Biological functions of mitochondrial dynamics	12
Protection of respiratory function	13
Essential developmental functions	13
Mitochondrial distribution and recruitment in neurons	14

Involvement in human disease	16
OPA1 and ADOA	16
Mfn2 and CMT2A	17
GDAP1 and CMT4A	19
Regulation of apoptosis	20
Lymphocyte chemotaxis	22
Perspectives	22
References	24
Figures	39
Thesis overview	45
Chapter 2: Multiple Independent Modes of Mitofusin Domain	
Interactions are Required for Mitochondrial Fusion	48
Abstract	49
Introduction	49
Results	51
Discussion	60
Experimental procedures	63
References	66
Figures	69
Chapter 3: Complementation Between Mouse Mfn1 and Mfn2 Protects	
Mitochondrial Fusion Defects Caused by CMT2A Disease Mutations	79

Abstract	80
Introduction	80
Results	81
Discussion	86
Materials and methods	88
References	88
Supplementary figures	90
Chapter 4: Mfn2 Disease Allele Causes Gait Defects and Axonopathy in Transgenic Mouse Model of CMT2A	95
Introduction	96
Results	98
Discussion	105
Experimental procedures	107
References	110
Figures	114
Chapter 5: Generation of Mitofusin 2 Knock-In Mouse Models of Charcot-Marie-Tooth Disease Type 2A	125
Introduction	126
Results and discussion	127
References	136
Table and figures	139

Chapter 6: Future Directions	143
References	149

List of Figures and Tables

Chapter 1:

Figure 1-1. Mitochondria as dynamic organelles	41
Figure 1-2. Mitochondrial fusion and fission determine morphology	42
Figure 1-3. Mitochondrial fusion	43
Figure 1-4. Mitochondrial fission	44

Chapter 2:

Figure 2-1. Structure-function analysis of Mfn1	72
Figure 2-2. Structure-function analysis of Mfn2	73
Figure 2-3. Co-immunoprecipitation of full-length Mfn1 mutants	74
Figure 2-4. Mitofusin N-N and N-C domain interactions	75
Figure 2-5. Characterization of Mfn1 N-C interaction	76
Figure 2-6. Characterization of non-HR N-C interaction	77
Figure 2-7. Mfn2 CMT2A disease mutations disrupt N-C interaction	78

Chapter 3:

Figure 3-1. Functional analysis of Mfn2 CMT2A alleles	81
Figure 3-2. Lack of mitochondrial fusion activity in many CMT2A alleles	82
Figure 3-3. Construction of MEFs containing homozygous Mfn2 ^{R94Q} Knockin mutations	83
Figure 3-4. Tubular mitochondria in Mfn2 ^{R94Q} —Mfn2 ^{R94Q} cells	84
Figure 3-5. Physical association of mutant Mfn2 with wild-type Mfn1 and Mfn2	84

Figure 3-6. Mfn1 but not Mfn2 complements Mfn2 CMT2A alleles	85
Figure 3-7. Mfn1 complements Mfn2 CMT2A mutants in trans	86
Figure 3-8. Mfn1 complements mutant Mfn2 to preserve mitochondrial fusion in most CMT2A cells	87
Supplementary figure 3-1. Mitochondrial profiles in MEFs expressing Mfn2 CMT2A alleles	92
Supplementary figure 3-2. Mitochondrial aggregation in wild-type cells highly overexpressing Mfn2 CMT2A alleles	93
Supplementary figure 3-3. Quantification of retroviral expression levels	94
Chapter 4:	
Figure 4-1. Generation of Mfn2 T105M transgenic mice	118
Figure 4-2. Tg1/Tg1 mouse phenotype	119
Figure 4-3. Transgene expression in motor neurons	120
Figure 4-4. Hindlimb muscle mass	121
Figure 4-5. Loss of motor neurons in Tg1/Tg1 animals	122
Figure 4-6. Altered mitochondrial distribution in Tg1/Tg1 motor neurons	123
Supplementary figure 4-1. Transgene allelic series for tail phenotype	124
Chapter 5:	
Table 5-1. Summary of genotype/phenotype for knock-in animals	140
Figure 5-1. 94Q/94Q animals have runted phenotype	141
Figure 5-2. Mitochondrial morphologies in CMT2A MEFs	142

Chapter 1

New functions for mitochondrial dynamics

Scott A. Detmer and David C. Chan

This chapter has been submitted to *Nature Reviews Molecular Cell Biology*.

Introduction

Seminal electron microscopy studies in the 1950s revealed the double-membranes and cristae that are hallmarks of mitochondria. These studies of fixed samples led to the canonical view of mitochondria as bean-shaped organelles, although little was known about their versatile and dynamic nature. It is now clear that mitochondria have drastically different morphologies depending on the cell type. Even within the same cell, mitochondria can take on a range of morphologies, from small spheres or short rods to long tubules. In fibroblasts, for example, mitochondria visualized with fluorescent proteins or specific dyes typically form tubules with diameters of approximately 0.5 microns, but their lengths can range from one to ten or more microns.

Even more remarkably, when mitochondria are tracked in living cells, they behave as dynamic organelles that move constantly and undergo structural transitions. Mitochondrial tubules move with their long axis aligned along cytoskeletal tracks. Moreover, individual mitochondria can encounter each other during these movements and undergo fusion. Fusion results in merging of the double membranes, resulting in both lipid and content mixing. Conversely, an individual mitochondrion can divide by fission to yield two or more shorter mitochondria.

What are the molecular mechanisms underlying these unusual behaviors, and do they have consequences for mitochondrial function and cell physiology? In this review, we discuss the dynamic nature of mitochondria and summarize the mechanisms that drive mitochondrial fusion and fission. In addition, we discuss recent insights into how these processes affect the function of mitochondria. Fusion and fission control not only the

shape of mitochondria, but also the functional capacity of the mitochondrial population, including its respiratory activity. Moreover, mitochondrial dynamics plays a key role in mammalian development, neuronal function and several neurodegenerative diseases, and apoptosis.

Mitochondria as dynamic organelles

Control of mitochondrial shape by fusion and fission

It is very clear that an important function of mitochondrial fusion and fission is to control the shape, size, and number of mitochondria (Fig. 1a). At steady-state, the frequencies of fusion and fission events are balanced (Nunnari et al., 1997) to maintain the overall morphology of the mitochondrial population. When this balance is experimentally perturbed, dramatic transitions in mitochondrial shape can occur. Genetic studies in yeast and mammals indicate that cells with a high fusion-to-fission ratio have fewer mitochondria that are longer and more highly interconnected (Fig. 2) (Bleazard et al., 1999; Chen et al., 2003; Sesaki and Jensen, 1999; Smirnova et al., 2001). Conversely, cells with a low fusion-to-fission ratio have numerous mitochondria that are small spheres or short rods, often referred to as "fragmented mitochondria." Such changes in mitochondrial dynamics are used in vivo to developmentally control mitochondrial morphology, as during *Drosophila* spermatogenesis, when many mitochondria synchronously fuse to form the Nebenkern structure that is required for sperm motility (Hales and Fuller, 1997).

Control of mitochondrial distribution by active mitochondrial transport

Mitochondrial transport is required to distribute mitochondria throughout the cell (Fig. 1b). In most cells, mitochondria are highly motile and travel along cytoskeletal tracks. Mitochondrial transport depends on the actin cytoskeleton in budding yeast (Fehrenbacher et al., 2004) and on both actin and microtubules in mammalian cells (Hollenbeck and Saxton, 2005; Ligon and Steward, 2000b; Morris and Hollenbeck, 1995). Depending of the cellular context, these transport processes serve to ensure proper inheritance of mitochondria or to recruit mitochondria to active regions of the cell. For example, in budding yeast, mitochondria are transported into and retained in the developing bud to ensure mitochondrial inheritance to the daughter cell (Fehrenbacher et al., 2004). In neurons, mitochondria are specifically recruited to active growth cones where demand for ATP is presumed to be great (Morris and Hollenbeck, 1993).

Rates of neuronal mitochondria transport have been reported between 0.4 micron/min (Li et al., 2004) and 0.1-1 micron/sec (Miller and Sheetz, 2004; Morris and Hollenbeck, 1995; Pilling et al., 2006). Mitochondria move in a saltatory manner, with pauses often followed by reversal of direction. At a given time, 50-75% of mitochondria are stationary (Bereiter-Hahn and Voth, 1994; Chang et al., 2006; Ligon and Steward, 2000a; Miller and Sheetz, 2004; Morris and Hollenbeck, 1995; Pilling et al., 2006). These pauses and reversals of direction may reflect attachment and detachment of cytoskeletal motors. Although these movements can appear chaotic, several lines of evidence from neuronal studies suggest that mitochondrial transport is not random. First,

neuronal mitochondria most often pause at sites lacking other mitochondria, resulting in a well-spaced axonal mitochondrial distribution (Miller and Sheetz, 2004). Second, nearly 90% of mitochondria with high membrane potential move in the anterograde direction, whereas 80% of mitochondria with low potential move in the retrograde direction (Miller and Sheetz, 2004). These results suggest that active mitochondria are recruited to distal regions with high-energy requirements, whereas impaired mitochondria are returned to the cell soma for destruction or repair. Third, mitochondria accumulate at both pre- and post-synaptic sites in an activity-dependent manner (Chang et al., 2006; Li et al., 2004). Finally, mitochondria, but not other organelles, accumulate at axonal sites of with high local nerve growth factor concentration, perhaps related to mitochondrial collection at active growth cones (Chada and Hollenbeck, 2004; Morris and Hollenbeck, 1993).

Dynamic internal structure

In addition to changes in the overall shape of mitochondria, the internal structures of mitochondria are also dynamic. Three-dimensional tomography of cryo-preserved samples (Mannella et al., 1994; Perkins et al., 1997) has provided new views of mitochondrial internal structure and its plasticity. The inner membrane can be divided into distinct regions: the inner boundary membrane, the cristae membrane, and the cristae junctions (Fig. 1c). The inner boundary membranes are the regions where inner membrane is in close proximity to the outer membrane. These regions are likely important for protein import and may be the sites of coupled outer and inner membrane

fusion. The cristae junctions are narrow "neck" regions that separate the inner boundary membrane from the involuted cristae membrane.

The various regions of the mitochondrial inner membrane are not only morphologically distinct, they appear to constitute separate functional domains of the inner membrane. Proteins involved in translocation of proteins through the inner membrane, such as the TIM23 complex, are enriched in the inner boundary membrane, whereas proteins involved in oxidative phosphorylation are enriched in the cristae membranes (Gilkerson et al., 2003; Vogel et al., 2006; Wurm and Jakobs, 2006). In addition, the structure of mitochondrial membranes is linked to the metabolic state of mitochondria (Fig. 1c). "Orthodox" cristae morphology, with narrow cristae and few cristae junctions per cristae compartment, is found in low ATP conditions. "Condensed" morphology, with larger cristae having several junctions per cristae, is found in high ATP conditions (Mannella, 2006). The conversion between these states likely involves inner membrane fusion and fission (Mannella, 2006). Taken together, these observations suggest that inner membrane morphology is dynamically related to bioenergetics, although the causal relationship remains unclear.

Mechanisms of mitochondrial dynamics

Mediators of fusion

An important inroad into the molecular analysis of mitochondrial morphology came with the discovery in 1997 of the *Drosophila* fusion factor fuzzy onions (Fzo), a

mitochondrial outer membrane GTPase required for the fusion of mitochondria during spermatogenesis (Hales and Fuller, 1997). The yeast ortholog, Fzo1, was found to have a conserved role in mitochondrial fusion (Hermann et al., 1998), and yeast genetics provided the tools to identify additional modulators of mitochondrial fusion and fission (Okamoto and Shaw, 2005; Shaw and Nunnari, 2002). Therefore, the core machineries mediating mitochondrial fusion and fission are most fully understood in yeast. Several of these components have functionally conserved mammalian homologs. More comprehensive discussions of the molecular mechanisms of mitochondria fusion and fission have been presented in recent reviews (Chan, 2006; Griffin et al., 2006).

In yeast, the core mitochondrial fusion machinery consists of two GTPases, Fzo1p and Mgm1p (Fig. 3). Fzo1 is located on the mitochondrial outer membrane and is essential for fusion of the outer membranes (Hermann et al., 1998; Meeusen et al., 2004). The mammalian orthologs of Fzo1 are the mitofusins Mfn1 and Mfn2. These two related proteins form homo-oligomeric and hetero-oligomeric complexes that are functional for fusion (Chen et al., 2003). Mitofusins are required on adjacent mitochondria during the fusion process, implying that they form complexes in trans between apposing mitochondria (Koshiba et al., 2004; Meeusen et al., 2004). A heptad repeat region of Mfn1 has been shown to form an anti-parallel coiled coil that is likely involved in tethering mitochondria during fusion (Koshiba et al., 2004). Mgm1 is a dynamin-related protein that is essential for fusion of the mitochondrial inner membranes, a function consistent with its localization to the intermembrane space and association of the inner membrane (Meeusen et al., 2006). The mammalian ortholog OPA1 is also essential for mitochondrial fusion (Chen et al., 2005; Cipolat et al., 2004). In yeast, the outer

membrane protein Ugo1 physically links Fzo1 and Mgm1, but no mammalian ortholog has been discovered.

The membrane potential across the mitochondrial inner membrane, maintained by the electron transport chain, is essential for mitochondrial fusion (Legros et al., 2002; Meeusen et al., 2004). Ionophores that dissipate the mitochondrial membrane potential cause mitochondrial fragmentation due to an inhibition of mitochondrial fusion (Legros et al., 2002; Malka et al., 2005). In an in vitro fusion assay, both the proton and electrical gradient are important components of the requirement for membrane potential (Meeusen et al., 2004). The link between membrane potential and fusion remains to be resolved, but one factor appears the dependence of OPA1 post-translational processing on the membrane potential (Ishihara et al., 2006).

Recent work has also identified mitochondrial lipids as important factors in fusion. Mitochondrial morphology screens in yeast identified members of the ergosterol synthesis pathway as being required for normal mitochondrial morphology (Altmann and Westermann, 2005; Dimmer et al., 2002). Recently, MitoPLD has been identified as important for mitochondrial fusion (Choi et al., 2006). This mitochondrial outer membrane enzyme hydrolyzes cardiolipin to generate phosphatidic acid. Interestingly, ergosterol has been linked to yeast vacuole fusion (Fratti et al., 2004), and phosphatidic acid is thought to play a role in generating membrane curvature required for SNARE-mediated fusion (Vitale et al., 2001). Thus, specific lipids may play similar roles in distinct types of membrane fusion.

Mediators of fission

The opposing process, mitochondrial fission, requires the recruitment of a dynamin-related protein (Dnm1 in yeast and Drp1 in mammals) from the cytosol to mitochondria (Fig. 4). Both Dnm1 and Drp1 assemble into punctate spots on mitochondrial tubules, and a subset of these complexes lead to a productive fission event (Bleazard et al., 1999; Sesaki and Jensen, 1999; Smirnova et al., 2001). By analogy with classical dynamin in endocytosis, Dnm1 and Drp1 are thought to assemble into rings and spirals that encircle and constrict the mitochondrial tubule during fission (Shaw and Nunnari, 2002). Consistent with this model, purified Dnm1 indeed can form helical rings and spirals in vitro, with dimensions similar to those of constricted mitochondria (Ingerman et al., 2005). Moreover, Dnm1 assembly is required for fission activity (Bhar et al., 2006).

Recruitment of Dnm1 to yeast mitochondrial fission sites involves three other components. It is dependent on Fis1, a mitochondrial integral outer membrane protein that is essential for fission (Fekkes et al., 2000; Mozdy et al., 2000; Tieu and Nunnari, 2000). Fis1 binds indirectly to Dnm1 through either one of two molecular adaptors, Mdv1 and Caf4 (Fig. 4b) (Griffin et al., 2005). Either Mdv1 or Caf4 are sufficient to allow Fis1-dependent recruitment of Dnm1, although Mdv1 has a more important role in mediating fission. Fis1 in mammals is also essential for mitochondrial fission (Lee et al., 2004), but no orthologs of Mdv1 and Caf4 are currently known. Both Fis1 and Drp1 are also required for fission of peroxisomes (Koch et al., 2003; Koch et al., 2005).

Other regulators of morphology

In addition to these core fusion and fission components, other genes can affect mitochondrial morphology. For example, genes such as Mmm1, Mdm10, and Mdm12 are required to maintain yeast mitochondria in a tubular shape (Okamoto and Shaw, 2005). Additional genes have been identified through visual screens for aberrant mitochondrial morphology in large-scale collections of mutant yeast (Altmann and Westermann, 2005; Dimmer et al., 2002). These screens suggest that several cellular pathways influence mitochondrial morphology and inheritance, including ergosterol biosynthesis, mitochondrial protein import, actin dynamics, vesicular fusion, and ubiquitin-mediated protein degradation. Another fruitful approach has been the identification of proteins that physically associate with the core components, such as Mfn2, Mgm1, and Drp1 (Eura et al., 2006; Hajek et al., 2006; Herlan et al., 2003; McQuibban et al., 2003; Nakamura et al., 2006).

Proteins required for mitochondrial transport

Kinesin and dynein microtubule motors are known to be required for anterograde and retrograde mitochondrial transport, respectively (Hollenbeck and Saxton, 2005). Recent work has clarified the linkage between mitochondria and the molecular motors. Screens for essential genes in drosophila identified Milton and dMiro, both of which are required for anterograde mitochondrial transport in neurons (Guo et al., 2005; Stowers et al., 2002). Milton interacts directly with kinesin and associates indirectly with

mitochondria. dMiro is a mitochondrial outer membrane protein that interacts directly with Milton. Thus, dMiro links Milton and kinesin to mitochondria (Glater et al., 2006). dMiro contains both GTPase and EF hand domains which are likely important in regulating mitochondrial transport.

Proteins mediating inner membrane morphology

Studies of mitochondrial inner membrane structure are complicated by the intimate link, discussed above, between mitochondrial bioenergetics and cristae structure. Nevertheless, several proteins have been shown to have a specific role in control of cristae structure. In addition to their roles in mitochondrial fusion, Mgm1 and OPA1 are important for cristae structure. Loss of Mgm1 in yeast or knock-down of OPA1 in mammalian cells results in disorganized inner membrane structures (Amutha et al., 2004; Frezza et al., 2006; Olichon et al., 2003; Sesaki et al., 2003). In both cases, Mgm1 or OPA1 homo-oligomeric interactions are involved (Frezza et al., 2006; Meeusen et al., 2006). The role of OPA1 in cristae structure appears separable from its role in mitochondrial fusion (Frezza et al., 2006).

Mitochondrial F_1F_0 ATP synthase, a rotary enzyme embedded in the inner membrane that couples proton pumping to ATP synthesis, is essential for normal cristae structure (Paumard et al., 2002). This role in inner membrane structure involves a dimeric form of ATP synthase containing the additional subunits e and g. As visualized by electron microscopy, the ATP synthase dimer has a dimeric interface with a sharp angle that could distort the local lipid membrane. This distortion may contribute to the

high membrane curvature that characterizes cristae tubules (Dudkina et al., 2005; Minauro-Sanmiguel et al., 2005). Mgm1 is required for oligomerization of ATP synthase, providing a link between these two modulators of cristae structure (Amutha et al., 2004).

Additional proteins modulate inner membrane dynamics. In yeast, Mdm33 is required for normal mitochondrial morphology, and its over-expression leads to septation and vesiculation of the inner membranes (Messerschmitt et al., 2003). Because of these phenotypes, Mdm33 has been suggested to play a role in inner membrane fission. Depletion of Mitofilin by RNAi in mammalian cells results in formation of complex sworls of inner membrane (John et al., 2005). Depletion of Mmm1p, Mdm31 and Mdm32, yeast proteins implicated in mtDNA maintenance, also cause aberrant cristae morphologies (Dimmer et al., 2005; Hobbs et al., 2001). A challenge for the future will be determining whether these proteins have direct or indirect effects on cristae morphology.

Biological functions of mitochondrial dynamics

Mitochondrial fusion and fission were first studied because of their important role in regulation of mitochondrial morphology. In addition to this function, it is now clear that these processes have additional roles in maintaining the health of the mitochondrial population, with consequences for development, disease, and apoptosis.

Protection of respiratory function

Cells with abnormalities in mitochondrial fusion have severe mitochondrial dysfunction in addition to mitochondrial fragmentation. Mouse fibroblasts lacking either Mfn1 or Mfn2 show mild heterogeneity in mitochondrial membrane potential (Chen et al., 2003), although respiratory activity is intact. Cells lacking both mitofusins, however, show great heterogeneity in mitochondrial shape and membrane potential and reduced respiratory capacity (Chen et al., 2005). Cells lacking OPA1 show similar defects, with an even greater reduction in respiratory capacity. Because other cells with fragmented mitochondria can have normal mitochondrial function, these observations show that fusion is beneficial to the mitochondrial population apart from its effect on mitochondrial shape. Fusion and fission allow the mitochondrial population to form a dynamic network capable of genetic and biochemical complementation. Indeed, functional complementation between mutant mitochondrial DNA genomes has been observed (D'Aurelio et al., 2004; Ono et al., 2001)

Essential developmental functions

Perturbations in mitochondrial dynamics result in specific developmental defects. Mice with loss of either mitofusins die in mid-gestation, with Mfn2-null mice showing a specific defect in placental development (Chen et al., 2003). Mice lacking OPA1 also die in early embryogenesis (Alavi et al., 2007).

Mitochondrial fission is also an essential process. Worms deficient in mitochondrial division die before reaching adulthood (Labrousse et al., 1999). An infant with a dominant-negative Drp1 allele has been reported. This patient died at about one month of age and had a wide spectrum of abnormalities, including reduced head growth, increased lactic acid, and optic atrophy. Fibroblasts from this patient showed elongation of both mitochondria and peroxisomes (Waterham et al., 2007).

Mitochondrial distribution and recruitment in neurons

Mitochondrial dynamics is probably a ubiquitous phenomenon that is important for all cells. However, neurons appear to be particularly dependent on proper control of mitochondrial dynamics. Abundant mitochondria have been noted at neuronal synapses since the 1950s (Palay, 1956). More recent time-lapse imaging has confirmed enrichment and retention of mitochondria at both pre- and post-synaptic sites (Chang et al., 2006). Due to their extreme length (the longest are greater than half a body length), neurons rely heavily on active transport to recruit organelles, including mitochondria, to nerve termini. Fibroblasts lacking the anterograde mitochondrial motor Kif5b have perinuclearly aggregated mitochondria but no reported functional defects (Tanaka et al., 1998). In contrast, disruption of anterograde mitochondrial transport in neurons results in defective synaptic transmission (Guo et al., 2005; Stowers et al., 2002; Verstreken et al., 2005).

Fly neurons lacking Milton, Miro, or Drp1 show loss of synaptic mitochondria and are defective for synaptic transmission (Guo et al., 2005; Stowers et al., 2002;

Verstreken et al., 2005). Miro-deficient larvae had altered neuromuscular junctions with smaller and more abundant pre-synaptic boutons compared to wild-type larvae, indicating synaptic overgrowth in the absence of productive synapse formation (Guo et al., 2005). Both mutant Miro and Drp1 synapses were found to have elevated resting Ca^{2+} levels but normal Ca^{2+} dynamics upon moderate stimulation, with more severe defects appearing during sustained stimulation (Guo et al., 2005; Verstreken et al., 2005). Both studies suggest that mitochondria are critically important for Ca^{2+} homeostasis only during sustained and intense stimulation. The more important defect in Drp1 mutants appears to be decreased synaptic levels of ATP and subsequent immobilization of the reserve vesicle pool. Forward-filling of synapses with ATP partially rescued synaptic transmission in Drp1 mutant neuromuscular junctions (Verstreken et al., 2005).

Mitochondria are also required post-synaptically in dendrites of hippocampal neurons. Mitochondrial localization at dendritic spines (potential post-synaptic sites) increased following repetitive stimulation (Li et al., 2004). Expression of mutant Drp1 caused elongation of mitochondria and a decrease in both the abundance of dendritic mitochondria and the density of dendritic spines. Conversely, over-expression of wild-type Drp1 decreased mean mitochondrial length and increased both the density of dendritic mitochondria and spines (Li et al., 2004). Dendritic spine density was also increased by creatine, which stimulates mitochondrial activity.

*Involvement in human disease**OPA1 and ADOA*

Heterozygous mutations in OPA1 cause autosomal dominant optic atrophy (ADOA). This disease is the most common heritable form of optic neuropathy and is due to degeneration of retinal ganglion cells, whose axons form the optic nerve (Delettre et al., 2000). Over 100 mutations in OPA1 have been reported, with the majority of the mutations occurring in the GTPase domain (Ferre et al., 2005). Roughly half of the pathogenic alleles contain nonsense mutations predicted to encode a truncated protein. A few nonsense mutations abolish nearly the entire coding sequence (Delettre et al., 2000), suggesting that haploinsufficiency of OPA1 can cause ADOA. It remains possible that other less severe truncations may have dominant-negative activity.

Fibroblasts knocked-down for OPA1 have fragmented mitochondria, defects in respiration, aberrant cristae structure, and increased susceptibility to apoptosis (Chen et al., 2005; Cipolat et al., 2004; Griparic et al., 2004; Olichon et al., 2003). In the disease state, the pathophysiology remains to be clarified. Monocytes from a patient with a C-terminal truncation in OPA1 had aggregated mitochondria (Delettre et al., 2000), and skin fibroblasts from a patient with a GTPase missense mutation in OPA1 had fragmented mitochondria and increased sensitivity to apoptosis (Olichon et al., 2006). In addition, OPA1 mutations have been associated with reduced ATP production and mtDNA content (Kim et al., 2005; Lodi et al., 2004). It is unclear why mutations in OPA1, which is broadly expressed, have such cell-type specific defects.

A mouse model of ADOA has been constructed with an OPA1 gene containing a splice site mutation that causes processed transcripts to lack exon 10 (Alavi et al., 2007). Although this mutation would be expected to produce an internally truncated protein, the mutant mice do not produce any detectable protein from the mutant OPA1 gene. Heterozygous mice show several features of ADOA, including progressive decline in retinal ganglion cell numbers and loss of axons in the optic nerve. These results further support haploinsufficiency of OPA1 as a mechanism for ADOA. Interestingly, mice homozygous for the OPA1 mutation die at mid-gestation (Alavi et al., 2007), consistent with an essential requirement for mitochondrial fusion during embryonic development (Chen et al., 2003).

Mfn2 and CMT2A

Charcot-Marie-Tooth (CMT) disease, one of the most common hereditary neuropathies, is caused by mutations in at least 30 different genes (Zuchner and Vance, 2006). Affected individuals have progressive distal motor and sensory impairments beginning in the feet and hands due to loss of function of long neurons. Depending on the type of CMT, these diseases can be caused by a primary defect in the Schwann cells that myelinate peripheral nerves or in the neurons themselves (Zuchner and Vance, 2006). CMT2A is an axonopathy caused by the latter defect, and has been associated with over 40 mutations in Mfn2. Nearly all of these disease alleles contain missense mutations or short, in-frame deletions (Zuchner et al., 2004). Most mutations cluster in or near the GTPase domain but some also occur in each of the heptad repeat domains of

Mfn2. In addition to loss of peripheral nerve function, a subset of CMT2A patients also have optic atrophy, suggesting a similar mechanistic and clinical outcome for disruption of mitochondrial dynamics with mutation of OPA1 and Mfn2 (Chung et al., 2006; Zuchner et al., 2006).

Because of difficulties in studying patient nerve tissue, the pathogenic mechanisms leading to peripheral nerve degeneration in CMT2A are not well understood. Only one study has examined ultrastructural defects in mitochondria from nerves of CMT2A patients. Mitochondria in the sural nerve of two patients show structural aberrations in the mitochondrial outer and inner membranes, along with swelling that is suggestive of mitochondrial dysfunction (Verhoeven et al., 2006). Aggregation of mitochondria is also observed. Interestingly, over-expression of Mfn2 CMT2A alleles (Baloh et al., 2007; Detmer and Chan, 2007) causes mitochondrial aggregation and subsequent mitochondrial transport defects in neurons (Baloh et al., 2007). In fibroblasts, the mitochondrial aggregation phenotype is dependent on significant over-expression of the CMT2A alleles (Detmer and Chan, 2007), and therefore its relevance to disease pathogenesis remains to be clarified.

Several perplexing issues remain to be resolved concerning the molecular genetics of CMT2A. How does mutation of one copy of Mfn2 lead to disease? Why are long peripheral neurons selectively affected, given that Mfn2 is a broadly expressed protein? Clues to these issues have come from analysis of CMT2A alleles in mice (Detmer and Chan, 2007). Many CMT2A alleles of Mfn2 are nonfunctional for fusion when expressed alone. However, the fusion activity of these nonfunctional alleles can be efficiently complemented by wild-type Mfn1 but not Mfn2. Because of this

complementation, in CMT2A patients, cells that express Mfn1 are protected from gross loss of fusion activity. In contrast, cells with little or no Mfn1 expression would suffer a greater relative loss of fusion activity. In part, these properties of the CMT2A alleles may underlie the selective loss of sensory and motor neurons. Consistent with this model, Mfn2 appears to be more highly expressed in central and peripheral nervous tissue than Mfn1 (S. A. Detmer and D. C. Chan, unpublished observations). Even within the peripheral nerves, it appears that mitochondrial fusion defects are partial, because only the longest nerves are affected. Most likely, the extreme dimensions of long peripheral nerves make them most vulnerable to changes in mitochondrial dynamics. Hopefully, the molecular basis of this effect can be dissected in animal models.

GDAP1 and CMT4A

Another form of CMT is associated with defects in mitochondrial dynamics. GDAP1 (ganglioside-induced differentiation-associated protein 1) is mutated in CMT4A, one of the few recessive forms of CMT disease. CMT4A contains both demyelinating and axonal features, and consistent with this mixed clinical presentation, GDAP1 is expressed in both Schwann cells and neurons (Niemann et al., 2005). GDAP1 is an integral outer membrane protein that likely affects mitochondrial division (Niemann et al., 2005; Pedrola et al., 2005). Disease alleles either fail to localize to mitochondria or are defective in stimulating mitochondrial division when over-expressed (Niemann et al., 2005). If GDAP1 disease alleles disrupt normal mitochondrial fission, they may cause mitochondrial distribution defects similar to those induced by Drp1 mutations discussed

above (Li et al., 2004; Verstreken et al., 2005). Again, it will be important determine whether patient samples substantiate these ideas.

Regulation of apoptosis

A regulated switch in mitochondrial morphology appears to be important for some forms of apoptosis. In apoptosis mediated by Bcl-2 family members, the outer membrane of mitochondria are permeabilized to release contents of the intermembrane space, such as cytochrome c, into the cytoplasm. Cytochrome c subsequently activates a cascade of caspases that propagate and execute the apoptotic program. This mitochondrial outer membrane permeabilization is an early step in apoptosis and is temporally associated with mitochondrial fragmentation (Desagher and Martinou, 2000; Frank et al., 2001). In principle, therefore, genes controlling mitochondrial morphology can potentially impact progression of apoptosis.

The first functional link between mitochondrial fission and apoptosis was the observation that inhibition of fission can partially block apoptosis (Frank et al., 2001). Over-expression of dominant-negative Drp1 prevents mitochondrial fragmentation and reduces membrane depolarization, cytochrome c release, and cell death in response to apoptotic stimuli (Frank et al., 2001). Similarly, RNAi-mediated down-regulation of Fis1 and Drp1 inhibits both fragmentation and apoptosis (Lee et al., 2004). These results suggest that mitochondrial fission is an important component of mitochondrial permeabilization and progression of apoptosis. In addition, over-expression of rat mitofusin protects against apoptosis, whereas RNAi down-regulation of mitofusin leads

to fragmentation of mitochondria and increased susceptibility to apoptosis (Sugioka et al., 2004). Mitochondrial fusion is inhibited during apoptosis following Bax activation (Karbowski et al., 2004). Interestingly, Bax, which localizes to discrete puncta on mitochondria upon induction of apoptosis, colocalize with both Drp1 and Mfn2 (Karbowski et al., 2002). The functional nature of these interactions is not understood but suggests that the fission and fusion machinery may be modified in early apoptosis. Surprisingly, the apoptotic proteins Bax and Bak appear to have a role in normal mitochondrial morphology. Bax and Bak double knock-out cells have fragmented mitochondria due to a fusion defect (Karbowski et al., 2006). In addition, Bax and Mfn2 interact in a yeast-2-hybrid analysis, and Bax may be involved in Mfn2 distribution on the mitochondrial outer membrane (Karbowski et al., 2006).

In spite of these compelling observations, the causal relationship of mitochondrial fission to apoptosis remains to be definitively resolved. Perplexingly, depending on the biological system, mitochondrial fragmentation has been reported to occur before cytochrome c release in some cases, but after in other cases (Arnoult, 2007). In some experimental systems, inhibition of mitochondrial fission by knock-down of Fis1 or Drp1 does not inhibit apoptosis, even though mitochondrial fragmentation is efficiently inhibited (Parone et al., 2006).

In addition to outer membrane permeabilization, remodeling of the cristae membranes is required for rapid and efficient release of cytochrome c (Goldstein et al., 2000; Scorrano et al., 2002). The reason for this requirement is that only a minority (~15%) of cytochrome c resides in the intermembrane space, with the bulk found in cristae compartments (Scorrano et al., 2002). OPA1 appears to be a regulator of cristae

junctions and therefore cytochrome c release (Cipolat et al., 2006; Frezza et al., 2006). Over-expression of OPA1 blocks cytochrome c release following induction of apoptosis by maintaining narrow cristae junctions (Frezza et al., 2006).

Lymphocyte chemotaxis

Mitochondrial dynamics appears to be important for proper mitochondrial redistribution in lymphocytes during chemotaxis (Campello et al., 2006). Mitochondria redistribute to the trailing edge in lymphocyte cell lines migrating in response to chemical attractants. Modulation of mitochondrial fusion or fission effected both mitochondrial redistribution and cell migration. For example, fragmentation of mitochondria enhanced both redistribution and migration whereas conditions that promoted fusion, and subsequently larger mitochondria, impaired both redistribution and migration. These observations suggest that mitochondrial dynamics is important for recruiting mitochondria to local cellular areas that have the greatest energy requirements.

Perspectives

The study of mitochondrial dynamics has undergone great advances in the last few years. It is now clear that, in addition to control of organelle morphology, mitochondrial dynamics is important for the functional state of mitochondria. As a result, these processes play crucial roles in mammalian development, apoptosis, and disease. As our knowledge of mitochondrial dynamics increases, we can expect to learn about its

involvement in other processes. The link between defects in mitochondrial fusion and neurodegenerative disease is particularly intriguing. In future studies, the pathophysiological mechanisms underlying such neurodegenerative diseases will hopefully be dissected in appropriate animal models.

References

- Alavi, M.V., S. Bette, S. Schimpf, F. Schuettauf, U. Schraermeyer, H.F. Wehrl, L. Ruttiger, S.C. Beck, F. Tonagel, B.J. Pichler, M. Knipper, T. Peters, J. Laufs, and B. Wissinger. 2007. A splice site mutation in the murine Opa1 gene features pathology of autosomal dominant optic atrophy. *Brain*.
- Altmann, K., and B. Westermann. 2005. Role of essential genes in mitochondrial morphogenesis in *Saccharomyces cerevisiae*. *Mol Biol Cell*. 16:5410-7.
- Amutha, B., D.M. Gordon, Y. Gu, and D. Pain. 2004. A novel role of Mgm1p, a dynamin-related GTPase, in ATP synthase assembly and cristae formation/maintenance. *Biochem J*. 381:19-23.
- Arnoult, D. 2007. Mitochondrial fragmentation in apoptosis. *Trends Cell Biol*. 17:6-12.
- Baloh, R.H., R.E. Schmidt, A. Pestronk, and J. Milbrandt. 2007. Altered axonal mitochondrial transport in the pathogenesis of Charcot-Marie-Tooth disease from mitofusin 2 mutations. *J Neurosci*. 27:422-30.
- Bereiter-Hahn, J., and M. Voth. 1994. Dynamics of mitochondria in living cells: shape changes, dislocations, fusion, and fission of mitochondria. *Microsc Res Tech*. 27:198-219.
- Bhar, D., M.A. Karren, M. Babst, and J.M. Shaw. 2006. Dimeric Dnm1-G385D interacts with Mdv1 on mitochondria and can be stimulated to assemble into fission complexes containing Mdv1 and Fis1. *J Biol Chem*. 281:17312-20.

- Bleazard, W., J.M. McCaffery, E.J. King, S. Bale, A. Mozdy, Q. Tieu, J. Nunnari, and J.M. Shaw. 1999. The dynamin-related GTPase Dnm1 regulates mitochondrial fission in yeast. *Nat Cell Biol.* 1:298-304.
- Campello, S., R.A. Lacalle, M. Bettella, S. Manes, L. Scorrano, and A. Viola. 2006. Orchestration of lymphocyte chemotaxis by mitochondrial dynamics. *J Exp Med.*
- Chada, S.R., and P.J. Hollenbeck. 2004. Nerve growth factor signaling regulates motility and docking of axonal mitochondria. *Curr Biol.* 14:1272-6.
- Chan, D.C. 2006. Mitochondrial fusion and fission in mammals. *Annu Rev Cell Dev Biol.* 22:79-99.
- Chang, D.T., A.S. Honick, and I.J. Reynolds. 2006. Mitochondrial trafficking to synapses in cultured primary cortical neurons. *J Neurosci.* 26:7035-45.
- Chen, H., A. Chomyn, and D.C. Chan. 2005. Disruption of fusion results in mitochondrial heterogeneity and dysfunction. *J Biol Chem.* 280:26185-92.
- Chen, H., S.A. Detmer, A.J. Ewald, E.E. Griffin, S.E. Fraser, and D.C. Chan. 2003. Mitofusins Mfn1 and Mfn2 coordinately regulate mitochondrial fusion and are essential for embryonic development. *J Cell Biol.* 160:189-200.
- Choi, S.Y., P. Huang, G.M. Jenkins, D.C. Chan, J. Schiller, and M.A. Frohman. 2006. A common lipid links Mfn-mediated mitochondrial fusion and SNARE-regulated exocytosis. *Nat Cell Biol.* 8:1255-62.
- Chung, K.W., S.B. Kim, K.D. Park, K.G. Choi, J.H. Lee, H.W. Eun, J.S. Suh, J.H. Hwang, W.K. Kim, B.C. Seo, S.H. Kim, I.H. Son, S.M. Kim, I.N. Sunwoo, and B.O. Choi. 2006. Early onset severe and late-onset mild Charcot-Marie-Tooth disease with mitofusin 2 (MFN2) mutations. *Brain.* 129:2103-18.

- Cipolat, S., O. Martins de Brito, B. Dal Zilio, and L. Scorrano. 2004. OPA1 requires mitofusin 1 to promote mitochondrial fusion. *Proc Natl Acad Sci U S A.* 101:15927-32.
- Cipolat, S., T. Rudka, D. Hartmann, V. Costa, L. Serneels, K. Craessaerts, K. Metzger, C. Frezza, W. Annaert, L. D'Adamio, C. Derks, T. Dejaegere, L. Pellegrini, R. D'Hooge, L. Scorrano, and B. De Strooper. 2006. Mitochondrial rhomboid PARL regulates cytochrome c release during apoptosis via OPA1-dependent cristae remodeling. *Cell.* 126:163-75.
- D'Aurelio, M., C.D. Gajewski, M.T. Lin, W.M. Mauck, L.Z. Shao, G. Lenaz, C.T. Moraes, and G. Manfredi. 2004. Heterologous mitochondrial DNA recombination in human cells. *Hum Mol Genet.* 13:3171-9.
- Delettre, C., G. Lenaers, J.M. Griffoin, N. Gigarel, C. Lorenzo, P. Belenguer, L. Pelloquin, J. Grosgeorge, C. Turc-Carel, E. Perret, C. Astarie-Dequeker, L. Lasquellec, B. Arnaud, B. Ducommun, J. Kaplan, and C.P. Hamel. 2000. Nuclear gene OPA1, encoding a mitochondrial dynamin-related protein, is mutated in dominant optic atrophy. *Nat Genet.* 26:207-10.
- Desagher, S., and J.C. Martinou. 2000. Mitochondria as the central control point of apoptosis. *Trends Cell Biol.* 10:369-77.
- Detmer, S.A., and D.C. Chan. 2007. Complementation between mouse Mfn1 and Mfn2 protects mitochondrial fusion defects caused by CMT2A disease mutations. *J Cell Biol.* 176:405-14.

- Dimmer, K.S., S. Fritz, F. Fuchs, M. Messerschmitt, N. Weinbach, W. Neupert, and B. Westermann. 2002. Genetic basis of mitochondrial function and morphology in *Saccharomyces cerevisiae*. *Mol Biol Cell*. 13:847-53.
- Dimmer, K.S., S. Jakobs, F. Vogel, K. Altmann, and B. Westermann. 2005. Mdm31 and Mdm32 are inner membrane proteins required for maintenance of mitochondrial shape and stability of mitochondrial DNA nucleoids in yeast. *J Cell Biol*. 168:103-15.
- Dudkina, N.V., J. Heinemeyer, W. Keegstra, E.J. Boekema, and H.P. Braun. 2005. Structure of dimeric ATP synthase from mitochondria: an angular association of monomers induces the strong curvature of the inner membrane. *FEBS Lett*. 579:5769-72.
- Eura, Y., N. Ishihara, T. Oka, and K. Mihara. 2006. Identification of a novel protein that regulates mitochondrial fusion by modulating mitofusin (Mfn) protein function. *J Cell Sci*. 119:4913-25.
- Fehrenbacher, K.L., H.C. Yang, A.C. Gay, T.M. Huckaba, and L.A. Pon. 2004. Live cell imaging of mitochondrial movement along actin cables in budding yeast. *Curr Biol*. 14:1996-2004.
- Fekkes, P., K.A. Shepard, and M.P. Yaffe. 2000. Gag3p, an outer membrane protein required for fission of mitochondrial tubules. *J Cell Biol*. 151:333-40.
- Ferre, M., P. Amati-Bonneau, Y. Tourmen, Y. Malthiery, and P. Reynier. 2005. eOPA1: an online database for OPA1 mutations. *Hum Mutat*. 25:423-8.

- Frank, S., B. Gaume, E.S. Bergmann-Leitner, W.W. Leitner, E.G. Robert, F. Catez, C.L. Smith, and R.J. Youle. 2001. The role of dynamin-related protein 1, a mediator of mitochondrial fission, in apoptosis. *Dev Cell*. 1:515-25.
- Fratti, R.A., Y. Jun, A.J. Merz, N. Margolis, and W. Wickner. 2004. Interdependent assembly of specific regulatory lipids and membrane fusion proteins into the vertex ring domain of docked vacuoles. *J Cell Biol*. 167:1087-98.
- Frezza, C., S. Cipolat, O. Martins de Brito, M. Micaroni, G.V. Beznoussenko, T. Rudka, D. Bartoli, R.S. Polishuck, N.N. Danial, B. De Strooper, and L. Scorrano. 2006. OPA1 controls apoptotic cristae remodeling independently from mitochondrial fusion. *Cell*. 126:177-89.
- Gilkerson, R.W., J.M. Selker, and R.A. Capaldi. 2003. The cristal membrane of mitochondria is the principal site of oxidative phosphorylation. *FEBS Lett*. 546:355-8.
- Glater, E.E., L.J. Megeath, R.S. Stowers, and T.L. Schwarz. 2006. Axonal transport of mitochondria requires milton to recruit kinesin heavy chain and is light chain independent. *J Cell Biol*. 173:545-57.
- Goldstein, J.C., N.J. Waterhouse, P. Juin, G.I. Evan, and D.R. Green. 2000. The coordinate release of cytochrome c during apoptosis is rapid, complete and kinetically invariant. *Nat Cell Biol*. 2:156-62.
- Griffin, E.E., S.A. Detmer, and D.C. Chan. 2006. Molecular mechanism of mitochondrial membrane fusion. *Biochim Biophys Acta*. 1763:482-9.

- Griffin, E.E., J. Graumann, and D.C. Chan. 2005. The WD40 protein Caf4p is a component of the mitochondrial fission machinery and recruits Dnm1p to mitochondria. *J Cell Biol.* 170:237-48.
- Griparic, L., N.N. van der Wel, I.J. Orozco, P.J. Peters, and A.M. van der Blik. 2004. Loss of the intermembrane space protein Mgm1/OPA1 induces swelling and localized constrictions along the lengths of mitochondria. *J Biol Chem.* 279:18792-8.
- Guo, X., G.T. Macleod, A. Wellington, F. Hu, S. Panchumarthi, M. Schoenfield, L. Marin, M.P. Charlton, H.L. Atwood, and K.E. Zinsmaier. 2005. The GTPase dMiro is required for axonal transport of mitochondria to Drosophila synapses. *Neuron.* 47:379-93.
- Hajek, P., A. Chomyn, and G. Attardi. 2006. Identification of a novel mitochondrial complex containing mitofusin 2 and stomatin-like protein 2. *J Biol Chem.*
- Hales, K.G., and M.T. Fuller. 1997. Developmentally regulated mitochondrial fusion mediated by a conserved, novel, predicted GTPase. *Cell.* 90:121-9.
- Herlan, M., F. Vogel, C. Bornhovd, W. Neupert, and A.S. Reichert. 2003. Processing of Mgm1 by the rhomboid-type protease Pcp1 is required for maintenance of mitochondrial morphology and of mitochondrial DNA. *J Biol Chem.* 278:27781-8.
- Hermann, G.J., J.W. Thatcher, J.P. Mills, K.G. Hales, M.T. Fuller, J. Nunnari, and J.M. Shaw. 1998. Mitochondrial fusion in yeast requires the transmembrane GTPase Fzo1p. *J Cell Biol.* 143:359-73.

- Hobbs, A.E., M. Srinivasan, J.M. McCaffery, and R.E. Jensen. 2001. Mmm1p, a mitochondrial outer membrane protein, is connected to mitochondrial DNA (mtDNA) nucleoids and required for mtDNA stability. *J Cell Biol.* 152:401-10.
- Hollenbeck, P.J., and W.M. Saxton. 2005. The axonal transport of mitochondria. *J Cell Sci.* 118:5411-9.
- Ingerman, E., E.M. Perkins, M. Marino, J.A. Mears, J.M. McCaffery, J.E. Hinshaw, and J. Nunnari. 2005. Dnm1 forms spirals that are structurally tailored to fit mitochondria. *J Cell Biol.* 170:1021-7.
- Ishihara, N., Y. Fujita, T. Oka, and K. Mihara. 2006. Regulation of mitochondrial morphology through proteolytic cleavage of OPA1. *Embo J.* 25:2966-77.
- Ishihara, N., A. Jofuku, Y. Eura, and K. Mihara. 2003. Regulation of mitochondrial morphology by membrane potential, and DRP1-dependent division and FZO1-dependent fusion reaction in mammalian cells. *Biochem Biophys Res Commun.* 301:891-8.
- John, G.B., Y. Shang, L. Li, C. Renken, C.A. Mannella, J.M. Selker, L. Rangell, M.J. Bennett, and J. Zha. 2005. The mitochondrial inner membrane protein mitofilin controls cristae morphology. *Mol Biol Cell.* 16:1543-54.
- Karbowski, M., D. Arnoult, H. Chen, D.C. Chan, C.L. Smith, and R.J. Youle. 2004. Quantitation of mitochondrial dynamics by photolabeling of individual organelles shows that mitochondrial fusion is blocked during the Bax activation phase of apoptosis. *J Cell Biol.* 164:493-9.
- Karbowski, M., Y.J. Lee, B. Gaume, S.Y. Jeong, S. Frank, A. Nechushtan, A. Santel, M. Fuller, C.L. Smith, and R.J. Youle. 2002. Spatial and temporal association of Bax

- with mitochondrial fission sites, Drp1, and Mfn2 during apoptosis. *J Cell Biol.* 159:931-8.
- Karbowski, M., K.L. Norris, M.M. Cleland, S.Y. Jeong, and R.J. Youle. 2006. Role of Bax and Bak in mitochondrial morphogenesis. *Nature.* 443:658-62.
- Kim, J.Y., J.M. Hwang, H.S. Ko, M.W. Seong, B.J. Park, and S.S. Park. 2005. Mitochondrial DNA content is decreased in autosomal dominant optic atrophy. *Neurology.* 64:966-72.
- Koch, A., M. Thiemann, M. Grabenbauer, Y. Yoon, M.A. McNiven, and M. Schrader. 2003. Dynamin-like protein 1 is involved in peroxisomal fission. *J Biol Chem.* 278:8597-605.
- Koch, A., Y. Yoon, N.A. Bonekamp, M.A. McNiven, and M. Schrader. 2005. A role for Fis1 in both mitochondrial and peroxisomal fission in mammalian cells. *Mol Biol Cell.* 16:5077-86.
- Koshiba, T., S.A. Detmer, J.T. Kaiser, H. Chen, J.M. McCaffery, and D.C. Chan. 2004. Structural basis of mitochondrial tethering by mitofusin complexes. *Science.* 305:858-62.
- Labrousse, A.M., M.D. Zappaterra, D.A. Rube, and A.M. van der Bliek. 1999. C. elegans dynamin-related protein DRP-1 controls severing of the mitochondrial outer membrane. *Mol Cell.* 4:815-26.
- Lee, Y.J., S.Y. Jeong, M. Karbowski, C.L. Smith, and R.J. Youle. 2004. Roles of the mammalian mitochondrial fission and fusion mediators Fis1, Drp1, and Opa1 in apoptosis. *Mol Biol Cell.* 15:5001-11.

- Legros, F., A. Lombes, P. Frachon, and M. Rojo. 2002. Mitochondrial fusion in human cells is efficient, requires the inner membrane potential, and is mediated by mitofusins. *Mol Biol Cell*. 13:4343-54.
- Legros, F., F. Malka, P. Frachon, A. Lombes, and M. Rojo. 2004. Organization and dynamics of human mitochondrial DNA. *J Cell Sci*. 117:2653-62.
- Li, Z., K. Okamoto, Y. Hayashi, and M. Sheng. 2004. The importance of dendritic mitochondria in the morphogenesis and plasticity of spines and synapses. *Cell*. 119:873-87.
- Ligon, L.A., and O. Steward. 2000a. Movement of mitochondria in the axons and dendrites of cultured hippocampal neurons. *J Comp Neurol*. 427:340-50.
- Ligon, L.A., and O. Steward. 2000b. Role of microtubules and actin filaments in the movement of mitochondria in the axons and dendrites of cultured hippocampal neurons. *J Comp Neurol*. 427:351-61.
- Lodi, R., C. Tonon, M.L. Valentino, S. Iotti, V. Clementi, E. Malucelli, P. Barboni, L. Longanesi, S. Schimpf, B. Wissinger, A. Baruzzi, B. Barbiroli, and V. Carelli. 2004. Deficit of in vivo mitochondrial ATP production in OPA1-related dominant optic atrophy. *Ann Neurol*. 56:719-23.
- Malka, F., O. Guillery, C. Cifuentes-Diaz, E. Guillou, P. Belenguer, A. Lombes, and M. Rojo. 2005. Separate fusion of outer and inner mitochondrial membranes. *EMBO Rep*. 6:853-9.
- Mannella, C.A. 2006. Structure and dynamics of the mitochondrial inner membrane cristae. *Biochim Biophys Acta*. 1763:542-8.

- Mannella, C.A., M. Marko, P. Penczek, D. Barnard, and J. Frank. 1994. The internal compartmentation of rat-liver mitochondria: tomographic study using the high-voltage transmission electron microscope. *Microsc Res Tech.* 27:278-83.
- Mattenberger, Y., D.I. James, and J.C. Martinou. 2003. Fusion of mitochondria in mammalian cells is dependent on the mitochondrial inner membrane potential and independent of microtubules or actin. *FEBS Lett.* 538:53-9.
- McQuibban, G.A., S. Saurya, and M. Freeman. 2003. Mitochondrial membrane remodelling regulated by a conserved rhomboid protease. *Nature.* 423:537-41.
- Meeusen, S., R. DeVay, J. Block, A. Cassidy-Stone, S. Wayson, J.M. McCaffery, and J. Nunnari. 2006. Mitochondrial inner-membrane fusion and crista maintenance requires the dynamin-related GTPase Mgm1. *Cell.* 127:383-95.
- Meeusen, S., J.M. McCaffery, and J. Nunnari. 2004. Mitochondrial fusion intermediates revealed in vitro. *Science.* 305:1747-52.
- Messerschmitt, M., S. Jakobs, F. Vogel, S. Fritz, K.S. Dimmer, W. Neupert, and B. Westermann. 2003. The inner membrane protein Mdm33 controls mitochondrial morphology in yeast. *J Cell Biol.* 160:553-64.
- Miller, K.E., and M.P. Sheetz. 2004. Axonal mitochondrial transport and potential are correlated. *J Cell Sci.* 117:2791-804.
- Minauro-Sanmiguel, F., S. Wilkens, and J.J. Garcia. 2005. Structure of dimeric mitochondrial ATP synthase: novel F₀ bridging features and the structural basis of mitochondrial cristae biogenesis. *Proc Natl Acad Sci U S A.* 102:12356-8.
- Morris, R.L., and P.J. Hollenbeck. 1993. The regulation of bidirectional mitochondrial transport is coordinated with axonal outgrowth. *J Cell Sci.* 104 (Pt 3):917-27.

- Morris, R.L., and P.J. Hollenbeck. 1995. Axonal transport of mitochondria along microtubules and F-actin in living vertebrate neurons. *J Cell Biol.* 131:1315-26.
- Mozdy, A.D., J.M. McCaffery, and J.M. Shaw. 2000. Dnm1p GTPase-mediated mitochondrial fission is a multi-step process requiring the novel integral membrane component Fis1p. *J Cell Biol.* 151:367-80.
- Nakamura, N., Y. Kimura, M. Tokuda, S. Honda, and S. Hirose. 2006. MARCH-V is a novel mitofusin 2- and Drp1-binding protein able to change mitochondrial morphology. *EMBO Rep.* 7:1019-22.
- Niemann, A., M. Ruegg, V. La Padula, A. Schenone, and U. Suter. 2005. Ganglioside-induced differentiation associated protein 1 is a regulator of the mitochondrial network: new implications for Charcot-Marie-Tooth disease. *J Cell Biol.* 170:1067-78.
- Nunnari, J., W.F. Marshall, A. Straight, A. Murray, J.W. Sedat, and P. Walter. 1997. Mitochondrial transmission during mating in *Saccharomyces cerevisiae* is determined by mitochondrial fusion and fission and the intramitochondrial segregation of mitochondrial DNA. *Mol Biol Cell.* 8:1233-42.
- Okamoto, K., and J.M. Shaw. 2005. Mitochondrial morphology and dynamics in yeast and multicellular eukaryotes. *Annu Rev Genet.* 39:503-36.
- Olichon, A., L. Baricault, N. Gas, E. Guillou, A. Valette, P. Belenguer, and G. Lenaers. 2003. Loss of OPA1 perturbs the mitochondrial inner membrane structure and integrity, leading to cytochrome c release and apoptosis. *J Biol Chem.* 278:7743-6.

- Olichon, A., T. Landes, L. Arnaune-Pelloquin, L.J. Emorine, V. Mils, A. Guichet, C. Delettre, C. Hamel, P. Amati-Bonneau, D. Bonneau, P. Reynier, G. Lenaers, and P. Belenguer. 2006. Effects of OPA1 mutations on mitochondrial morphology and apoptosis: Relevance to ADOA pathogenesis. *J Cell Physiol.*
- Ono, T., K. Isobe, K. Nakada, and J.I. Hayashi. 2001. Human cells are protected from mitochondrial dysfunction by complementation of DNA products in fused mitochondria. *Nat Genet.* 28:272-5.
- Palay, S.L. 1956. Synapses in the central nervous system. *J Biophys Biochem Cytol.* 2:193-202.
- Parone, P.A., D.I. James, S. Da Cruz, Y. Mattenberger, O. Donze, F. Barja, and J.C. Martinou. 2006. Inhibiting the mitochondrial fission machinery does not prevent Bax/Bak-dependent apoptosis. *Mol Cell Biol.* 26:7397-408.
- Paumard, P., J. Vaillier, B. Couлары, J. Schaeffer, V. Soubannier, D.M. Mueller, D. Brethes, J.P. di Rago, and J. Velours. 2002. The ATP synthase is involved in generating mitochondrial cristae morphology. *Embo J.* 21:221-30.
- Pedrola, L., A. Espert, X. Wu, R. Claramunt, M.E. Shy, and F. Palau. 2005. GDAP1, the protein causing Charcot-Marie-Tooth disease type 4A, is expressed in neurons and is associated with mitochondria. *Hum Mol Genet.* 14:1087-94.
- Perkins, G., C. Renken, M.E. Martone, S.J. Young, M. Ellisman, and T. Frey. 1997. Electron tomography of neuronal mitochondria: three-dimensional structure and organization of cristae and membrane contacts. *J Struct Biol.* 119:260-72.

- Pilling, A.D., D. Horiuchi, C.M. Lively, and W.M. Saxton. 2006. Kinesin-1 and Dynein are the primary motors for fast transport of mitochondria in *Drosophila* motor axons. *Mol Biol Cell*. 17:2057-68.
- Scorrano, L., M. Ashiya, K. Buttle, S. Weiler, S.A. Oakes, C.A. Mannella, and S.J. Korsmeyer. 2002. A distinct pathway remodels mitochondrial cristae and mobilizes cytochrome c during apoptosis. *Dev Cell*. 2:55-67.
- Sesaki, H., and R.E. Jensen. 1999. Division versus fusion: Dnm1p and Fzo1p antagonistically regulate mitochondrial shape. *J Cell Biol*. 147:699-706.
- Sesaki, H., S.M. Southard, M.P. Yaffe, and R.E. Jensen. 2003. Mgm1p, a dynamin-related GTPase, is essential for fusion of the mitochondrial outer membrane. *Mol Biol Cell*. 14:2342-56.
- Shaw, J.M., and J. Nunnari. 2002. Mitochondrial dynamics and division in budding yeast. *Trends Cell Biol*. 12:178-84.
- Smirnova, E., L. Griparic, D.L. Shurland, and A.M. van der Bliek. 2001. Dynamin-related protein Drp1 is required for mitochondrial division in mammalian cells. *Mol Biol Cell*. 12:2245-56.
- Stowers, R.S., L.J. Megeath, J. Gorska-Andrzejak, I.A. Meinertzhagen, and T.L. Schwarz. 2002. Axonal transport of mitochondria to synapses depends on Milton, a novel *Drosophila* protein. *Neuron*. 36:1063-77.
- Sugioka, R., S. Shimizu, and Y. Tsujimoto. 2004. Fzo1, a protein involved in mitochondrial fusion, inhibits apoptosis. *J Biol Chem*. 279:52726-34.

- Tanaka, Y., Y. Kanai, Y. Okada, S. Nonaka, S. Takeda, A. Harada, and N. Hirokawa. 1998. Targeted disruption of mouse conventional kinesin heavy chain, kif5B, results in abnormal perinuclear clustering of mitochondria. *Cell*. 93:1147-58.
- Tieu, Q., and J. Nunnari. 2000. Mdv1p is a WD repeat protein that interacts with the dynamin-related GTPase, Dnm1p, to trigger mitochondrial division. *J Cell Biol*. 151:353-66.
- Verhoeven, K., K.G. Claeys, S. Zuchner, J.M. Schroder, J. Weis, C. Ceuterick, A. Jordanova, E. Nelis, E. De Vriendt, M. Van Hul, P. Seeman, R. Mazanec, G.M. Saifi, K. Szigeti, P. Mancias, I.J. Butler, A. Kochanski, B. Ryniewicz, J. De Bleecker, P. Van den Bergh, C. Verellen, R. Van Coster, N. Goemans, M. Auer-Grumbach, W. Robberecht, V. Milic Rasic, Y. Nevo, I. Tournev, V. Guergueltcheva, F. Roelens, P. Vieregge, P. Vinci, M.T. Moreno, H.J. Christen, M.E. Shy, J.R. Lupski, J.M. Vance, P. De Jonghe, and V. Timmerman. 2006. MFN2 mutation distribution and genotype/phenotype correlation in Charcot-Marie-Tooth type 2. *Brain*. 129:2093-102.
- Verstreken, P., C.V. Ly, K.J. Venken, T.W. Koh, Y. Zhou, and H.J. Bellen. 2005. Synaptic mitochondria are critical for mobilization of reserve pool vesicles at *Drosophila* neuromuscular junctions. *Neuron*. 47:365-78.
- Vitale, N., A.S. Caumont, S. Chasserot-Golaz, G. Du, S. Wu, V.A. Sciorra, A.J. Morris, M.A. Frohman, and M.F. Bader. 2001. Phospholipase D1: a key factor for the exocytotic machinery in neuroendocrine cells. *Embo J*. 20:2424-34.

- Vogel, F., C. Bornhovd, W. Neupert, and A.S. Reichert. 2006. Dynamic subcompartmentalization of the mitochondrial inner membrane. *J Cell Biol.* 175:237-47.
- Waterham, H., J. Koster, C. van Roermund, P. Mooyer, R. Wanders, and J. Leonard. 2007. A Lethal Defect of Mitochondrial and Peroxisomal Fission. *New England Journal of Medicine*:in press.
- Wurm, C.A., and S. Jakobs. 2006. Differential protein distributions define two sub-compartments of the mitochondrial inner membrane in yeast. *FEBS Lett.* 580:5628-34.
- Zuchner, S., P. De Jonghe, A. Jordanova, K.G. Claeys, V. Guerguelcheva, S. Cherninkova, S.R. Hamilton, G. Van Stavern, K.M. Krajewski, J. Stajich, I. Tournev, K. Verhoeven, C.T. Langerhorst, M. de Visser, F. Baas, T. Bird, V. Timmerman, M. Shy, and J.M. Vance. 2006. Axonal neuropathy with optic atrophy is caused by mutations in mitofusin 2. *Ann Neurol.* 59:276-81.
- Zuchner, S., I.V. Mersiyanova, M. Muglia, N. Bissar-Tadmouri, J. Rochelle, E.L. Dadali, M. Zappia, E. Nelis, A. Patitucci, J. Senderek, Y. Parman, O. Evgrafov, P.D. Jonghe, Y. Takahashi, S. Tsuji, M.A. Pericak-Vance, A. Quattrone, E. Battaloglu, A.V. Polyakov, V. Timmerman, J.M. Schroder, and J.M. Vance. 2004. Mutations in the mitochondrial GTPase mitofusin 2 cause Charcot-Marie-Tooth neuropathy type 2A. *Nat Genet.* 36:449-51.
- Zuchner, S., and J.M. Vance. 2006. Mechanisms of disease: a molecular genetic update on hereditary axonal neuropathies. *Nat Clin Pract Neurol.* 2:45-53.

Figure Legends

Figure 1-1. Mitochondria as dynamic organelles. a. Mitochondrial fusion and fission control mitochondrial number and size. When mitochondria fuse, two mitochondria become a single larger mitochondrion with continuous outer and inner membranes. Conversely, single mitochondrion can divide to form two distinct mitochondria by fission. b. Mitochondria are distributed throughout the cytoplasm by active transport along microtubules and actin in mammalian systems. Distinct molecular motors transport mitochondria in anterograde or retrograde directions. c. Inner membrane dynamics. Cristae are dynamic and can have a variety of different shapes, often in response to the bioenergetic state of the cell. OM, outer membrane; IM, inner membrane; IMS, inner membrane space; IBM, inner boundary membrane; CM, cristae membrane; CJ, cristae junction.

Figure 1-2. Mitochondrial fusion and fission determine morphology. Mitochondrial morphology is determined by the relative rates of mitochondrial fusion and fission. In wild type cells (center), mitochondria form tubules of variable length. In the absence of mitochondrial fusion (left), unopposed fission results in fully fragmented mitochondria. Conversely, decreased fission relative to fusion (right) cause elongated and highly interconnected mitochondria. Drp1 K38A, dominant-negative form of Drp1; Mfn-null, cells lacking Mfn1 and Mfn2; scale bar, 10 μm .

Figure 1-3. Mitochondrial fusion. a. Mitochondrial fusion consists of outer membrane fusion followed by inner membrane fusion. Normally these events occur coordinately. .
b. Dynamin-related proteins Fzo1 and Mgm1 are key molecules in the yeast mitochondrial fusion machinery. Fzo1p is an integral outer-membrane protein with GTPase and heptad repeat domains facing the cytoplasm. Each domain is required for fusion activity. Mgm1 is present on the inner membrane facing the inner membrane space and is proteolytically processed by a rhomboid protease. Both long (l-Mgm1) and short (s-Mgm1) forms are required for mitochondrial fusion. In addition to inner membrane fusion, Mgm1 is required for maintenance of cristae structures. Ugo1 binds to both Fzo1 and Mgm1 and likely coordinates their function. All components are nuclearly encoded. The mitofusin proteins Mfn1 and Mfn2 are the mammalian homologs of Fzo1; OPA1 is the mammalian homolog of Mgm1. No homolog of Ugo1 has been identified.

Figure 1-4. Mitochondrial fission. a. Mitochondrial fission is mediated by the dynamin related protein Dnm1 in yeast. Cytoplasmic Dnm1 localizes to the mitochondrial outer membrane where it oligomerizes into a ring structure that constricts and severs the mitochondrion. In this model, Dnm1 functions in an analogous manner to dynamin in endocytosis. b. Localization of Dnm1 on the mitochondrial outer membrane is mediated by Fis1 and the adaptors Mdv1 and Caf4. Fis1 is an integral outer membrane protein that interacts with the N-terminus of Mdv1 and Caf4. In turn, the WD-40 C-terminal domain of Mdv1 and Caf4 bind to Dnm1. Fis1 and Dnm1 have mammalian homologs (Fis1 and Drp1) but no Mdv1 or Caf4 homologs have been identified.

Figure 1-1

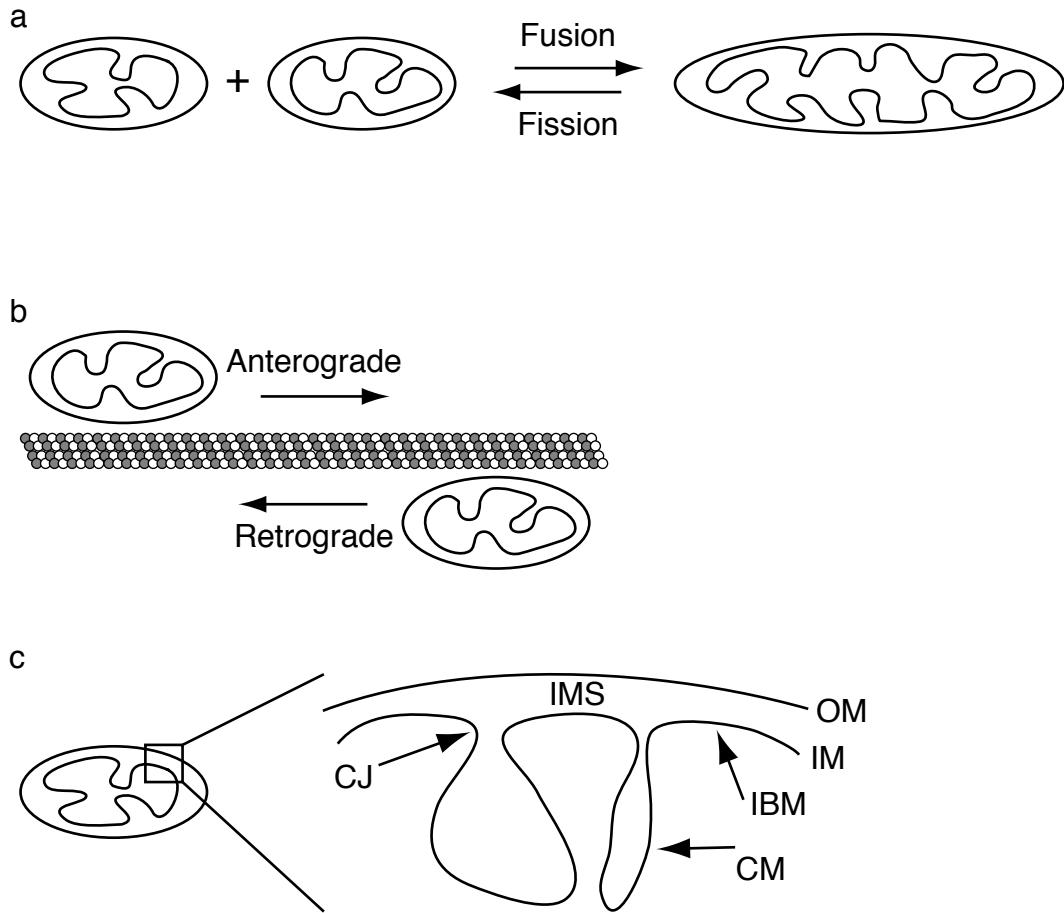


Figure 1-2

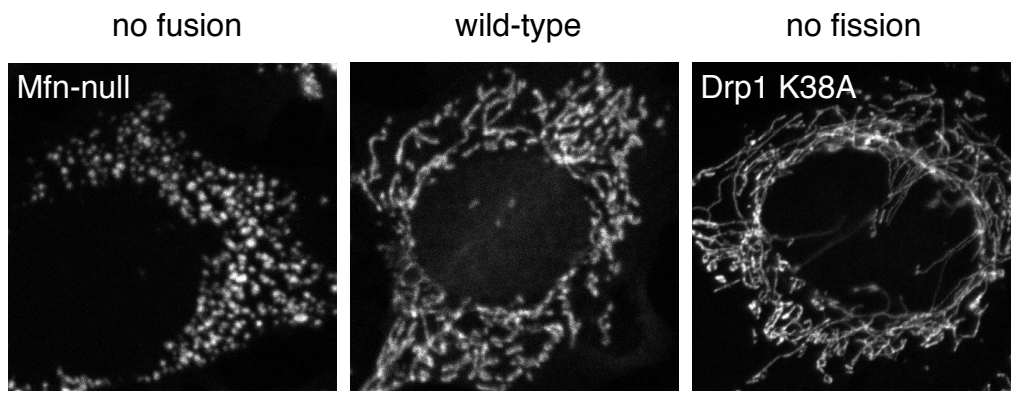


Figure 1-3

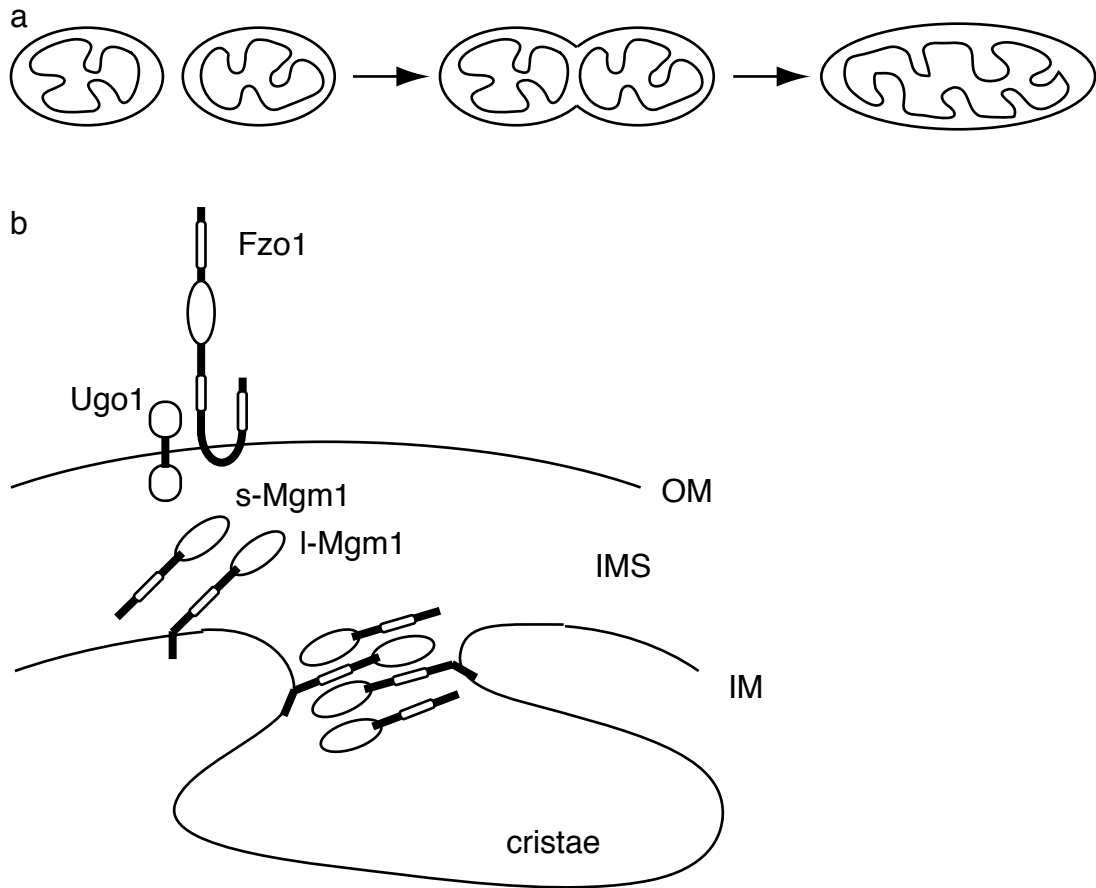
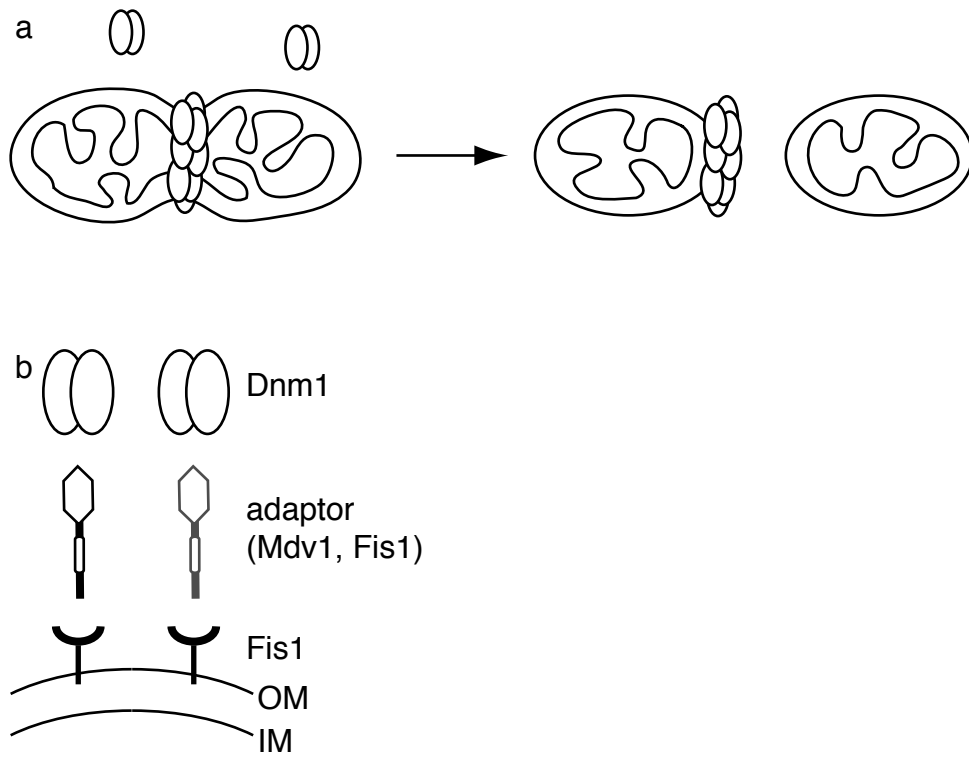


Figure 1-4



Thesis Overview

Chapter 2: Multiple, independent modes of Mitofusin domain interactions are required for mitochondrial fusion

The mitofusin proteins are required for mitochondrial fusion. In this chapter, we describe structure-function and domain interaction analysis of Mitofusin 1 and Mitofusin 2. We find that mitofusins interact extensively via multiple domains and that the GTPase domains and heptad-repeat domains are required for mitofusin function and for specific domain interactions. We characterize an N- and C-terminal mitofusin interaction by co-immunoprecipitation and show that it is disrupted by Charcot-Marie-Tooth disease mutations in Mitofusin 2.

Chapter 3: Complementation between mouse Mfn1 and Mfn2 protects mitochondrial fusion defects caused by CMT2A disease mutations

In this work we functionally characterize Mitofusin 2 alleles that cause the peripheral neuropathy Charcot-Marie-Tooth disease Type 2A. We find that disease alleles can be functional or non-functional for mitochondrial fusion. Significantly, wild-type Mitofusin 1, but not Mitofusin 2, can functionally complement non-functional Mitofusin 2 disease alleles. These results imply that expression of Mitofusin 1 is critical for the cell-type specificity observed in Charcot-Marie-Tooth disease Type 2A.

Chapter 4: Mfn2 disease allele causes gait defects and axonopathy in transgenic mouse model of CMT2A

In this chapter we report the generation of a transgenic mouse model for Charcot-Marie-Tooth disease Type 2A (CMT2A) caused by mutations in Mitofusin 2. We expressed a Mitofusin 2 disease allele in motor neurons and resulting animals mimic CMT2A patients in several regards, including gait impairments, lower limb muscle loss and axonopathy. Mitochondria in motor neurons expressing the transgene are aggregated and poorly distributed and are very likely the basis of the animal phenotype.

Chapter 5: Generation of Mitofusin 2 knock-in mouse models of Charcot-Marie-Tooth Disease Type 2A

In this chapter we report the generation and initial characterization of knock-in mouse models of Charcot-Marie-Tooth disease Type 2A (CMT2A). Using homologous recombination, we generated mice carrying Mitofusin 2 disease alleles L76P or R94Q at the endogenous Mitofusin 2 locus. Thus far, we have not identified defects in heterozygous animals, which are most relevant to the human disease state, but have found severe physiological consequences in animals with altered genomic ratios of wild-type and mutant Mitofusin proteins.

Chapter 6: Future Directions

Here, we briefly discuss future lines of investigation based on the work of the preceding chapters.

Chapter 2

**Multiple Independent Modes of Mitofusin Domain Interactions are Required for
Mitochondrial Fusion**

Scott A. Detmer and David C. Chan

Abstract

Mitofusin 1 and Mitofusin 2 (Mfn1 and Mfn2) are conserved outer mitochondrial membrane proteins required for mammalian mitochondrial fusion. Mfn1 and Mfn2 form homotypic and heterotypic oligomers, but the contributions of the GTPase and heptad repeat domains to these interactions are poorly understood. We identify multiple modes of interaction between Mfn1 and Mfn2 domains including N-terminal and N- and C-terminal interactions. Point mutations in the GTPase or either heptad-repeat domains disrupt domain interactions and result in non-functional full-length molecules. Mfn2 mutations that cause Charcot-Marie-Tooth Disease Type 2A disrupt the N-C interaction between Mfn2 N-C but not between Mfn1 C and Mfn2 N.

Introduction

Mitochondria undergo continuous cycles of fusion and fission and the relative rates of these opposing reactions determine the mitochondrial morphology within a cell. These mitochondrial dynamics are required for the maintenance of mitochondrial function because blocking mitochondrial fusion leads to energetic defects in cells and embryonic lethality in mice (Chen et al., 2005; Chen et al., 2003). Two mammalian mitochondrial fusion factors, Mitofusin2 and OPA1, are mutated in the human neuropathies Charcot-Marie-Tooth Disease type 2A and dominant optic atrophy, respectively (Delettre et al., 2000; Zuchner et al., 2004).

The Mitofusin proteins are required for mitochondrial fusion. Mitofusins are

nuclearly encoded, integral outer mitochondrial membrane proteins. They contain a GTPase domain and two heptad repeat domains, all oriented towards the cytoplasm (Rojo et al., 2002). As such, the mitofusins are perfectly positioned to mediate fusion of the mitochondrial outer membrane. In mammals there are two mitofusins, Mfn1 and Mfn2, and each is sufficient to promote mitochondrial fusion (Chen et al., 2003).

Heptad repeat and GTPase domains are key components in other well-characterized membrane fusion systems. In SNARE mediated fusion, heptad-repeat mediated coiled-coil formation drives membrane apposition and is an early step in the fusion reaction. Associated RAB GTPases are regulatory components of these fusion reactions. Transmitochondrial tethering mediated by Mfn1 heptad-repeat 2 coiled-coil formation is an early step in the fusion pathway (Koshihara et al., 2004). However, it is unclear how tethered mitochondria proceed in the fusion pathway.

Mitofusins are members of the dynamin superfamily. Dynamins are large GTPases that exhibit oligomerization dependent GTPase activity and are involved in a variety of membrane remodeling systems (Praefcke and McMahon, 2004). Dynamin family proteins are known to form complex inter- and intra-molecular interactions. Mfn1 and Mfn2 form both homotypic (Mfn1/Mfn1 and Mfn2/Mfn2) and heterotypic (Mfn1/Mfn2) complexes but the nature of this oligomerization is not well characterized (Chen et al., 2003; Eura et al., 2003).

Studies on the single budding yeast mitofusin homolog, yFzo1, have revealed that the GTPase domain and each heptad repeat domain are required for fusion activity (Griffin and Chan, 2006). Additionally, allelic complementation between distinct non-functional yfzo1 alleles demonstrates that yFzo1p functions as an oligomer (Griffin and

Chan, 2006). In this study we identify non-functional mutations in the GTPase and heptad repeat domains of Mfn1 and Mfn2. We demonstrate that the heptad repeat domains are required for mitofusin domain interactions and that loss-of-function mutations disrupt these domain interactions. We characterize an important mitofusin N- and C-terminal interaction and show that it is disrupted by Charcot-Marie-Tooth disease mutations in Mfn2.

Results

The GTPase and heptad repeat domains are required for Mitofusin function

Cell lines lacking both Mfn1 and Mfn2 (Mfn-null cells) have severely fragmented mitochondrial morphology and are completely deficient for mitochondrial fusion (Chen et al., 2003; Koshiba et al., 2004). Overexpression of either Mfn1 or Mfn2 in Mfn-null cells restores mitochondrial fusion, resulting in tubular mitochondrial morphology (Fig. 1, Fig. 2) (Koshiba et al., 2004). This defines a system for Mitofusin structure-function analysis: express mutant Mitofusin in Mfn-null cells and score the resulting mitochondrial morphology for the presence of tubules. The definitive test for mitochondrial fusion activity is the PEG-induced mitochondrial fusion assay (Chen et al., 2003; Legros et al., 2002); however, we have found excellent agreement between mitochondrial tubulation in Mfn-null cells and mitochondrial fusion activity in the PEG experiment (Detmer and Chan, 2007). It is important to use the Mfn-null cells in this structure-function analysis in contrast to single Mfn1 or Mfn2 deficient cells due to the

potential for complementation between the introduced mutant allele and the remaining endogenous wild-type allele (Detmer and Chan, 2007).

Mitofusins have four identified functional domains: an N-terminal GTPase domain and two heptad-repeat domains separated by a transmembrane domain (Fig. 1A, Fig. 2A). The transmembrane region passes through the outer mitochondrial membrane twice such that both the Mitofusin N- and C-termini face the cytosol (Rojo et al., 2002). We tested the functional importance of the GTPase and heptad-repeat domains by introducing mutations to these regions and testing for the ability of the mutant Mitofusin to tubulate mitochondria in Mfn-null cells. It has previously been reported that the GTPase domain is critical for Mitofusin function in fly, yeast and mammals (Chen et al., 2003; Hales and Fuller, 1997). We have expanded these results by testing additional GTPase mutations. The G1 motif (GxxxxGKS) of the GTPase domain is required for triphosphate nucleotide binding (Bourne et al., 1991). Mutation of either of the adjacent glycine and lysine residues in dynamin resulted in a greatly reduced affinity for GTP such that *in vivo* the mutant dynamin is predicted to be in the *apo* form (Marks et al., 2001). The analogous mutations in Mfn1 (K88A and S89N) result in non-functional alleles (Fig. 1C). Similarly, these G1 motif mutations in Mfn2 (K109A and S110N) are also non-functional (Fig. 2C). Disruption of the G2 motif by the Mfn1 mutation T109A is similarly non-functional (Fig. 1C). In dynamin, this mutation permits GTP binding, but is defective in hydrolysis (Marks et al., 2001). Each of these Mfn1 mutants (K88A, S89N, T109A) localize properly to mitochondria as judged by immunofluorescence and have no effect on the mitochondrial morphology in Mfn-null cells.

We next tested the importance of the heptad-repeat domains (HR1 and HR2) for mitofusin function. Heptad repeats are protein interaction domains that promote oligomerization by coiled-coil formation. Substitution of proline residues within a heptad repeat domain is predicted to preclude coiled-coil formation by disrupting the helical structure. Indeed, a dimeric, anti-parallel coiled-coil has been found to form between Mfn1 HR2 domains and this interaction is disrupted by proline mutations L691P and L705P (Koshiba et al., 2004). Experiments with the yeast mitofusin homolog yFZO1 demonstrate that point mutations in HR1 and HR2 can result in complete loss-of-function molecules (Griffin and Chan, 2006). We have identified two HR1 mutations that disrupt function of Mfn1: L355P is a complete loss-of-function mutation and L380P is partially functional though it is clearly less efficient at tubulating mitochondria than wild-type Mfn1 (Fig. 1C). Both L355P and L380P localize normally to mitochondria. These results are shown with the HR2 mutations described previously for comparison (L691P and L705P, Fig. 1C) (Koshiba et al., 2004). Similarly, we find that substitution of proline residues in Mfn2 HR1 (L411P, L417P) and HR2 (L717P, L724P) results in partial or complete loss-of-function molecules (Fig. 2C).

Non-functional Mitofusin1 point mutants maintain full-length interactions

Mfn1 and Mfn2 form both homotypic and heterotypic oligomers (Chen et al., 2003; Eura et al., 2003). That is, Mfn1/Mfn1, Mfn2/Mfn2 and Mfn1/Mfn2 oligomers are detected in co-immunoprecipitation experiments. It is not known if these complexes represent oligomers formed in cis (on the same mitochondria) or in trans (on opposing

mitochondria, presumably preceding fusion). Nevertheless, the presence of oligomerization domains, the demonstrated Mfn1 C-terminal coiled-coil interaction, and the readily detected interaction between full-length Mitofusins makes it likely that these interactions are relevant to their function. Moreover, allelic complementation studies in yeast demonstrate that the single yeast Mitofusin, yFzo1, functions as an oligomer (Griffin and Chan, 2006).

One mechanism to explain the loss-of-function phenotype in the Mfn1 and Mfn2 point mutants is that they disrupt oligomerization. We tested each of the Mfn1 GTPase and heptad repeat mutants in a co-immunoprecipitation assay for their ability to interact with themselves (Fig. 2). C-terminally Myc- and HA- tagged Mfn1 constructs were co-transfected in 293T cells, cultured for 48 hours, and then lysed and subjected to an anti-Myc immunoprecipitation. As a control for non-specific binding of HA constructs during the immunoprecipitation, we included a transfection that contained no Myc construct. In no case did a non-functional mutation disrupt the interaction between full-length molecules (Fig. 2). This suggests that Mitofusin oligomerization is achieved through multiple, redundant interacting domains.

Mitofusins have multiple, distinct domain interactions

In an effort to dissect the mitofusin domains that mediate the full-length mitofusin interactions, we generated domain fragments and tested them in the co-immunoprecipitation interaction assay. We dissected the mitofusins into their soluble N- and C-terminal fragments such that each fragment lacked transmembrane domain

residues: Mfn1 N (residues 1-579) and C (629-741) and Mfn2 N (1-598) and C (648-758). We previously reported that Mfn1 C could interact both with itself and with Mfn2 C. Here, we report that the Mfn1 N and Mfn2 N constructs can form both homotypic and heterotypic interactions (Fig. 4A). Thus, two distinct and non-overlapping fragments can contribute to mitofusin oligomerization: N-N interactions and C-C interactions.

Two previous reports have demonstrated that the N- and C-terminal domains of Mfn2 interact. In the first, expression of a mitochondrially localized C-terminal construct of Mfn2 containing the transmembrane domain promoted mitochondrial recruitment of an otherwise cytoplasmic N-terminal fragment (Rojo et al., 2002). In the second, co-immunoprecipitation experiments demonstrated that Mfn2 N- and C-terminal constructs could interact and that they depend on an intact GTPase domain (Honda et al., 2005). We sought to extend these observations to Mfn1 and to test for heterotypic N- and C-terminal interactions.

Both Mfn1 and Mfn2 N and C fragments interact with themselves in the co-immunoprecipitation assay (Fig. 4B). This is a much stronger interaction than we find in any other fragment or full-length Mitofusin co-immunoprecipitation experiment. Additionally, we find that the Mfn1 C-terminus interacts strongly with the Mfn2 N-terminus, but that the Mfn2 C-terminus does not interact with the Mfn1 N-terminus (Fig. 4B). This is the only non-reciprocal interaction we detect between Mfn1 and Mfn2 and the functional significance has yet to be determined.

GTPase and HR1/HR2 fragments of yFzo1p have been shown to co-immunoprecipitate and functionally complement each other in yeast (Griffin and Chan, 2006). We tested if analogous constructs of mammalian Mfn1 behaved similarly. Co-

immunoprecipitation experiments between the GTPase and HR1/HR2 fragments of mammalian Mfn1 and Mfn2 resulted in only very weak binding and no functional complementation between these fragments was detected (data not shown). Notably, yFzo1p has an additional N-terminal heptad repeat domain that is not found in the mammalian Mitofusin proteins.

Characterization of Mfn1 N- and C-terminal interaction

Mfn1 HR2 forms a dimeric coiled-coil that can be completely disrupted by the introduction of the L705P mutation in the middle of HR2 (Koshiba et al., 2004). Using the L705P mutation, we sought to confirm that the Mfn1 C-terminus binds to the Mfn1 N-terminus.

First, we found that the Mfn1 C (residues 629-741) binds to full-length Mfn1 (Fig. 5A). This interaction could occur either by the C-terminal fragment binding to the C-terminus or to the N-terminus of the full-length molecule. To remove the former possibility, we tested interaction between Mfn1 C and full-length Mfn1 L705P. We find that Mfn1 C binds to the mutant full-length molecule (Fig. 5A) and conclude that this interaction must be independent of the C-terminus in the full-length molecule. Furthermore, the interaction between Mfn1 C and Mfn1 L705 is consistently stronger than the interaction with wild-type Mfn1 suggesting that the L705P mutation is disrupting an N-terminal binding site in the mutant molecule that is normally occupied by the C-terminus in wild-type molecules. In a control reaction, a C-terminal fragment containing

L705P binds very poorly to wild-type full-length Mfn1, which means that the Mfn1 C interaction with full-length Mfn1 is largely dependent on the HR2 domain.

To determine the sequence requirements of the N- and C- terminal interactions we tested incrementally smaller N-terminal fragments (Fig. 5B). We find little difference in the strength of interaction between the C-terminus binding to the full N-terminus (1-579) and GTPase/HR1 (1-453). However, the C-terminal construct binds to a GTPase domain-only fragment (1-330) significantly less well than it does to the longer fragments. Furthermore, deletion of the first 50 residues of either of the longer N-terminal constructs drastically reduces interaction with the C-terminus (data not shown); this is similar to a previous finding with Mfn2 (Honda et al., 2005).

Mutations in the GTPase, HR1 and HR2 domains disrupt the N-C interaction

To further characterize the Mfn1 N-C interaction, we tested the effect of mutations in the GTPase and heptad-repeat domains in the co-immunoprecipitation assay. For these experiments, we used the Mfn1 N-terminal construct 1-453 as it is the smallest construct found to retain strong interaction with the C-terminus. Loss-of-function proline mutations in HR1 (L355P and L380P) and HR2 (L691P and L705P) strongly disrupt the N- and C-terminal interaction (Fig. 5C). Together, these data provide indirect evidence for an HR1-HR2 interaction as mutation of either domain greatly reduces binding. We were unable to test for an HR1-HR2 interaction directly as all HR1 constructs we tested were expressed at only very low levels.

GTPase domain mutations in the Mfn1 1-453 construct also disrupt the N- and C-terminal interaction, though to a lesser extent than the HR1 or HR2 mutations. The G1 mutations (K88A and S89N) have an intermediate decrease in the interaction compared to wild-type and the HR point mutations. The G2 mutation (T109A), though a non-functional mutation in full-length Mfn1, appears to have only a modest effect on the N-C interaction. In Mfn2, a G1 mutation (K109A) has a more severe effect on the N-C interaction (Fig. 7A, B).

Mfn1 C-GTPase domain interaction

The C-terminus of Mfn1 (629-741) interacts with the GTPase domain (1-330) much more weakly than it does with the GTPase/HR1 domain (1-453) (Fig. 5B). We reasoned that this binding might represent a different mode of interaction due to the absence of HR1. Indeed, we found that a shorter HR2-only Mfn1 C-terminal fragment (660-737) did not interact with the GTPase domain fragment (Fig. 6B). Furthermore, HR2 proline mutations L691P and L705P did not disrupt the interaction between the longer C-terminal fragment (629-741) and the GTPase domain (Fig. 6B). Together, these data demonstrate that the relatively weak interaction in Mfn1 between the C-terminus and the GTPase-only domain does not depend on HR2. This mode of interaction is likely responsible for the weak binding observed between the Mfn1 C L705P and full-length Mfn1 (Fig. 5A).

We examined the residues between 629 and 660 and found several well-conserved charged residues in Mitofusin proteins (Fig. 6A). We tested the importance of

these conserved charged residues by mutating them to alanine and testing them in the Mfn1 C-GTPase domain interaction. Mutations E639A, K643A and K653A each disrupted the C-GTPase interaction (Fig. 6C). In contrast, K638A and R640A had no effect on the interaction. None of these mutations affected the C-GTPase/HR1 interaction (data not shown).

Having found an interaction defect, we asked if these charged residues are functionally important. We made the charge mutations in full-length Mfn1 molecules and tested them in Mfn-null and wild-type cells (Fig. 6D-G). All of the mutant full-length molecules localized normally to mitochondria and only K643A has clear functional consequence. Mfn1 K643A is non-functional for mitochondrial fusion when expressed in Mfn-null cells (Fig. 6D-E). Further, it causes dramatic fragmentation of mitochondria when expressed in wild-type cells (Fig. 6F-G). Thus, Mfn1 K643A is a non-functional allele that has dominant mitochondrial fragmentation activity.

Mfn2 CMT2A alleles disrupt N-C interaction

Mutations in Mfn2 cause Charcot-Marie-Tooth disease type 2A (CMT2A), a peripheral neuropathy that results in loss of the longest motor and sensory neurons. Over 40 missense mutations have been reported in Mfn2 thus far and the majority of these cluster in and around the GTPase domain and in HR1 and HR2 (Zuchner et al., 2004). Only a subset of the mutant Mfn2 alleles have been functionally characterized, and these include alleles that are functional and non-functional for mitochondrial fusion (Detmer and Chan, 2007). A majority of these alleles cause mitochondrial aggregation when

overexpressed in neurons or fibroblasts (Baloh et al., 2007; Detmer and Chan, 2007). We tested if the Mfn2 CMT2A mutations had an effect on the Mfn2 N-C interaction. Four of the nine CMT2A alleles tested (L76P, R94W, T105M, P251A) are defective in the N-C interaction. The reduction in binding with these CMT2A mutations is comparable to the low level of binding found with the designed Mfn2 GTPase mutation K109A. The remaining CMT2A alleles (V69F, R94Q, R274Q, R280H, W740S) interact at levels similar to wild-type fragments. The ability to interact in the N-C interaction assay does not completely correlate with the CMT2A allele function. Alleles V69F, R274Q, and W740S are functional and do interact, whereas R94W, T105M and P251A are non-functional and do not interact. However, L76P is a functional allele that does not interact and R94Q and R280H are non-functional alleles that do interact. It is surprising that mutations R94Q and R94W, both of which are non-functional, have different interaction properties.

We next tested whether the Mfn2 N-terminal CMT2A mutant constructs could interact with Mfn1 C. In this assay, the GTPase mutation K109A and CMT2A mutation T105M have clearly reduced interactions. However, the remaining CMT2A alleles retain wild-type or significant levels of interaction.

Discussion

This study confirms and extends the functional importance of the GTPase and heptad-repeat domains of Mfn1 and Mfn2. Specifically, mutation of any of these

domains can result in a non-functional molecule. Moreover, the heptad-repeat mutations can be linked to disruption of specific domain interactions within the Mitofusins.

Mitofusin oligomerization is clearly complex as there are multiple modes of interaction between non-overlapping fragments. For Mfn1, the N-terminus can interact with itself, the C-terminus can interact with itself, and the N- and C-termini can interact with each other. Furthermore, there is the capacity for significant cross-interaction between Mfn1 and Mfn2 through the formation of N-N, C-C and N-C interactions. These extensive hetero-interactions strongly suggest that when Mfn1 and Mfn2 are both present in a cell they function coordinately and are likely required for the observed complementation between wild-type Mfn1 and non-functional Mfn2 mutants (Detmer and Chan, 2007).

We find that the C-terminus of Mfn1 interacts strongly with an N-terminal GTPase/HR1 fragment and that this interaction is disrupted by loss-of-function proline mutations in either HR1 or HR2. These results imply an HR1-HR2 interaction. We have been unable to test this prediction directly as all of the HR1 constructs we made expressed very poorly. Mfn1 HR2 is known to dimerize with itself to form an anti-parallel coiled-coil (Koshiba et al., 2004). The possibilities that (1) an HR2 dimer could interact with HR1 to form a larger helical bundle or that (2) HR2 could alternatively interact with itself or with HR1 are intriguing. In either case, it seems likely that the GTPase domain could regulate such interactions. First, GTPase domain point mutations designed to decrease GTP binding in Mfn1 and Mfn2 disrupt the N-C interaction. Second, GTPase domain point mutations behave distinctly from an N-terminal truncation that removes the GTPase domain. This construct (residues 331-741) causes

mitochondrial aggregation that likely represents tethered mitochondria that cannot proceed to fusion in the absence of the GTPase domain (Koshihara et al., 2004). Thus, there is likely a structural requirement for the GTPase domain in addition to its enzymatic activity.

We find that four of the nine Mfn2 CMT2A alleles tested are defective in the Mfn2 N-C interaction. However, there is an imperfect correlation between Mfn2 CMT2A alleles that can interact in the N-C assay and that are functional for mitochondrial fusion. Most surprising is allele L76P which is functional but does not interact; this result suggests that the N-C interaction is not strictly required for mitofusin function. However, Mfn2 L76P does induce mitochondrial aggregation, even at low expression level (Baloh et al., 2007; Detmer and Chan, 2007). When we test for Mfn1 C binding to CMT2A allele Mfn2 N we find that seven of eight constructs interact well. Only Mfn2 N T105M does not interact with Mfn1 C. Interestingly, T105M is the only Mfn2 CMT2A allele that is not complemented by Mfn1 in trans (Detmer and Chan, 2007).

In addition to the N-C interaction, we find a distinct interaction between Mfn1 C and a GTPase-only construct. This interaction is weaker than the GTPase/HR1 interaction, is independent of HR2 and requires charged residues between the transmembrane domain and HR2. Mutation K643A disrupts the Mfn1 C-GTPase interaction. In full-length Mfn1, K643A is non-functional for mitochondrial fusion and causes mitochondrial fragmentation when expressed in wild-type cells. The K643A mutation does not disrupt the C-GTPase/HR1 interaction yet has significant functional

effects, suggesting that this region of Mfn1 has a critical interaction with the GTPase domain.

Dynamins are large proteins with extensive intra- and inter-molecular interactions. Though Mitofusins are most closely related to dynamins in the GTPase domain, they also share a similar domain structure and organization (Praefcke and McMahon, 2004). It remains to be determined if mitofusins, like dynamins, have assembly-dependent regulation of GTPase activity and if the C-terminus can function as a GTPase effector domain. Future structural and biochemical studies of the N- and C-terminal fragments will be required to precisely define these interactions as well as the enzymatic and functional consequences relating to mitofusin activity in mitochondrial membrane fusion.

Experimental Procedures

Cloning

The mitofusin 7xMyc and 3xHA constructs were described previously (Chen et al., 2003). Point mutations were introduced by PCR with primers encoding the mutations to Mfn1-7xMyc or Mfn2-7xMyc constructs in pcDNA3.1. Mfn1 and Mfn2 fragments were generated by PCR and cloned into 7xMyc or 3xHA pcDNA3.1 vectors. In both cases, the entire region amplified by PCR was verified by sequencing. Full-length mutant constructs were subcloned into retroviral pCLBW constructs for functional testing.

Cell culture and retroviral transduction

Wild-type MEFs were cultured in DMEM supplemented with 10% BCS, l-glutamine and Pen/Strep (all from Gibco). Mfn-null MEFs were cultured as above, but with 10% FCS. Retroviral supernatants were generated as described (Chen et al., 2003). All infections were completed at low multiplicity of infection to limit the level of overexpression (Detmer and Chan, 2007). Cells were processed for immunofluorescence approximately one week after retroviral infection.

Immunofluorescence

Immunofluorescence against Myc-tagged mitofusins has been described previously (Chen et al., 2003). 9E10 primary antibody and Cy3-conjugated secondary antibody was used to detect the Myc epitope in fixed cells grown on coverslips. Imaging was achieved on a Zeiss Pascal laser scanning confocal microscope with a Pan NeoFluar 63x oil immersion objective (N.A. 1.25) and controlled by Zeiss LSM v3 software. Images were resized in Adobe Photoshop CS.

Co-immunoprecipitation

1.8 micrograms of DNA of Myc and HA pcDNA3.1 constructs were transfected to 293T cells in 6 well plates using calcium phosphate. Media was replaced twelve hours post-transfection and 36 hours later cells were processed. Cells were lysed in 400 microliters lysis buffer (1X TBS, 1% TX-100, 4mM MgCl₂, and 1X protease inhibitor cocktail (Roche)). Post-nuclear lysates were immunoprecipitated with 9E10 antibody coupled to protein A sepharose beads. HA.11 (Covance) and 9E10 antibodies were used

for immunoblotting. All gels have immunoprecipitated material at 14 times the relative load of lysate.

References

- Baloh, R.H., R.E. Schmidt, A. Pestronk, and J. Milbrandt. 2007. Altered axonal mitochondrial transport in the pathogenesis of Charcot-Marie-Tooth disease from mitofusin 2 mutations. *J Neurosci.* 27:422-30.
- Bourne, H.R., D.A. Sanders, and F. McCormick. 1991. The GTPase superfamily: conserved structure and molecular mechanism. *Nature.* 349:117-27.
- Chen, H., A. Chomyn, and D.C. Chan. 2005. Disruption of fusion results in mitochondrial heterogeneity and dysfunction. *J Biol Chem.* 280:26185-92.
- Chen, H., S.A. Detmer, A.J. Ewald, E.E. Griffin, S.E. Fraser, and D.C. Chan. 2003. Mitofusins Mfn1 and Mfn2 coordinately regulate mitochondrial fusion and are essential for embryonic development. *J Cell Biol.* 160:189-200.
- Delettre, C., G. Lenaers, J.M. Griffoin, N. Gigarel, C. Lorenzo, P. Belenguer, L. Pelloquin, J. Grosgeorge, C. Turc-Carel, E. Perret, C. Astarie-Dequeker, L. Lasquellec, B. Arnaud, B. Ducommun, J. Kaplan, and C.P. Hamel. 2000. Nuclear gene OPA1, encoding a mitochondrial dynamin-related protein, is mutated in dominant optic atrophy. *Nat Genet.* 26:207-10.
- Detmer, S.A., and D.C. Chan. 2007. Complementation between mouse Mfn1 and Mfn2 protects mitochondrial fusion defects caused by CMT2A disease mutations. *J Cell Biol.* 176:405-414.
- Eura, Y., N. Ishihara, S. Yokota, and K. Mihara. 2003. Two mitofusin proteins, mammalian homologues of FZO, with distinct functions are both required for mitochondrial fusion. *J Biochem (Tokyo).* 134:333-44.

- Griffin, E.E., and D.C. Chan. 2006. Domain interactions within Fzo1 oligomers are essential for mitochondrial fusion. *J Biol Chem.* 281:16599-606.
- Hales, K.G., and M.T. Fuller. 1997. Developmentally regulated mitochondrial fusion mediated by a conserved, novel, predicted GTPase. *Cell.* 90:121-9.
- Honda, S., T. Aihara, M. Hontani, K. Okubo, and S. Hirose. 2005. Mutational analysis of action of mitochondrial fusion factor mitofusin-2. *J Cell Sci.* 118:3153-61.
- Koshihara, T., S.A. Detmer, J.T. Kaiser, H. Chen, J.M. McCaffery, and D.C. Chan. 2004. Structural basis of mitochondrial tethering by mitofusin complexes. *Science.* 305:858-62.
- Legros, F., A. Lombes, P. Frachon, and M. Rojo. 2002. Mitochondrial fusion in human cells is efficient, requires the inner membrane potential, and is mediated by mitofusins. *Mol Biol Cell.* 13:4343-54.
- Marks, B., M.H. Stowell, Y. Vallis, I.G. Mills, A. Gibson, C.R. Hopkins, and H.T. McMahon. 2001. GTPase activity of dynamin and resulting conformation change are essential for endocytosis. *Nature.* 410:231-5.
- Praefcke, G.J., and H.T. McMahon. 2004. The dynamin superfamily: universal membrane tubulation and fission molecules? *Nat Rev Mol Cell Biol.* 5:133-47.
- Rojo, M., F. Legros, D. Chateau, and A. Lombes. 2002. Membrane topology and mitochondrial targeting of mitofusins, ubiquitous mammalian homologs of the transmembrane GTPase Fzo. *J Cell Sci.* 115:1663-74.
- Zuchner, S., I.V. Mersiyanova, M. Muglia, N. Bissar-Tadmouri, J. Rochelle, E.L. Dadali, M. Zappia, E. Nelis, A. Patitucci, J. Senderek, Y. Parman, O. Evgrafov, P.D. Jonghe, Y. Takahashi, S. Tsuji, M.A. Pericak-Vance, A. Quattrone, E. Battaloglu,

A.V. Polyakov, V. Timmerman, J.M. Schroder, and J.M. Vance. 2004. Mutations in the mitochondrial GTPase mitofusin 2 cause Charcot-Marie-Tooth neuropathy type 2A. *Nat Genet.* 36:449-51.

Figure Legends

Figure 2-1. Structure-function analysis of Mfn1. A. Schematic of Mfn1, with domains and mutations (HR, heptad repeat; TM, transmembrane). Position of domains indicated by residue numbers below schematic. B. Representative images of Mfn1-Myc constructs expressed in Mfn-null cells by retroviral infection. Mitochondria are labeled with EGFP (green) and Mfn1 is labeled by immunofluorescence against the Myc epitope (red). Scale bar = 10 micrometers. C. Quantitation of mitochondrial morphology in Mfn-null cells expressing wild-type and mutant Mfn1-Myc. At least 150 cells were scored for each infection; morphology was scored blind.

Figure 2-2. Structure-function analysis of Mfn2. A. Domain structure of Mfn2, as in Fig. 1, with mutations indicated. B. Representative images of Mfn2-Myc constructs expressed in Mfn-null cells. C. Quantitation of mitochondrial morphology in Mfn-null cells expressing wild-type and mutant Mfn2-Myc. At least 150 cells scored, blind.

Figure 2-3. Co-immunoprecipitation of full-length Mfn1 mutants. Myc- and HA-tagged Mfn1 point mutants were co-transfected in 293T cells. Anti-Myc immunoprecipitates (labeled Myc IP) and post-nuclear lysates (labeled lysate) were analyzed by Western blot with anti-Myc (9E10) and anti-HA (HA.11) antibodies. The relative load of immunoprecipitates was 14 times that of lysates. The positions of molecular weight markers (in kDa) are indicated.

Figure 2-4. Mitofusin N-N and N-C domain interactions. Co-immunoprecipitation as described in Fig 3. A. Mfn1 N-terminal construct (1N), residues 1-579. Mfn2 N-terminal construct (2N), residues 1-598. B. Mfn1 C-terminal construct (1C), residues 629-741. Mfn2 C-terminal construct (2C), residues 648-758. N-terminal constructs as in A.

Figure 2-5. Characterization of Mfn1 N-C interaction. Co-immunoprecipitation as described in Fig 3. A. Mfn1 C-terminal construct (C-Myc, residues 629-741), wild-type (wt) or L705P, co-immunoprecipitations with Mfn1 full length (full length-HA, residues 1-741), wild-type and L705P. B. C-Myc co-immunoprecipitations with Mfn1 N-terminal constructs (N-fragment-HA) of indicated residues. Construct 1-579 includes the full N-terminus until the TM domain; construct 1-453 includes the GTPase and HR1 domains; construct 1-330 includes only the GTPase domain. C. C-Myc co-immunoprecipitations with Mfn1 N-terminal construct (1-453-HA) with point mutations as indicated.

Figure 2-6. Characterization of non-HR N-C interaction. A. Alignment of Mfn1 C-terminal region between TM and HR2. Non-conserved residues are highlighted in black. Conserved charged mutations at indicated positions are boxed. B. Co-immunoprecipitations as described in Fig. 3 between Mfn1 C-terminal constructs (Mfn1 C-Myc) of indicated residues and Mfn1 GTPase domain (Mfn1 1-330-HA). C. Co-immunoprecipitations between Mfn1 C-terminal construct (Mfn1 629-741-Myc) and Mfn1 GTPase domain. D and F. Quantitation of mitochondrial morphology in Mfn-null cells (D) and wild-type cells (F) expressing full-length Mfn1-7xMyc with charge point

mutations. E and G. Representative image of an Mfn-null cell (E) and wild-type cell (G) expressing Mfn1 K643A 7xMyc. Immunofluorescence as described in Fig 1, 2. Scale bar = 10 micrometers.

Figure 2-7. Mfn2 CMT2A disease mutations disrupt N-C interaction. Co-immunoprecipitations as described in Fig 3. A. Mfn2 C-terminal constructs (Mfn2 C-Myc, residues 648-758) co-immunoprecipitations with Mfn2 N-terminal constructs (Mfn2 N-HA, residues 1-598). Constructs are wild-type (wt) or contain a designed GTPase mutation (K109A) or CMT2A point mutations as indicated. B. Mfn1 C-terminal construct (Mfn1 C-Myc, residues 629-741) co-immunoprecipitations with Mfn 2 N-HA constructs.

Figure 2-1

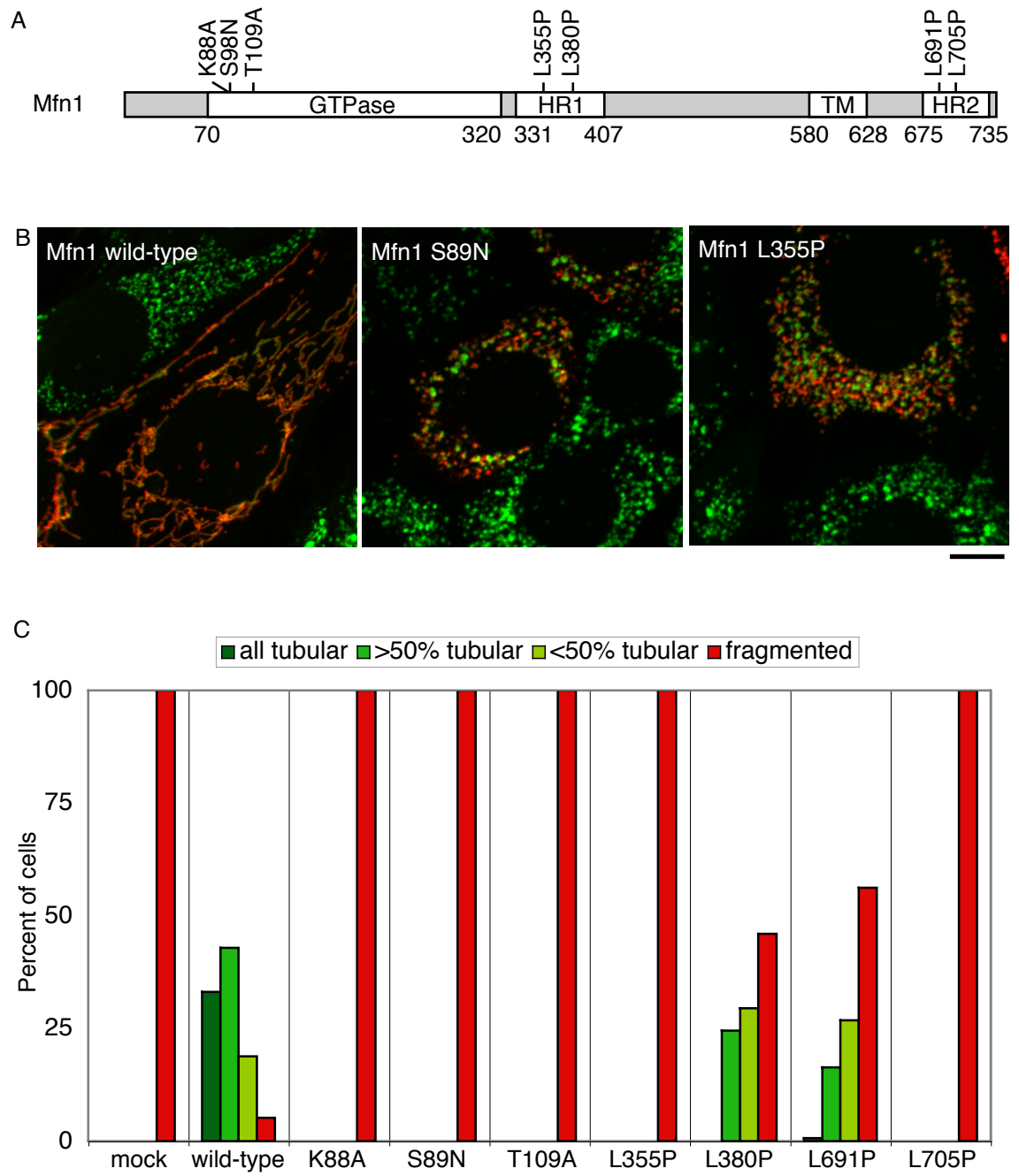


Figure 2-2

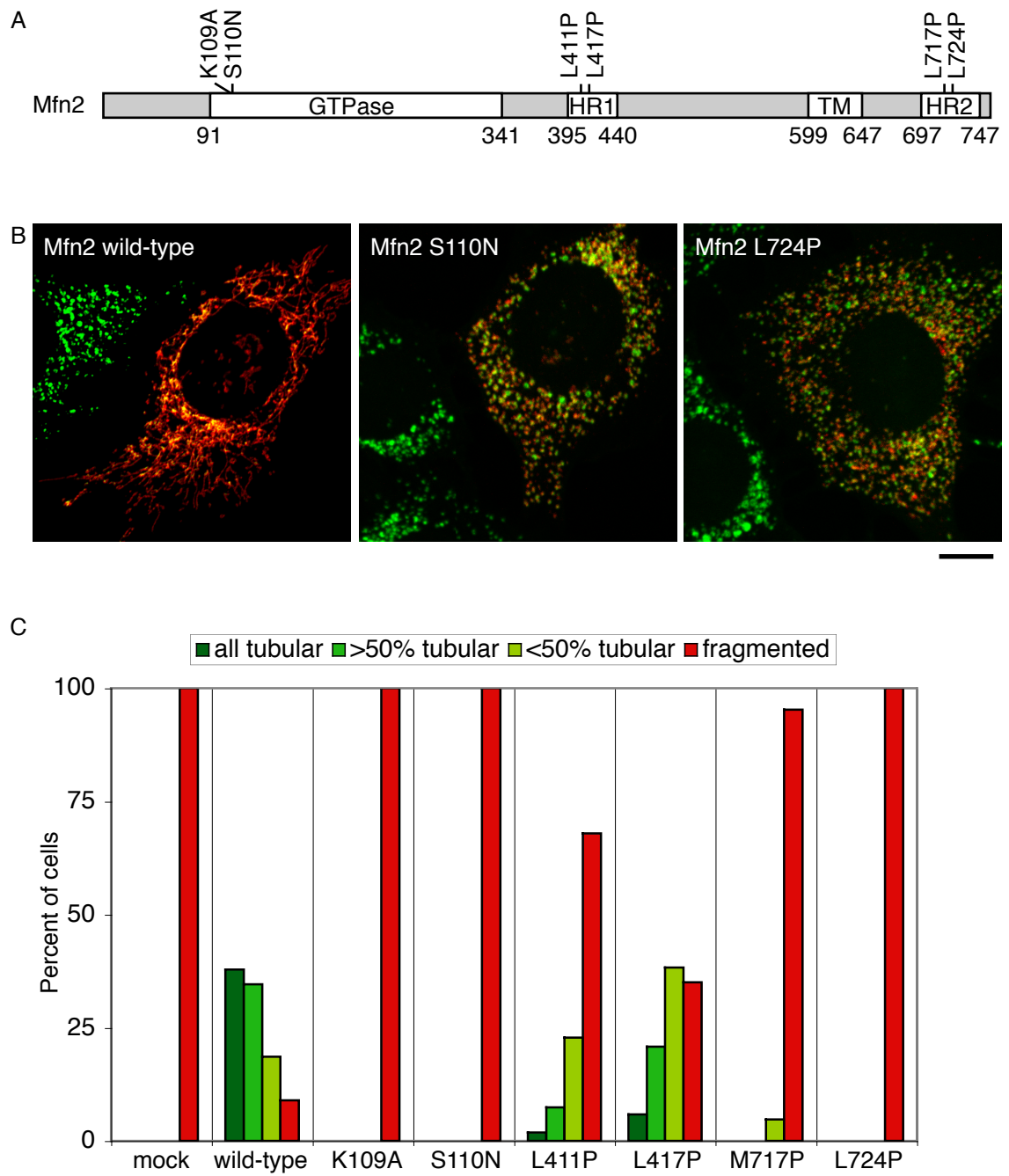


Figure 2-3

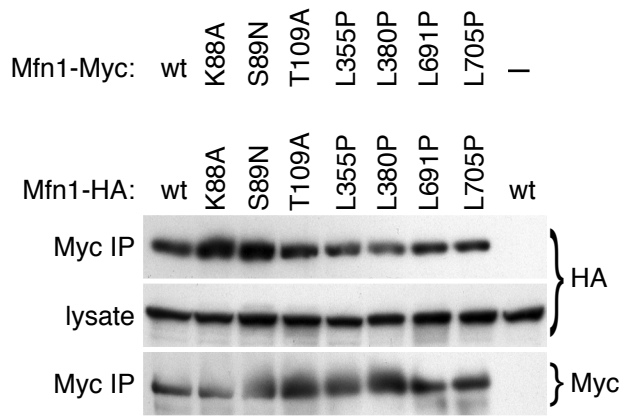


Figure 2-4

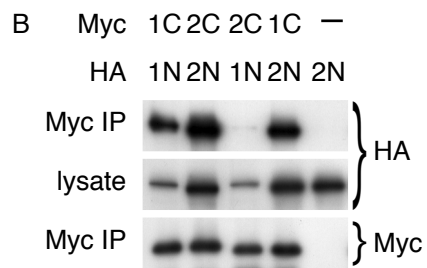
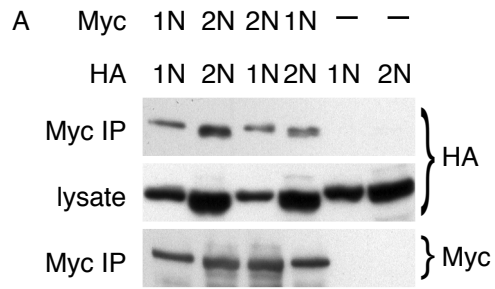


Figure 2-5

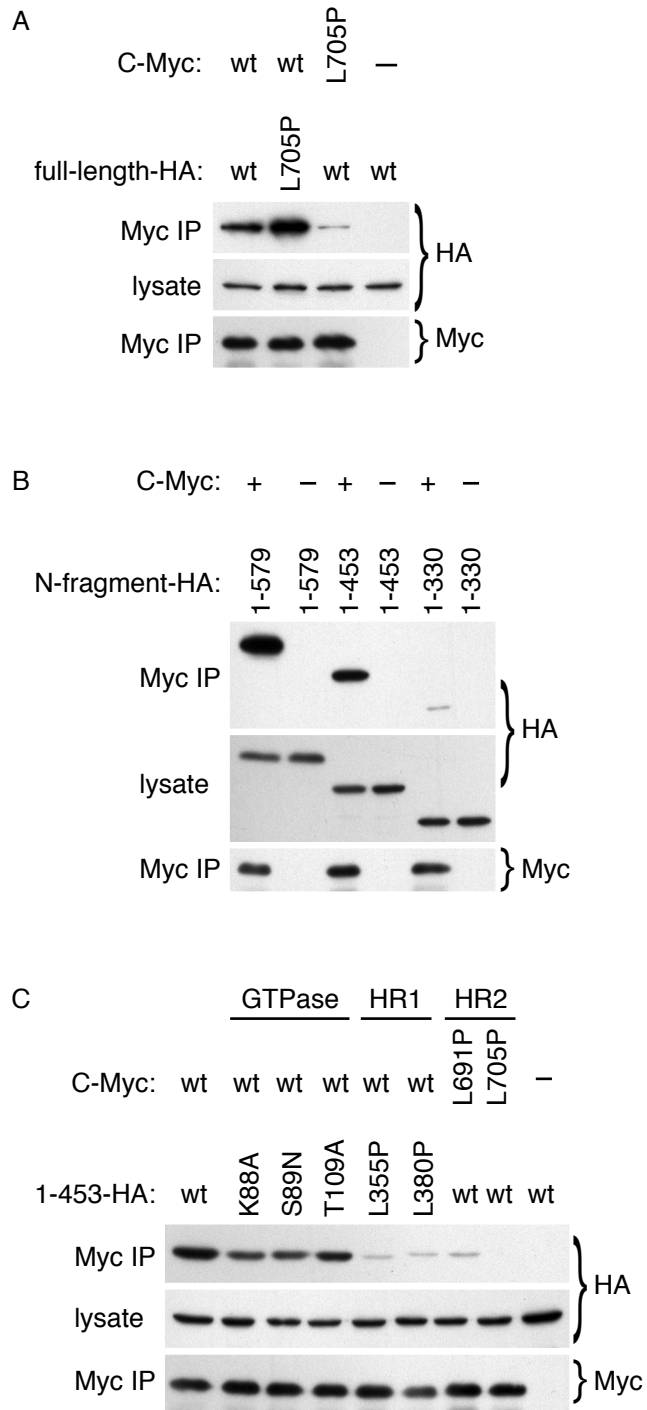


Figure 2-6

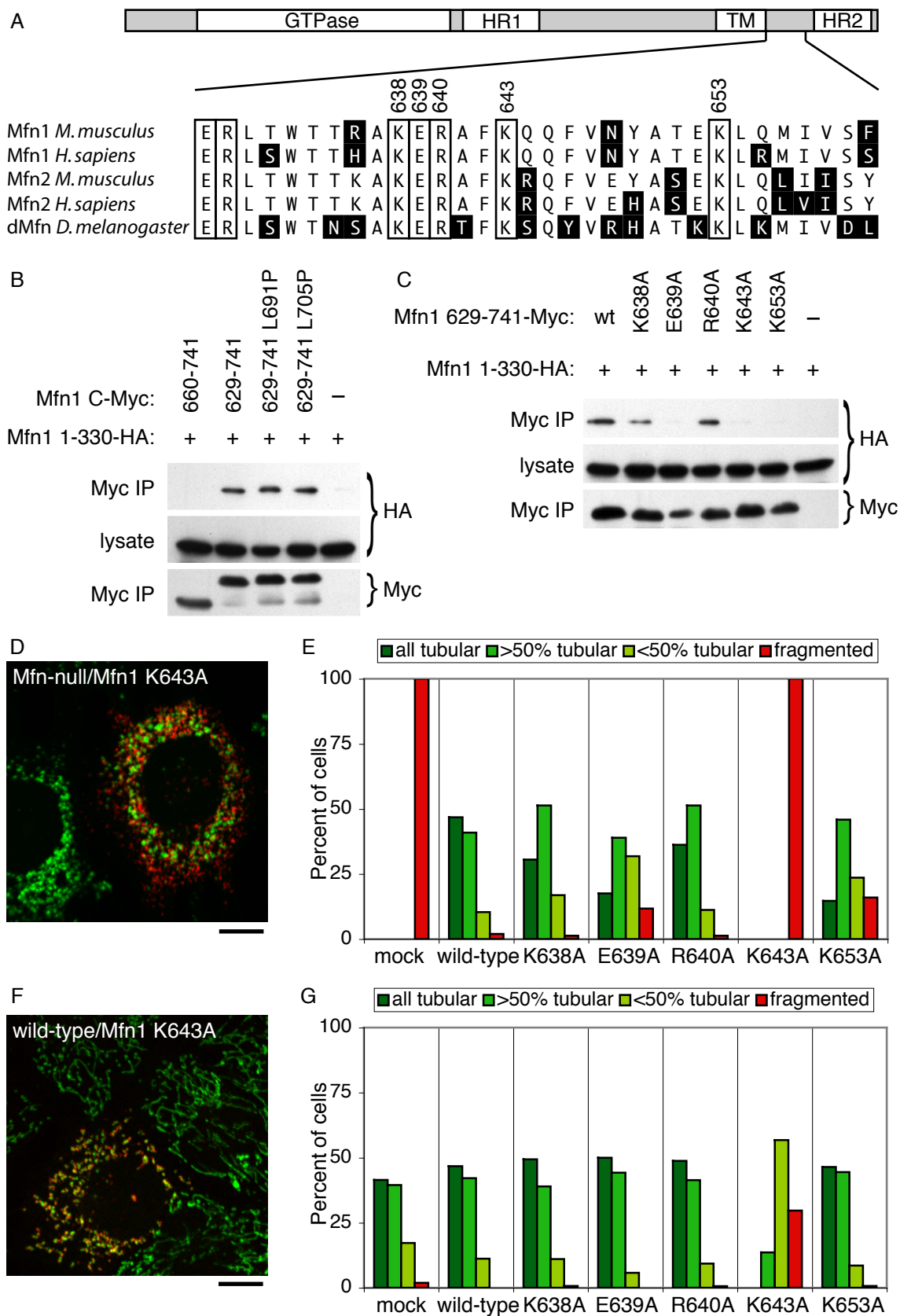
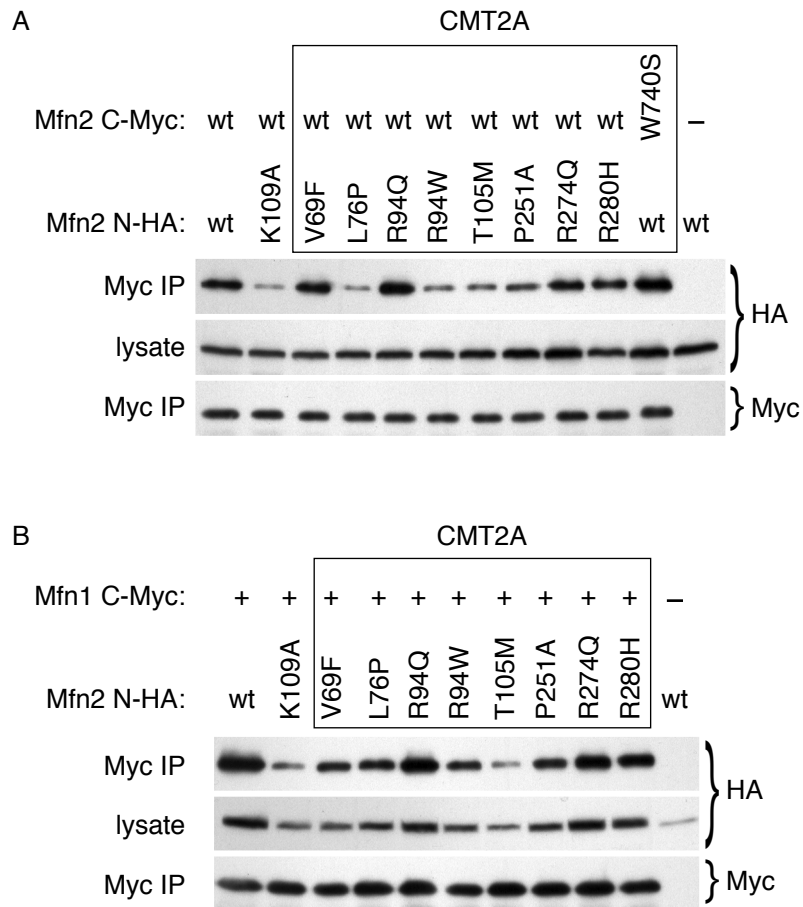


Figure 2-7



Chapter 3

Complementation Between Mouse Mfn1 and Mfn2 Protects Mitochondrial Fusion Defects Caused by CMT2A Disease Mutations

Scott A. Detmer and David C. Chan

This chapter has been published in the *Journal of Cell Biology* (2007) 176: 405-414.

Complementation between mouse Mfn1 and Mfn2 protects mitochondrial fusion defects caused by CMT2A disease mutations

Scott A. Detmer and David C. Chan

Division of Biology, California Institute of Technology, Pasadena, CA 91125

Mfn2, an oligomeric mitochondrial protein important for mitochondrial fusion, is mutated in Charcot-Marie-Tooth disease (CMT) type 2A, a peripheral neuropathy characterized by axonal degeneration. In addition to homooligomeric complexes, Mfn2 also associates with Mfn1, but the functional significance of such heterooligomeric complexes is unknown. Also unknown is why Mfn2 mutations in CMT2A lead to cell type-specific defects given the widespread expression of Mfn2. In this study, we show that homooligomeric complexes formed by many Mfn2 disease mutants are nonfunctional for mitochondrial fusion.

However, wild-type Mfn1 complements mutant Mfn2 through the formation of heterooligomeric complexes, including complexes that form in trans between mitochondria. Wild-type Mfn2 cannot complement the disease alleles. Our results highlight the functional importance of Mfn1–Mfn2 heterooligomeric complexes and the close interplay between the two mitofusins in the control of mitochondrial fusion. Furthermore, they suggest that tissues with low Mfn1 expression are vulnerable in CMT2A and that methods to increase Mfn1 expression in the peripheral nervous system would benefit CMT2A patients.

Introduction

Mitofusins are mitochondrial outer membrane GTPases required for mitochondrial fusion (Chan, 2006). Although yeast have one mitofusin, Fzo1 (Okamoto and Shaw, 2005), mammals contain two mitofusins, Mfn1 and Mfn2 (Santel and Fuller, 2001; Rojo et al., 2002; Chen et al., 2003). In the absence of either Mfn1 or Mfn2, cells have greatly reduced levels of mitochondrial fusion, and the imbalance of fusion and fission events leads to mitochondrial fragmentation (Chen et al., 2003). In the absence of both Mfn1 and Mfn2, no mitochondrial fusion can occur, leading to severe mitochondrial and cellular dysfunction (Chen et al., 2005). Moreover, mitochondrial dynamics play an important role in apoptosis (Youle and Karbowski, 2005), and maintenance of mitochondrial fusion has been linked to protection against apoptosis (Olichon et al., 2003; Sugioka et al., 2004; Neuspiel et al., 2005).

Mutations in Mfn2 cause Charcot-Marie-Tooth disease (CMT) type 2A, an autosomal dominant peripheral neuropathy (Zuchner et al., 2004). Most types of CMT disease involve

Schwann cell dysfunction, resulting in the demyelination of peripheral nerves. However, CMT2A is an axonal form in which the axons of the longest sensory and motor nerves are selectively affected (Zuchner and Vance, 2005). There is currently no effective treatment for this disease. Interestingly, another neurodegenerative disease, dominant optic atrophy, is caused by mutations in OPA1 (Alexander et al., 2000; Delettre et al., 2000), a mitochondrial intermembrane space protein that is also necessary for mitochondrial fusion. The sensitivity of neurons to mutations in Mfn2 and OPA1 suggests that such cells are particularly dependent on mitochondrial dynamics, which likely impacts the recruitment of mitochondria to extended neuronal processes (Chen and Chan, 2006). Indeed, the disruption of mitochondrial dynamics has been experimentally linked to neuronal dysfunction (Stowers et al., 2002; Li et al., 2004; Guo et al., 2005; Verstreken et al., 2005).

Several issues regarding mitofusin function and its relation to neurodegenerative disease remain poorly understood. First, it is unclear to what extent there is functional interplay between Mfn1 and Mfn2 during mitochondrial fusion. In experiments with Mfn1- or Mfn2-null cells, either mitofusin can functionally replace the other, indicating functional redundancy (Chen et al., 2003, 2005). However, some studies

Correspondence to David C. Chan: dchan@caltech.edu

Abbreviations used in this paper: CMT, Charcot-Marie-Tooth disease; ES, embryonic stem; MEF, mouse embryonic fibroblast; PEG, polyethylene glycol.

The online version of this article contains supplemental material.

suggest distinct pathways or mechanisms for Mfn1 versus Mfn2 (Cipolat et al., 2004; Ishihara et al., 2004). OPA1 action has been reported to depend on Mfn1 but not Mfn2 (Cipolat et al., 2004). An in vitro study indicates that overexpressed Mfn1 is more effective than Mfn2 in tethering mitochondria, an effect that is correlated with a higher rate of GTP hydrolysis for Mfn1 (Ishihara et al., 2004). Second, Mfn1 and Mfn2 have been shown to physically associate with each other (Chen et al., 2003; Eura et al., 2003), but the functional significance of such heterooligomeric complexes is poorly understood. Finally, it is unknown why Mfn2 mutations in CMT2A cause such highly cell type-specific defects. Patients with CMT2A show deficits in the longest sensory and motor peripheral nerves, with a subset showing additional degeneration in the optic nerve (Zuchner and Vance, 2005). The length-dependent degeneration of peripheral nerves likely reflects an inherent challenge of neurons to supply functional mitochondria to the nerve terminals, but it remains unclear why primarily the peripheral and optic nerves are affected.

In this study, we have analyzed Mfn2 disease alleles that cause CMT2A. We find that most of these mutants are not functional for fusion when allowed to form only homotypic complexes. However, these Mfn2 mutants can be complemented

through the formation of heterotypic complexes with wild-type Mfn1. These results emphasize the close interplay between Mfn1 and Mfn2 in the mitochondrial fusion reaction, demonstrate the functional importance of Mfn1–Mfn2 heterooligomeric complexes, and provide insights into the pathogenesis of Mfn2-dependent neuropathy.

Results

Many Mfn2 CMT2A alleles fail to rescue mitochondrial morphology in double Mfn-null cells

We have previously generated mouse embryonic fibroblast (MEF) cell lines with null mutations in both Mfn1 and Mfn2 (double Mfn-null cells; Koshiba et al., 2004; Chen et al., 2005). These cell lines enable straightforward structure-function analysis of mouse mitofusins. Human and mouse Mfn2 are 95% identical, and all of the residues that were found mutated in the original CMT2A study (Zuchner et al., 2004) are conserved in mouse Mfn2. In the present study, we introduced nine of the originally reported point mutations into mouse Mfn2; these include mutations occurring immediately before the GTPase domain (V69F and L76P), within the GTPase domain (R94Q, R94W,

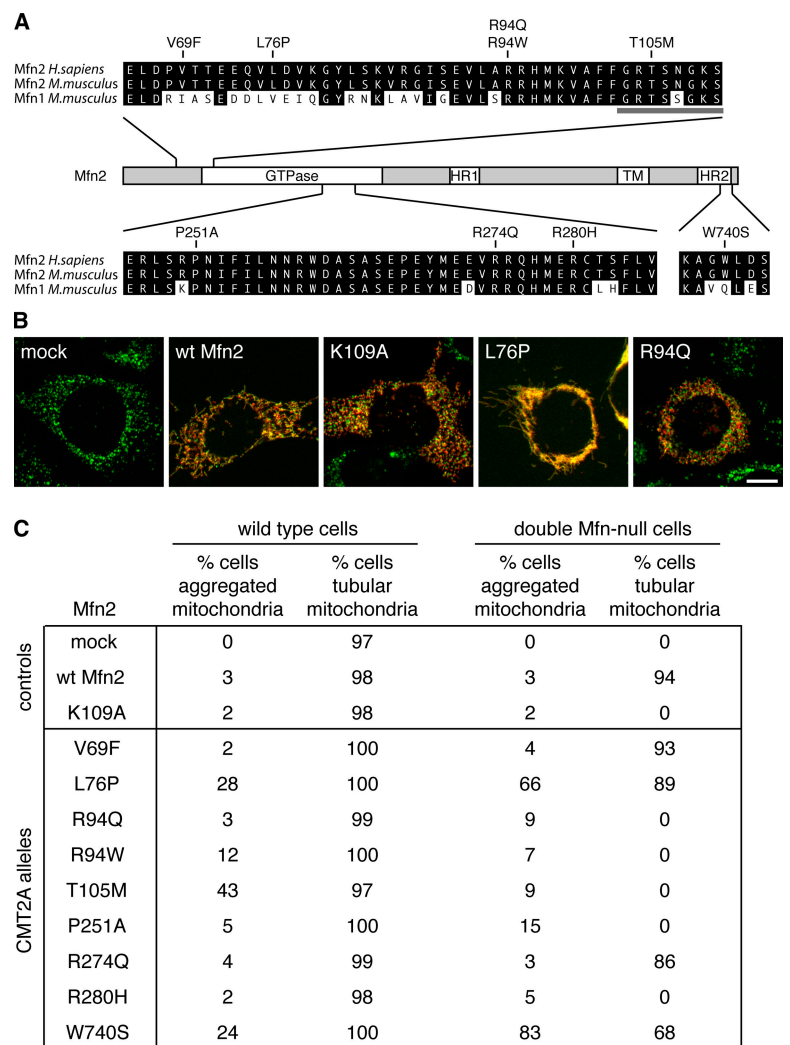


Figure 1. Functional analysis of Mfn2 CMT2A alleles. (A) Domain structure of Mfn2 with the GTPase, hydrophobic heptad repeat (HR), and transmembrane regions (TM) indicated. A sequence alignment of human Mfn2 with mouse Mfn2 and Mfn1 is shown for the regions surrounding CMT2A point mutations. Note that the residues mutated in CMT2A disease are conserved between human and mouse Mfn2. The horizontal gray bar indicates the GTPase G1 motif. (B) Representative images of double Mfn-null cells expressing myc-tagged Mfn2 at a low multiplicity of infection. Mitochondria are visualized by matrix-targeted EGFP (green), and Mfn2-expressing cells are identified by immunofluorescence against the myc epitope (red). Note mitochondrial aggregation induced by the CMT2A allele L76P. Bar, 10 μ m. (C) Summary of mitochondrial profiles when Mfn2 CMT2A alleles are expressed in wild-type MEFs (left two columns) and double Mfn-null MEFs (right two columns). In each case, infected cells were scored for mitochondrial morphology, and the three categories of tubular mitochondria (Fig. S1, A and B; available at <http://www.jcb.org/cgi/content/full/jcb.200611080/DC1>) were added to yield the percentage of cells with tubular mitochondria. Mitochondrial aggregation was independently scored. More than 150 cells were scored for each experiment. As additional reference points, using the same scoring criteria, we find that 0% of Mfn1-null cells and 10% of Mfn2-null cells have tubular mitochondria (see controls in Fig. 6, C and D).

T105M, P251A, R274Q, and R280H), and in a C-terminal heptad repeat region (W740S; Fig. 1 A). By expressing these disease alleles in wild-type and double Mfn-null MEFs, we could assess their subcellular localization, effects on mitochondrial morphology, and ability to mediate mitochondrial fusion.

Mock-infected wild-type MEFs have a range of mitochondrial profiles, but the vast majority of cells show considerable amounts of tubular mitochondria (Fig. 1 C and Fig. S1 A, available at <http://www.jcb.org/cgi/content/full/jcb.200611080/DC1>). The expression of wild-type Mfn2 or the GTPase mutant Mfn2^{K109A} by retroviral transduction did not affect mitochondrial morphology. We found that all of the CMT2A mutants properly localized to mitochondria as determined by immunofluorescence. However, seven of the nine CMT2A alleles (all except Mfn2^{V69F} and Mfn2^{R274Q}) caused substantial mitochondrial aggregation when cells were infected at a high multiplicity of infection (Fig. S2). At low infection rates, most infected cells have only one proviral copy and express about fourfold Mfn2 compared with endogenous Mfn2 in wild-type cells (Fig. S3). Under these conditions, only Mfn2^{L76P}, Mfn2^{T105M}, and Mfn2^{W740S} caused high levels of mitochondrial aggregation (Fig. 1 C). In contrast, such mitochondrial aggregation was not found in cells expressing wild-type Mfn2 and was found only in a few cells expressing Mfn2^{K109A}. This mitochondrial aggregation phenotype may reflect the aberration of Mfn2 function by CMT2A mutations; however, the effect is clearly dosage dependent and is not observed at physiological expression levels (see Fig. 4). Therefore, its relevance to CMT2A disease remains to be determined.

To evaluate the Mfn2 CMT2A alleles for mitochondrial fusion activity, we expressed them in double Mfn-null cells. Cells lacking mitofusins are fully deficient for mitochondrial fusion and show completely fragmented mitochondrial morphology (Chen et al., 2005). The expression of wild-type Mfn2 restored mitochondrial fusion, resulting in tubular mitochondrial morphology (Fig. 1, B and C; and Fig. S1 B). In contrast, the GTPase mutant Mfn2^{K109A} behaved as a complete loss of

function allele, showing no ability to restore mitochondrial tubules. The CMT2A mutants Mfn2^{R94Q}, Mfn2^{R94W}, Mfn2^{T105M}, Mfn2^{P251A}, and Mfn2^{R280H} are similarly unable to promote mitochondrial tubules in double Mfn-null cells. In contrast, cells expressing Mfn2^{V69F}, Mfn2^{L76P}, Mfn2^{R274Q}, or Mfn2^{W740S} showed a considerable restoration of mitochondrial tubules. Therefore, more than half of the CMT2A mutants are nonfunctional.

Nonrescuing CMT2A alleles lack mitochondrial fusion activity

To definitively evaluate the fusion activity of CMT2A alleles, we tested them in a polyethylene glycol (PEG) mitochondrial fusion assay. In this assay, double Mfn-null cells containing either mitochondrially targeted EGFP or mito-DsRed were each infected with retrovirus expressing a CMT2A allele. Hybrids between the two cell lines were scored for mitochondrial fusion. Cell hybrids that formed between double Mfn-null cells or cells expressing Mfn2^{K109A} never showed mitochondrial fusion (Fig. 2). In contrast, the expression of wild-type Mfn2 resulted in extensive mitochondrial fusion: 75% of the cell hybrids exhibited a complete overlay of EGFP and DsRed (scored as full fusion) or a nearly complete overlay with some singly labeled mitochondria remaining (scored as extensive fusion). 20% of these hybrids had no colabeled mitochondria (scored as no fusion) and invariably had fragmented mitochondria. These hybrids likely arose from uninfected cells. When clonal infected cell lines were used (Koshiba et al., 2004), all cell hybrids showed extensive mitochondrial fusion.

We found excellent agreement between the ability of a CMT2A allele to restore mitochondrial tubules to double Mfn-null cells and their fusion activity in the PEG assay. The Mfn2 CMT2A alleles Mfn2^{V69F}, Mfn2^{L76P}, Mfn2^{R274Q}, and Mfn2^{W740S} induced fluorophore mixing as efficiently as wild-type Mfn2, indicating that they are highly functional. In contrast, mutants Mfn2^{R94Q}, Mfn2^{R94W}, Mfn2^{T105M}, Mfn2^{P251A}, and Mfn2^{R280H} were all completely deficient for mitochondrial fusion. Interestingly, the five nonfunctional alleles are all in positions that are

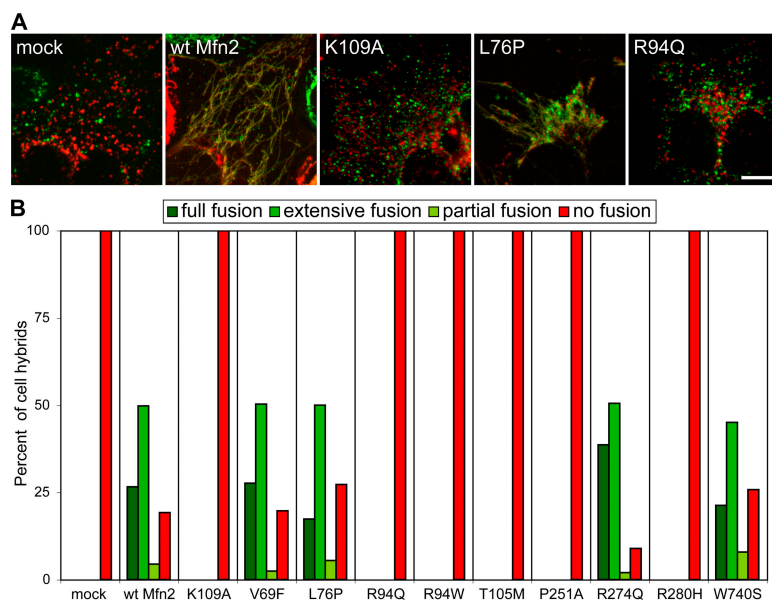


Figure 2. **Lack of mitochondrial fusion activity in many CMT2A alleles.** Double Mfn-null cells expressing either mito-DsRed or mito-EFG were infected with the same Mfn2 construct. The PEG fusion assay was used to evaluate mitochondrial fusion activity in cell hybrids formed from such cells. (A) Representative merged images of cell hybrids. No fusion is detected with mock-, Mfn2^{K109A}-, or Mfn2^{R94Q}-infected cells. Extensive fusion is observed with wild-type Mfn2 and Mfn2^{L76P}. Bar, 10 μ m. (B) Quantitation of mitochondrial fusion in cell hybrids. More than 200 cell hybrids were scored per experiment.

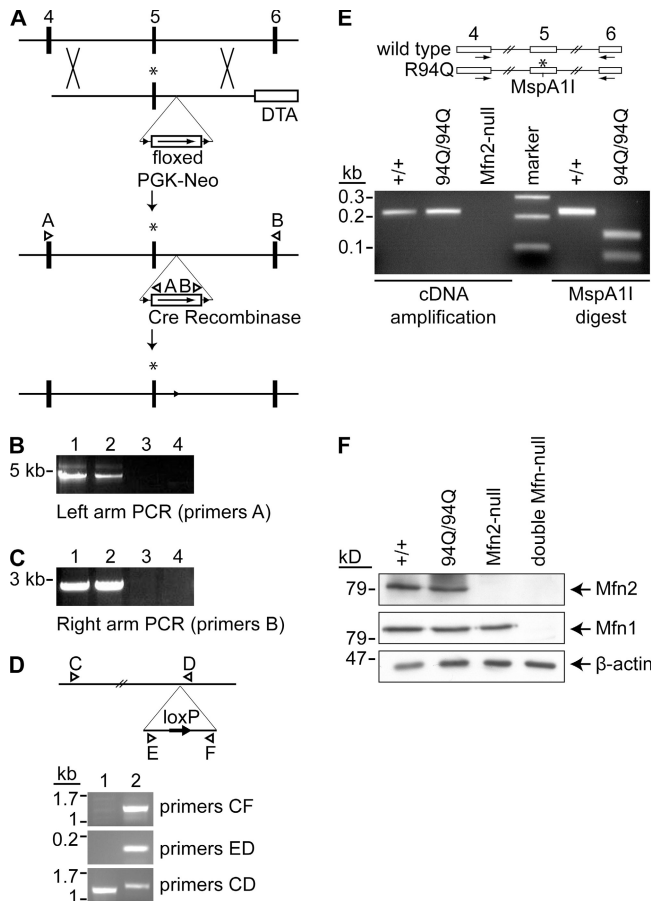


Figure 3. Construction of MEFs containing homozygous *Mfn2*^{R94Q} knockin mutations. (A) Schematic of *Mfn2* targeting construct and strategy. A portion of the *Mfn2* genomic locus containing exons 4–6 is shown on top based on Ensembl transcript ID ENSMUST0000030884 (www.ensembl.org). The knockin targeting vector below contains the R94Q mutation (*) placed in exon 5 as well as a floxed neomycin cassette for positive selection and a diphtheria toxin cassette (DTA) for negative selection. Homologous recombination in ES cells leads to the configuration in the third line, which can be detected by PCR using the A and B pairs of primers (triangles), as shown in B and C. Mice were generated with the targeted ES cells, and Cre recombination in vivo was used to excise the neomycin cassette, leading to the bottom configuration containing the R94Q mutation and *loxP* scar (arrowhead). (B) PCR screen of ES cells using primer set A for detection of the correct targeting of the left arm. Four ES cell clones are shown; the first two clones are positive. Because the 5' primer is outside the targeting construct, only correctly targeted clones will yield the desired PCR product. (C) PCR screen of ES cells using primer set B for detection of the correct targeting of the right arm. The same two ES cell clones are positive. Note that the 3' primer is outside the targeting construct. (D) PCR screen of *Mfn2* genomic structure after in vivo Cre-mediated excision of the PGK-neomycin cassette. Excision leaves behind a 140-bp *loxP* scar as diagrammed. Three sets of PCR reactions were used to confirm the presence of the *loxP* scar in *Mfn2*^{R94Q} homozygous MEFs (lane 2) but not wild-type MEFs (lane 1). (E) Genotype assay for *Mfn2* transcripts. The schematic on top shows the genomic *Mfn2* locus containing exons 4–6. Exon 5 encodes residue 94. A cDNA fragment was amplified using the indicated primers in exons 4 and 6. cDNA amplification and restriction digestion was performed on first-strand cDNA from wild-type (+/+), *Mfn2*^{R94Q} homozygous, and *Mfn2*-null cells. In the *Mfn2*^{R94Q} cDNA, the engineered R94Q mutation (*) introduces an *MspA11* site, resulting in cleavage of the 233-bp PCR product into 146- and 87-bp fragments. (F) Expression of Mfn1 and the *Mfn2*^{R94Q} allele at endogenous levels. Postnuclear whole cell lysates from the indicated MEFs were separated by SDS-PAGE and immunoblotted with an anti-Mfn2 (top) or Mfn1 antibody (middle). β-actin was used as a loading control (bottom).

conserved between Mfn1 and Mfn2. Three of the four functional alleles are in nonconserved positions.

Endogenous Mfn1 functionally complements the CMT2A mutant *Mfn2*^{R94Q} to induce mitochondrial fusion

Our PEG fusion assays showed that *Mfn2*^{R94Q}, along with four other CMT2A alleles, has no mitochondrial fusion activity in double *Mfn*-null cells. This allele is particularly interesting because position 94 is the most commonly mutated residue found in CMT2A. Multiple clinical studies have found familial or de novo mutations of residue 94 to either Q or W (Zuchner et al., 2004, 2006; Kijima et al., 2005; Chung et al., 2006; Verhoeven et al., 2006). To definitively study the in vivo properties of this allele, we used homologous recombination to place the R94Q mutation into the endogenous mouse *Mfn2* locus in embryonic stem (ES) cells (Fig. 3, A–D). For positive selection, the targeting construct contained a neomycin expression cassette flanked by *loxP* sites. After the generation of mice containing the knockin allele, Cre-mediated recombination was used to excise the neomycin cassette in vivo, resulting in an *MFN2* locus containing the R94Q mutation and a short *loxP* scar located in the adjacent intron (Fig. 3, A and D). We mated mice heterozygous for the *Mfn2*^{R94Q} allele, and homozygous embryos were used to derive *Mfn2*^{R94Q} homozygous MEF cell lines.

Our molecular analyses indicate that these cell lines express no wild-type *Mfn2* while expressing endogenous levels of *Mfn2*^{R94Q} (Fig. 3, E and F). To confirm the expression of *Mfn2*^{R94Q} in these cell lines, we used RT-PCR to analyze *Mfn2* RNA transcripts. We amplified exon 5 (which encodes residue 94) and the adjoining sequences of *Mfn2* cDNA by PCR. The presence of the R94Q mutation within the amplified cDNA fragment was diagnosed by digestion with the restriction enzyme *MspA11*, which cuts uniquely at a site introduced by the R94Q mutation. As expected, the cDNA fragment was amplified from cDNA of wild-type and *Mfn2*^{R94Q} homozygous cells but not *Mfn2*-null cells (Fig. 3 E). The cDNA from wild-type cells is completely resistant to *MspA11* digestion, whereas the cDNA from *Mfn2*^{R94Q} homozygous cells was completely digested by *MspA11*, demonstrating that all *Mfn2* transcripts contain the R94Q mutation. Having confirmed mRNA expression of the mutant allele, we next confirmed protein expression. Immunoblot analysis indicated that endogenous levels of Mfn1 and Mfn2 are present in wild-type and *Mfn2*^{R94Q} homozygous cell lines (Fig. 3 F).

Given that *Mfn2*^{R94Q} has no fusion activity in double *Mfn*-null cells (Figs. 1 and 2), we expected *Mfn2*^{R94Q} homozygous cells to have fragmented mitochondria similar to those found in *Mfn2*-null cells (Chen et al., 2003, 2005). Surprisingly, the scoring of mitochondrial profiles indicated that most *Mfn2*^{R94Q} homozygous cells have predominantly tubular mitochondria; this is in striking contrast to *Mfn2*-null cells, which have extensive mitochondrial fragmentation (Fig. 4, A and B). In addition, we did not find any mitochondrial aggregation in the *Mfn2*^{R94Q} homozygous cell line.

Therefore, although *Mfn2*^{R94Q} behaves as a null allele when expressed in double *Mfn*-null cells, it is clearly highly functional in our homozygous knockin cells. In evaluating these results, it is important to consider the total complement

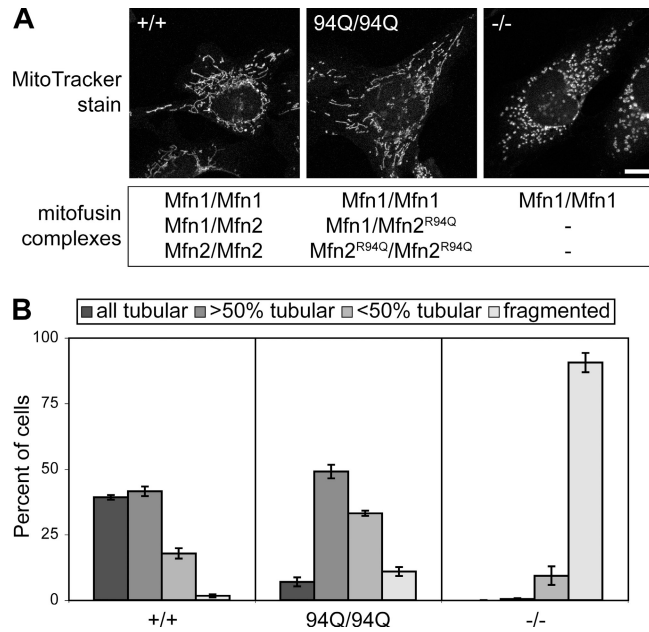


Figure 4. **Tubular mitochondria in Mfn2^{R94Q}-Mfn2^{R94Q} cells.** (A) Representative images of mitochondrial morphology in wild-type (+/+), Mfn2^{R94Q}-Mfn2^{R94Q}, and Mfn2-null (-/-) cells. Mitochondria were visualized by MitoTracker red staining. Below each cell, the potential mitofusin oligomers are listed. Bar, 10 μ m. (B) Quantitation of mitochondrial morphology. For each cell line, 100 cells were scored in three independent experiments. Error bars indicate SD.

of mitofusins in each cellular context because Mfn1 and Mfn2 can form both homooligomeric (Mfn1-Mfn1 or Mfn2-Mfn2) and heterooligomeric (Mfn1-Mfn2) complexes (Chen et al., 2003; Eura et al., 2003). When Mfn2^{R94Q} is expressed in double Mfn-null cells, only Mfn2^{R94Q}-Mfn2^{R94Q} homooligomeric complexes can be formed, and such complexes are clearly inactive for mitochondrial fusion. In Mfn2^{R94Q} homozygous knockin cells, endogenous Mfn1 is still present (Fig. 3 F). Therefore, three possible complexes can be formed: Mfn1-Mfn1, Mfn1-Mfn2^{R94Q}, and Mfn2^{R94Q}-Mfn2^{R94Q} (Fig. 4 A). The phenotype of Mfn2-null cells (which contain only Mfn1-Mfn1 homooligomeric complexes) indicates that endogenous levels of Mfn1-Mfn1 complexes alone are not sufficient to promote tubular mitochondria. Given that Mfn2^{R94Q}-Mfn2^{R94Q} complexes are nonfunctional (Fig. 2), these results strongly suggest that Mfn2^{R94Q} can cooperate with Mfn1 to form Mfn1-Mfn2^{R94Q} complexes capable of promoting fusion.

Mfn2 CMT2A mutants physically associate with wild-type Mfn1 and Mfn2

If this model of complementation is correct, Mfn2^{R94Q} should be able to physically associate with wild-type Mfn1. We tested whether the Mfn2 CMT2A mutants could coimmunoprecipitate with wild-type Mfn1 and Mfn2. In MEFs, all of the Mfn2 CMT2A mutants associated with Mfn1 at normal levels with the exception of Mfn2^{T105M}, which showed lower levels (Fig. 5 A). Similarly, the Mfn2 CMT2A mutants associated with Mfn2, although at slightly reduced levels compared with wild-type Mfn2. Again, Mfn2^{T105M} had low binding. It should be noted that when analogous immunoprecipitation experiments were performed in transfected 293T cells, the reduction in Mfn2^{T105M} binding was subtle (unpublished data). Therefore, although Mfn2^{T105M} has reduced binding to wild-type Mfn1 and Mfn2, this defect is not observed at high expression levels. The engineered GTPase mutant Mfn2^{K109A}, which interacted strongly with Mfn1, interacted poorly with Mfn2. These results suggest that the mutant Mfn2 molecules can interact with wild-type Mfn1 and Mfn2 and can potentially participate in or modify the fusion reaction.

Mfn1 but not Mfn2 complements CMT2A alleles to induce mitochondrial fusion

To learn more about the complementation of Mfn1 and Mfn2^{R94Q} and whether this is a unique property of the Mfn2^{R94Q} allele, we tested all of the nonfunctional Mfn2 CMT2A alleles for complementation with wild-type Mfn1 and Mfn2. We expressed alleles Mfn2^{R94Q}, Mfn2^{R94W}, Mfn2^{T105M}, Mfn2^{P251A}, and Mfn2^{R280H} in either Mfn2- or Mfn1-null cells and scored mitochondrial profiles. Most Mfn2-null cells have fragmented mitochondrial morphology, with only ~13% of the cells having short mitochondrial tubules. The expression of wild-type Mfn2 in these cells restores normal tubular mitochondrial morphology (Fig. 6, A and C). Remarkably, the expression of each of the five CMT2A alleles into Mfn2-null cells resulted in extensive mitochondrial tubulation. The GTPase mutant Mfn2^{K109A} was also able to induce mitochondrial tubulation, although its effect was considerably weaker than that of the CMT2A alleles. Because Mfn2-null cells contain Mfn1, the expression of CMT2A alleles in Mfn2-null cells results in the formation of three possible complexes: Mfn1-Mfn1, Mfn1-Mfn2^{CMT2A}, and Mfn2^{CMT2A}-Mfn2^{CMT2A} (Fig. 6 A). These results strongly support and generalize our interpretation of the Mfn2^{R94Q} homozygous

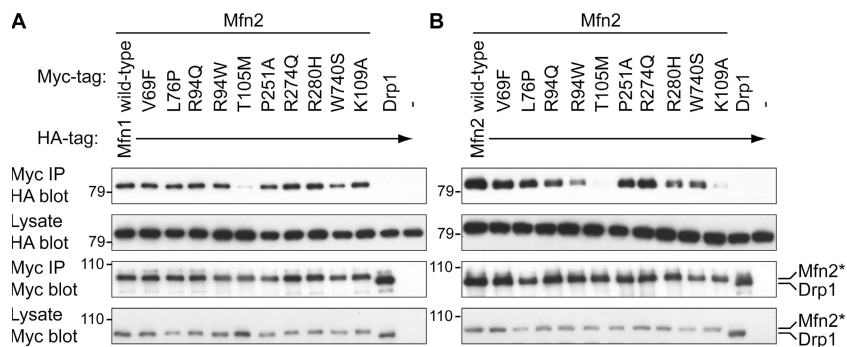


Figure 5. **Physical association of mutant Mfn2 with wild-type Mfn1 and Mfn2.** (A) Myc-tagged Mfn2 mutants were expressed in double Mfn-null cell lines stably expressing HA-tagged Mfn1. Anti-myc immunoprecipitates (myc IP) and postnuclear lysates (lysate) were analyzed by Western blotting with anti-myc and anti-HA antibodies. Mock (-) or Drp1-myc-infected cells were used as negative controls. The relative load of the immunoprecipitates was 14 times that of the lysates. (B) Same as in A except performed in double Mfn-null cell lines stably expressing HA-tagged Mfn2. Positions of the Mfn2-myc and Drp1-myc bands and positions of molecular mass markers (given in kilodaltons) are indicated.

knockin cell line: Mfn2 disease alleles can cooperate with Mfn1 to promote fusion activity. This activity is likely mediated by Mfn1–Mfn2^{CMT2A} heterooligomers. Because even mutant Mfn2^{K109A} shows a low level of complementation with Mfn1, Mfn2 need not have GTPase activity to cooperate with Mfn1.

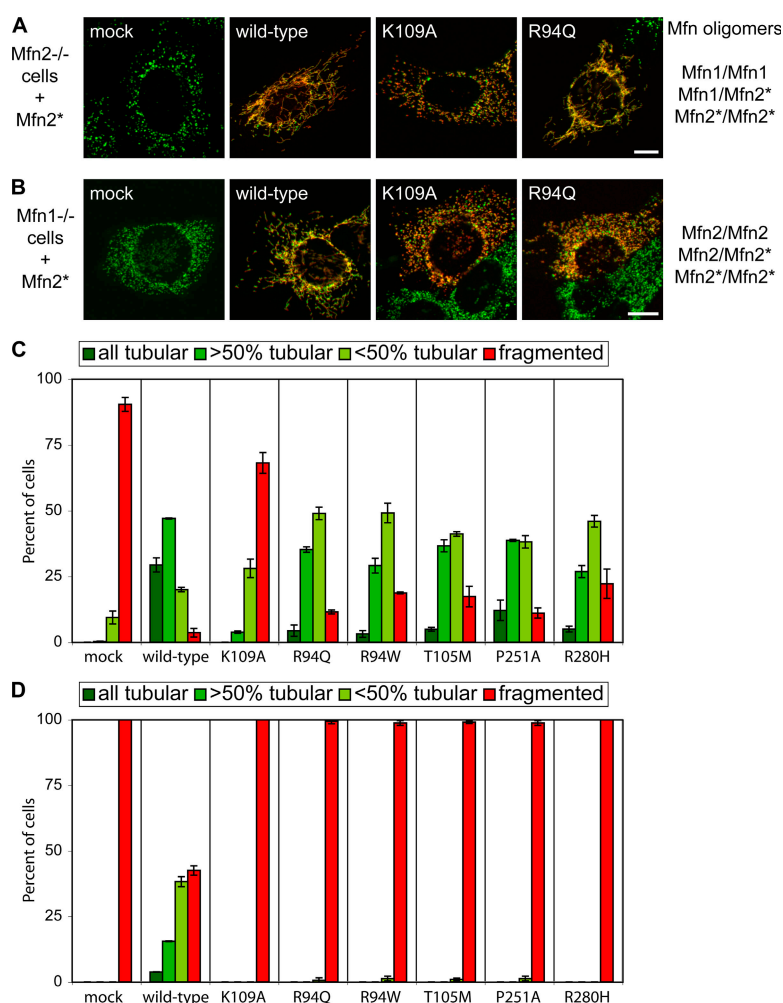
In contrast, the expression of mutants Mfn2^{R94Q}, Mfn2^{R94W}, Mfn2^{T105M}, Mfn2^{P251A}, and Mfn2^{R280H} in Mfn1-null cells did not induce tubulation (Fig. 6, B and D). Mfn1-null cells expressing these alleles had extensively fragmented mitochondria. In this experiment, only Mfn2 complexes can be formed: Mfn2–Mfn2, Mfn2^{CMT2A}–Mfn2^{CMT2A}, and Mfn2–Mfn2^{CMT2A} (Fig. 6 B). Therefore, in contrast to Mfn1–Mfn2^{CMT2A} complexes, Mfn2–Mfn2^{CMT2A} complexes do not appear to be competent for fusion.

Complementation between mutant Mfn2 and Mfn1 in trans

The aforementioned experiments demonstrate that Mfn1 can complement Mfn2 CMT2A alleles. By the nature of the experiment, it is impossible to know whether the complementation is occurring on the same mitochondria (in cis), between adjacent mitochondria (in trans), or both. To test whether the nonfunctional Mfn2 mutants can support fusion with wild-type mitochondria in trans, we returned to the PEG cell hybrid assay for mitochondrial fusion. In this assay, mitochondria from double

Mfn-null cells cannot fuse with mitochondria from wild-type cells, indicating a requirement for mitofusins on adjacent mitochondria (Koshiba et al., 2004; Chen et al., 2005). We expressed Mfn2 alleles in double Mfn-null cells and assessed mitochondrial fusion in cell hybrids with wild-type cells. In this experimental scheme, Mfn2^{CMT2A}–Mfn2^{CMT2A} complexes present on one set of mitochondria are tested for fusion with mitochondria containing a full complement of wild-type mitofusin complexes (Mfn1–Mfn1, Mfn2–Mfn2, and Mfn1–Mfn2 complexes). As expected, when double Mfn-null cells expressing wild-type Mfn2 were fused with wild-type cells, we found extensive colabeling of mitochondria (Fig. 7 B). Moreover, the Mfn2 CMT2A alleles Mfn2^{R94Q}, Mfn2^{R94W}, Mfn2^{P251A}, and Mfn2^{R280H} induce readily detectable but moderate levels of fusion that are lower than those of wild-type Mfn2 but are much more than those of Mfn2^{K109A} (Fig. 7, A and B). However, the Mfn2^{T105M} allele allows essentially no mitochondrial fusion. These results indicate that most Mfn2 CMT2A mutants can function in trans with wild-type mitofusin complexes.

To determine whether this complementation is caused by interactions with wild-type Mfn1–Mfn1 or Mfn2–Mfn2 complexes, we next tested the Mfn2 CMT2A alleles in mitochondrial fusion assays with Mfn2-null and Mfn1-null cells. Mfn2 mutants Mfn2^{R94Q}, Mfn2^{R94W}, Mfn2^{P251A}, and Mfn2^{R280H}



promoted moderate levels of mitochondrial fusion in cell hybrids with Mfn2-null cells (Fig. 7, A and C). In contrast, the same mutants induced no mitochondrial fusion in hybrids with Mfn1-null cells (Fig. 7, A and D). These results demonstrate that most Mfn2^{CMT2A} alleles can promote fusion when exposed to membranes containing Mfn1 but not Mfn2. As expected from its failure to promote fusion with wild-type mitochondria, Mfn2^{T105M} showed no fusion activity with either the Mfn2- or Mfn1-null cells.

Discussion

The Mfn1–Mfn2 heterooligomeric complex is an important regulator of mitochondrial dynamics

Previous immunoprecipitation studies indicated that Mfn1 and Mfn2 form heterooligomeric complexes (Chen et al., 2003; Eura et al., 2003). However, most functional studies have focused on Mfn1 or Mfn2 in isolation, and, therefore, we have little information on the functional importance of the heterooligomeric complex. The only direct demonstration that this complex is functional comes from the observation that cell hybrids between Mfn1- and Mfn2-null cells show low levels of mitochondrial fusion, suggesting that Mfn1–Mfn2 heterotypic complexes formed in trans have fusion activities that are roughly comparable with homooligomeric Mfn1 or Mfn2 complexes alone (Chen et al., 2005). Our current study of Mfn2 disease alleles reveals an intimate interplay between Mfn1 and Mfn2 in mediating mitochondrial fusion. A subset of Mfn2 disease alleles lack mitochondrial fusion activity in isolation but show substantial fusion activity in the presence of Mfn1. In addition, PEG fusion assays (Fig. 7) indicate that this cooperation between Mfn1 and mutant Mfn2 at least partially occurs through interactions in trans. Such close physical and functional interactions between Mfn1 and Mfn2 support the view that they have similar biochemical functions during mitochondrial membrane fusion. These results highlight the importance of heterooligomeric Mfn1–Mfn2 complexes in the control of mitochondrial dynamics.

Our study greatly extends a different type of complementation demonstrated in the yeast mitofusin Fzo1p. Fzo1p demonstrates strong complementation between specific pairs of null alleles, resulting in the restoration of mitochondrial tubules (Griffin and Chan, 2006). For example, an *fzo1* mutant containing a GTPase mutation can cooperate with an *fzo1* mutant containing a heptad repeat mutation to promote mitochondrial fusion. Such complementation reflects the oligomeric nature of mitofusin complexes and indicates that each subunit of the oligomer need not be fully functional to provide function to the complex. However, this previous study (Griffin and Chan, 2006) was limited to Fzo1 homooligomeric complexes, unlike the heterooligomeric complexes studied here. Indeed, we have not been able to demonstrate a similar type of complementation in Mfn1 or Mfn2 homooligomeric complexes (unpublished data).

Functional heterogeneity of CMT2A alleles

Our results reveal some functional heterogeneity in Mfn2 mutants that underlie CMT2A disease. The Mfn2^{T105M} allele

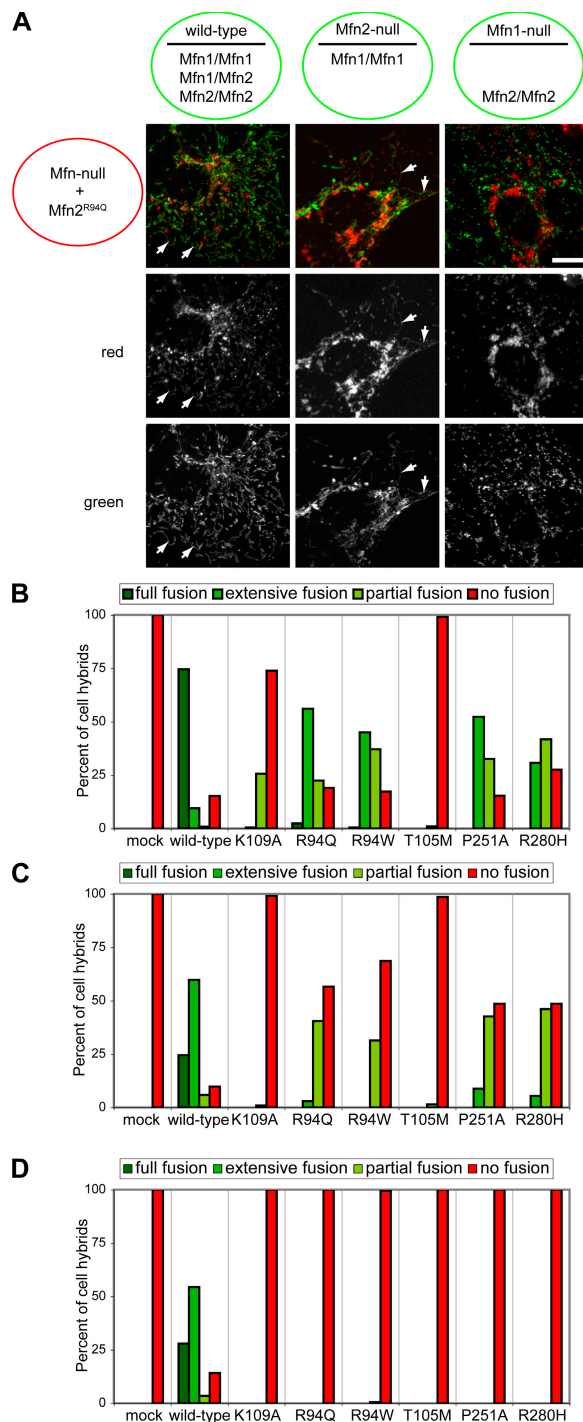


Figure 7. Mfn1 complements Mfn2 CMT2A mutants in trans. (A) Double Mfn-null MEFs expressing mitochondrial DsRed and Mfn2R94Q were fused to wild-type cells (left), Mfn2-null cells (middle), or Mfn1-null cells (right). As indicated by the green circles, the latter three cell lines expressed mitochondrial EGFP. For each cell line, all potential mitofusin oligomers are listed under the horizontal line. Colabeled mitochondrial tubules (indicated with arrows) are clearly observed in cell hybrids with wild-type and Mfn2-null cells but not with Mfn1-null cells. Bar, 10 μ m. (B–D) Double Mfn-null cells expressing the indicated Mfn2 mutant were assayed for mitochondrial fusion in cell hybrids with wild-type cells (B), Mfn2-null cells (C), and Mfn1-null cells (D). For each PEG fusion assay, at least 200 cell hybrids were scored.

behaved somewhat differently from the other nonfunctional alleles. Mfn2^{T105M}, like the other nonfunctional alleles, could be complemented by wild-type Mfn1. However, it showed reduced physical interactions with Mfn1 and did not show complementation with Mfn1 in trans. Presumably, Mfn2^{T105M} can be complemented by Mfn1 in cis but not in trans.

Over half of the CMT2A alleles are nonfunctional in double Mfn-null cells, but the rest show substantial fusion activity. More sensitive assays will be necessary to understand how the functional alleles affect mitochondrial dynamics. Some of the functional alleles caused severe mitochondrial aggregation when overexpressed. Future studies will determine the physiological significance of this phenotype.

Implications for pathogenesis and treatment of CMT2A

Our results have important implications for understanding the pathogenesis of CMT2A, especially because four of the five nonfunctional mutant alleles described in this study (Mfn2^{R94Q}, Mfn2^{R94W}, Mfn2^{T105M}, and Mfn2^{R280H}) are among the most commonly identified Mfn2 mutations (Zuchner et al., 2004, 2006; Kijima et al., 2005; Lawson et al., 2005; Chung et al., 2006; Verhoeven et al., 2006). In contrast to the broad expression pattern of Mfn2, one of the remarkable features of CMT2A disease is its apparent cell type specificity. In most patients, the clinical features are restricted to the motor and sensory neurons of the peripheral nervous system. In a subset of patients (designated as hereditary motor and sensory neuropathy type VI), the optic nerve is additionally affected (Zuchner et al., 2006). A recent study has suggested possible involvement of the central nervous system (Chung et al., 2006). This clinical picture suggests that most cells in CMT2A patients likely have only mild perturbations in mitochondrial dynamics. Moreover, in a typical patient, only the longest peripheral sensory and motor neurons are affected. This length dependence suggests that even in the peripheral nervous system, the defects in mitochondrial dynamics are not catastrophic because only the neurons with the highest demands for precise control of mitochondrial fusion are damaged.

Our studies of the Mfn2^{R94Q} knockin mice are ongoing, but initial observations support the conclusion that CMT2A disease results from a mild perturbation in mitochondrial dynamics. Thus far, we have not observed a neurological phenotype in the heterozygous knockin mice. The lack of an obvious peripheral neuropathy in these mice may reflect the fact that motor neurons in mice are much shorter than in humans, where their extreme length likely places more stringent requirements on the precise regulation of mitochondrial fusion. Although Mfn2-null animals die in utero, Mfn2^{R94Q} homozygous animals are born live and die at ~3 wk of age. The much milder phenotype of Mfn2^{R94Q} homozygous animals compared with Mfn2-null animals further supports our conclusion that Mfn2^{R94Q} can be partially complemented by endogenous Mfn1. Mfn2^{R94Q} homozygous animals have severe movement defects (unpublished data), and we are currently analyzing the basis for this phenotype.

In considering the effects of Mfn2 mutations, our results indicate that the full complement of mitofusins in any given cell

A	Mitofusin complexes		
	I	II	III
Wild-type cells	Mfn1/Mfn1	Mfn1/Mfn2	Mfn2/Mfn2
B CMT2A patients	most cells		
	Mfn1/Mfn1	Mfn1/Mfn2 Mfn1/Mfn2*	Mfn2/Mfn2 Mfn2/Mfn2* Mfn2*/Mfn2*
cells with no Mfn1 expression	—	—	Mfn2/Mfn2 Mfn2/Mfn2* Mfn2*/Mfn2*

Figure 8. Mfn1 complements mutant Mfn2 to preserve mitochondrial fusion in most CMT2A cells. (A) In most wild-type cell types, there are three classes of mitofusin complexes (I, II, and III) that maintain mitochondria in a highly dynamic state. (B) CMT2A patients are heterozygous for a mutant Mfn2 allele (designated Mfn2*). In most cells, defects in mitochondrial dynamics are mild because only a subset of class III complexes are nonfunctional (highlighted in black). In contrast, cells expressing little or no Mfn1 would suffer a large decline in mitochondrial fusion activity. Such cells contain only class III complexes, and the majority of these are nonfunctional.

type is the most relevant parameter in determining the dysfunction of mitochondrial fusion. This concept is clearly illustrated in our analysis of Mfn2 CMT2A mutations in MEFs. When Mfn2^{R94Q} is expressed in double Mfn-null cells, it is completely deficient for fusion activity, indicating that homooligomeric Mfn2^{R94Q} complexes are nonfunctional. In contrast, MEFs containing homozygous Mfn2^{R94Q} knockin mutations show only mild defects in mitochondrial morphology, a phenotype that is quite different from the extensive mitochondrial fragmentation observed in Mfn2-null MEFs. This observation indicates that in the presence of endogenous wild-type Mfn1, Mfn2^{R94Q} is actually highly functional. By expressing Mfn2^{R94Q} and other mutant alleles in Mfn1-null versus Mfn2-null cells, we found that wild-type Mfn1 but not Mfn2 can cooperate with mutant Mfn2 to promote mitochondrial fusion.

These results suggest that the widespread expression pattern of Mfn1 (Rojo et al., 2002; Santel et al., 2003) protects mitochondrial dynamics in most cells in CMT2A patients carrying nonfunctional alleles of Mfn2. CMT2A is an autosomal dominant disease, with patients carrying one mutant and one wild-type allele of Mfn2. In cell types that express Mfn1, Mfn1 homooligomeric complexes would be normal, and Mfn1–Mfn2 heterooligomeric complexes would also be largely normal as a result of the cooperation between Mfn1 and mutant Mfn2 (Fig. 8). For Mfn2 homooligomeric complexes, Mfn2^{wt}–Mfn2^{wt} complexes would be functional, whereas Mfn2^{wt}–Mfn2^{CMT2A} and Mfn2^{CMT2A}–Mfn2^{CMT2A} complexes would be nonfunctional. Therefore, of the three classes of mitofusin complexes, only a subset of one class is nonfunctional, resulting in mild mitochondrial fusion defects in most cells. In cell types with low or no Mfn1 expression, the full complement of mitofusin complexes consists primarily of Mfn2 homotypic complexes. In relative terms, such cells would experience a severe loss of mitochondrial fusion because the majority of mitofusin complexes (Mfn2^{wt}–Mfn2^{CMT2A} and Mfn2^{CMT2A}–Mfn2^{CMT2A}) lack mitochondrial fusion activity. Therefore, we propose that in CMT2A disease, the widespread expression pattern of Mfn1 serves to protect mitochondrial fusion in most cells through

heterooligomeric complex formation with mutant Mfn2. Peripheral nerves may contain little or no Mfn1 expression to compensate for mutant Mfn2. The resulting defects in mitochondrial dynamics coupled with the extreme length of these neurons lead to neuronal dysfunction and axon degeneration.

Our results emphasize the close interplay between Mfn1 and Mfn2 and the importance of the Mfn1–Mfn2 heterooligomer complex in control of mitochondrial fusion. Finally, our results suggest that an important area of future study is the regulation of Mfn1 levels. Methods to increase Mfn1 expression in the peripheral nervous system may benefit CMT2A patients by promoting the complementation of mitochondrial fusion.

Materials and methods

Cloning and retroviral transduction

The mitofusins 7xMyc and 3xHA constructs were described previously (Chen et al., 2003). The CMT2A point mutations were introduced to Mfn2-7xMyc in pCDNA3.1 by PCR with primers encoding the mutations. After cloning, the entire amplified region was verified by sequencing. The mutant cDNAs were then cloned into the retroviral construct pCLBW, and viral supernatant was produced and collected as described previously (Chen et al., 2003).

Immunofluorescence

Immunofluorescence against Mfn2-7xMyc was performed as described previously (Chen et al., 2003). In brief, cells were grown on poly-L-lysine-treated coverslips, fixed in formalin, permeabilized with 0.1% Triton X-100 in PBS, and blocked with 5% bovine calf serum in PBS. The 9E10 primary antibody was detected with a Cy3-labeled secondary antibody. Coverslips were mounted with GelMount and imaged with a plan NeoFluar 63× NA 1.25 oil immersion objective (Carl Zeiss MicroImaging, Inc.) on a laser-scanning confocal microscope (model 410; Carl Zeiss MicroImaging, Inc.). Images were acquired with LSM software (version 1; Carl Zeiss MicroImaging, Inc.) and pseudocolored in Photoshop CS (Adobe). Mitochondria were visualized by mitochondrially targeted GFP or DsRed as previously described (Chen et al., 2005). In other cases, mitochondria were stained using 150 nM MitoTracker red CMXRos (Invitrogen) and post-fixed in acetone.

PEG fusion assay

PEG fusion assays were performed in the presence of cycloheximide as described previously (Chen et al., 2003, 2005). Cell hybrids were fixed 7 h after PEG treatment. The mitochondrial GFP signal was enhanced by incubation with an anti-GFP antibody conjugated to AlexaFluor488 (Invitrogen).

Derivation of Mfn2^{R94Q} homozygous MEFs

The two arms of the targeting construct were derived from Mfn2 genomic sequence (129/SvJ background) and subcloned into the targeting vector pPGKneobpAlox2PGKDTA. Before subcloning of the left arm, the R94Q mutation was engineered into exon 5 by PCR. The targeting construct was verified by DNA sequencing. The linearized targeting construct was electroporated into low-passage 129/SvEv ES cells as described previously (Chen et al., 2003). Correctly targeted ES clones were identified by PCR using the primer sets A and B depicted in Fig. 3 A. Chimeric mice were generated by the injection of ES cells into C57BL/6 blastocysts. After confirmation of germline transmission, the floxed neomycin cassette was removed by mating the knockin mice with the EIIA-cre deleter line (Lakso et al., 1996). Heterozygous knockin animals were mated, and MEFs were derived from day 10.5 embryos as described previously (Chen et al., 2003). Homozygous embryos were identified by PCR genotyping of extra-embryonic membranes. Wild-type, Mfn1-null, Mfn2-null, and Mfn2^{R94Q}–Mfn2^{R94Q} MEFs were cultured in DME containing 10% bovine calf serum, 1 mM L-glutamine, and penicillin/streptomycin. Double Mfn-null MEFs were cultured with 10% FCS in place of bovine calf serum.

RNA isolation and RT-PCR

MEFs were resuspended directly in 800 μl STAT-60 (IsoTex Diagnostics, Inc.), and RNA was isolated according to the manufacturer's instructions. cDNA was generated by first-strand synthesis on total RNA using oligo(dT)

and Superscript II RT (Invitrogen). A cDNA fragment containing exon 5 was subsequently amplified (primers 5'-GGGGCCTACATCCAAGAGAG-3' and 5'-GCAGAACTTGTCCCAGAGC-3'). This product was digested overnight at 37°C with MspA11.

MEF lysates

MEF cell lysates were prepared from confluent 6-cm plates. For protein lysates, cells were washed once with PBS and resuspended in 400 μl lysis buffer (150 mM NaCl, 50 mM Tris, pH 8.0, 4 mM MgCl₂, 1% Triton X-100, and protease inhibitor cocktail [Roche]). Nuclei were removed by centrifugation, and postnuclear lysates were quantified with a protein assay (Bio-Rad Laboratories). 12 μg of each sample was separated by an 8% SDS-PAGE and immunoblotted with an anti-Mfn2 antibody (Sigma-Aldrich), an anti-Mfn1 antibody (Chen et al., 2003), or anti-β-actin as a loading control. Mitofusin antibodies (diluted 1:1,000) were detected by HRP-conjugated secondary antibodies and ECL detection reagents (GE Healthcare).

Coimmunoprecipitation assay

Double Mfn-null cells were infected with retrovirus encoding Mfn1-3xHA or Mfn2-3xHA. Infected cells were selected by culture in media containing bovine calf serum, which does not support uninfected double Mfn-null cells. Each cell line was subsequently infected with virus encoding Mfn2-7xMyc constructs or Drp1-7xMyc. Postnuclear lysates were generated as described above for MEFs (5–6 d after infection) and were immunoprecipitated with 9E10 antibody coupled to protein A–Sepharose beads. HA.11 (Covance) and 9E10 antibodies were used for immunoblotting.

Online supplemental material

Fig. S1 shows the mitochondrial profiles of MEFs expressing Mfn2 CMT2A alleles; this data is summarized in Fig. 1 C. Fig. S2 shows mitochondrial aggregation in MEFs highly overexpressing Mfn2 CMT2A alleles. Fig. S3 shows that at low infection rates, recombinant Mfn2 is present at approximately fourfold the level of endogenous Mfn2. Online supplemental material is available at <http://www.jcb.org/cgi/content/full/jcb.200611080/DC1>.

We are grateful to Hsiuchen Chen for helpful comments on the manuscript, members of the laboratory for encouragement, and the Beckman Imaging Center for use of confocal microscopes.

This work was supported by National Institutes of Health (NIH) grant GM062967. D.C. Chan was a Bren Scholar. S.A. Detmer was partially supported by NIH/National Research Service Award training grant 5T32GM07616.

Submitted: 15 November 2006

Accepted: 16 January 2007

References

- Alexander, C., M. Votruba, U.E. Pesch, D.L. Thiselton, S. Mayer, A. Moore, M. Rodriguez, U. Kellner, B. Leo-Kottler, G. Auburger, et al. 2000. OPA1, encoding a dynamin-related GTPase, is mutated in autosomal dominant optic atrophy linked to chromosome 3q28. *Nat. Genet.* 26:211–215.
- Chan, D.C. 2006. Mitochondrial fusion and fission in mammals. *Annu. Rev. Cell Dev. Biol.* 22:79–99.
- Chen, H., and D.C. Chan. 2006. Critical dependence of neurons on mitochondrial dynamics. *Curr. Opin. Cell Biol.* 18:453–459.
- Chen, H., S.A. Detmer, A.J. Ewald, E.E. Griffin, S.E. Fraser, and D.C. Chan. 2003. Mitofusins Mfn1 and Mfn2 coordinately regulate mitochondrial fusion and are essential for embryonic development. *J. Cell Biol.* 160:189–200.
- Chen, H., A. Chomyn, and D.C. Chan. 2005. Disruption of fusion results in mitochondrial heterogeneity and dysfunction. *J. Biol. Chem.* 280:26185–26192.
- Chung, K.W., S.B. Kim, K.D. Park, K.G. Choi, J.H. Lee, H.W. Eun, J.S. Suh, J.H. Hwang, W.K. Kim, B.C. Seo, et al. 2006. Early onset severe and late-onset mild Charcot-Marie-Tooth disease with mitofusin 2 (MFN2) mutations. *Brain.* 129:2103–2118.
- Cipolat, S., O. Martins de Brito, B. Dal Zilio, and L. Scorrano. 2004. OPA1 requires mitofusin 1 to promote mitochondrial fusion. *Proc. Natl. Acad. Sci. USA.* 101:15927–15932.
- Delettre, C., G. Lenaers, J.M. Griffoin, N. Gigarel, C. Lorenzo, P. Belenguer, L. Pelloquin, J. Grosgeorge, C. Turc-Carel, E. Perret, et al. 2000. Nuclear gene OPA1, encoding a mitochondrial dynamin-related protein, is mutated in dominant optic atrophy. *Nat. Genet.* 26:207–210.

- Eura, Y., N. Ishihara, S. Yokota, and K. Mihara. 2003. Two mitofusin proteins, mammalian homologues of FZO, with distinct functions are both required for mitochondrial fusion. *J. Biochem. (Tokyo)*. 134:333–344.
- Griffin, E.E., and D.C. Chan. 2006. Domain interactions within Fzo1 oligomers are essential for mitochondrial fusion. *J. Biol. Chem.* 281:16599–16606.
- Guo, X., G.T. Macleod, A. Wellington, F. Hu, S. Panchumarthi, M. Schoenfield, L. Marin, M.P. Charlton, H.L. Atwood, and K.E. Zinsmaier. 2005. The GTPase dMiro is required for axonal transport of mitochondria to *Drosophila* synapses. *Neuron*. 47:379–393.
- Ishihara, N., Y. Eura, and K. Mihara. 2004. Mitofusin 1 and 2 play distinct roles in mitochondrial fusion reactions via GTPase activity. *J. Cell Sci.* 117:6535–6546.
- Kijima, K., C. Numakura, H. Izumino, K. Umetsu, A. Nezu, T. Shiiki, M. Ogawa, Y. Ishizaki, T. Kitamura, Y. Shozawa, and K. Hayasaka. 2005. Mitochondrial GTPase mitofusin 2 mutation in Charcot-Marie-Tooth neuropathy type 2A. *Hum. Genet.* 116:23–27.
- Koshihara, T., S.A. Detmer, J.T. Kaiser, H. Chen, J.M. McCaffery, and D.C. Chan. 2004. Structural basis of mitochondrial tethering by mitofusin complexes. *Science*. 305:858–862.
- Lakso, M., J.G. Pichel, J.R. Gorman, B. Sauer, Y. Okamoto, E. Lee, F.W. Alt, and H. Westphal. 1996. Efficient in vivo manipulation of mouse genomic sequences at the zygote stage. *Proc. Natl. Acad. Sci. USA*. 93:5860–5865.
- Lawson, V.H., B.V. Graham, and K.M. Flanigan. 2005. Clinical and electrophysiologic features of CMT2A with mutations in the mitofusin 2 gene. *Neurology*. 65:197–204.
- Li, Z., K. Okamoto, Y. Hayashi, and M. Sheng. 2004. The importance of dendritic mitochondria in the morphogenesis and plasticity of spines and synapses. *Cell*. 119:873–887.
- Neuspiel, M., R. Zunino, S. Gangaraju, P. Rippstein, and H. McBride. 2005. Activated mitofusin 2 signals mitochondrial fusion, interferes with Bax activation, and reduces susceptibility to radical induced depolarization. *J. Biol. Chem.* 280:25060–25070.
- Okamoto, K., and J.M. Shaw. 2005. Mitochondrial morphology and dynamics in yeast and multicellular eukaryotes. *Annu. Rev. Genet.* 39:503–536.
- Olichon, A., L. Baricault, N. Gas, E. Guillou, A. Valette, P. Belenguer, and G. Lenaers. 2003. Loss of OPA1 perturbs the mitochondrial inner membrane structure and integrity, leading to cytochrome c release and apoptosis. *J. Biol. Chem.* 278:7743–7746.
- Rojo, M., F. Legros, D. Chateau, and A. Lombes. 2002. Membrane topology and mitochondrial targeting of mitofusins, ubiquitous mammalian homologs of the transmembrane GTPase Fzo. *J. Cell Sci.* 115:1663–1674.
- Santel, A., and M.T. Fuller. 2001. Control of mitochondrial morphology by a human mitofusin. *J. Cell Sci.* 114:867–874.
- Santel, A., S. Frank, B. Gaume, M. Herrler, R.J. Youle, and M.T. Fuller. 2003. Mitofusin-1 protein is a generally expressed mediator of mitochondrial fusion in mammalian cells. *J. Cell Sci.* 116:2763–2774.
- Stowers, R.S., L.J. Megeath, J. Gorska-Andrzejak, I.A. Meinertzhagen, and T.L. Schwarz. 2002. Axonal transport of mitochondria to synapses depends on Milton, a novel *Drosophila* protein. *Neuron*. 36:1063–1077.
- Sugioka, R., S. Shimizu, and Y. Tsujimoto. 2004. Fzo1, a protein involved in mitochondrial fusion, inhibits apoptosis. *J. Biol. Chem.* 279:52726–52734.
- Verhoeven, K., K.G. Claeys, S. Zuchner, J.M. Schroder, J. Weis, C. Ceuterick, A. Jordanova, E. Nelis, E. De Vriendt, M. Van Hul, et al. 2006. MFN2 mutation distribution and genotype/phenotype correlation in Charcot-Marie-Tooth type 2. *Brain*. 129:2093–2102.
- Verstreken, P., C.V. Ly, K.J. Venken, T.W. Koh, Y. Zhou, and H.J. Bellen. 2005. Synaptic mitochondria are critical for mobilization of reserve pool vesicles at *Drosophila* neuromuscular junctions. *Neuron*. 47:365–378.
- Youle, R.J., and M. Karbowski. 2005. Mitochondrial fission in apoptosis. *Nat. Rev. Mol. Cell Biol.* 6:657–663.
- Zuchner, S., and J.M. Vance. 2005. Emerging pathways for hereditary axonopathies. *J. Mol. Med.* 83:935–943.
- Zuchner, S., I.V. Mersyanova, M. Muglia, N. Bissar-Tadmouri, J. Rochelle, E.L. Dadali, M. Zappia, E. Nelis, A. Patitucci, J. Senderek, et al. 2004. Mutations in the mitochondrial GTPase mitofusin 2 cause Charcot-Marie-Tooth neuropathy type 2A. *Nat. Genet.* 36:449–451.
- Zuchner, S., P. De Jonghe, A. Jordanova, K.G. Claeys, V. Guerguelcheva, S. Cherninkova, S.R. Hamilton, G. Van Stavern, K.M. Krajewski, J. Stajich, et al. 2006. Axonal neuropathy with optic atrophy is caused by mutations in mitofusin 2. *Ann. Neurol.* 59:276–281.

Supplementary Figures

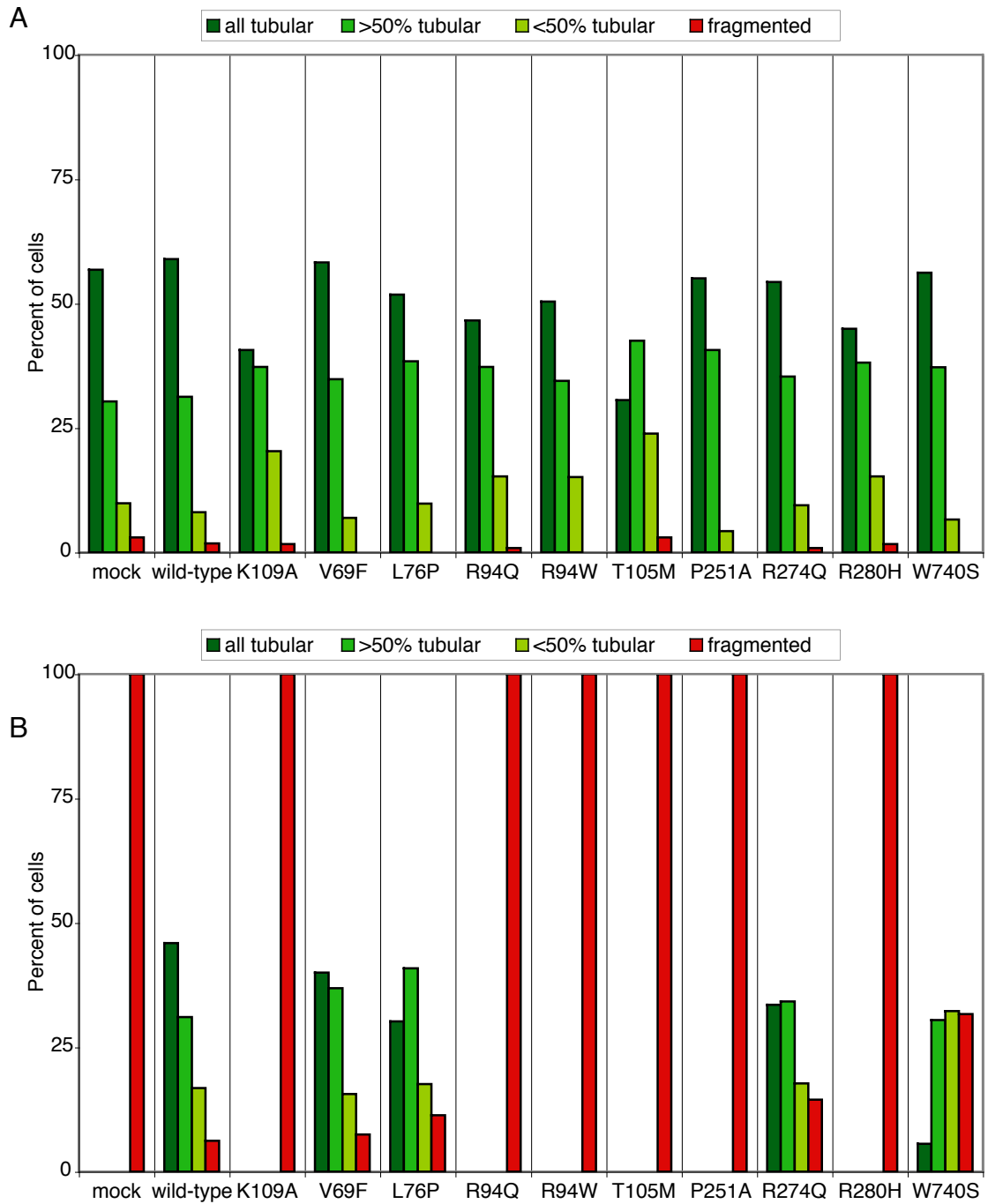
Supplementary figure 1. Mitochondrial profiles in MEFs expressing Mfn2 CMT2A alleles. A., Histogram of mitochondrial profiles in wild-type MEFs infected with mutant Mfn2 retroviruses at low multiplicity of infection. The percentage of cells with tubular mitochondria presented in Figure 1C is the sum of the categories “all tubular,” “>50% tubular” and “<50% tubular.” For each histogram, at least 150 cells were scored. B., As in A, but in double Mfn-null MEFs.

Supplementary figure 2. Mitochondrial aggregation in wild-type cells highly over-expressing Mfn2 CMT2A alleles. A., Representative overlay images of wild-type MEFs infected with mutant Mfn2-Myc retrovirus at a high multiplicity of infection. Mitochondria are visualized by matrix-targeted EGFP (green), and Mfn2-expressing cells are identified by immunofluorescence against the Myc epitope (red). Note the extensive mitochondrial aggregation caused by some of the CMT2A alleles. B., Histograms of mitochondrial morphology in these cells. For each histogram, at least 200 cells were counted. Scale bar = 10 microns.

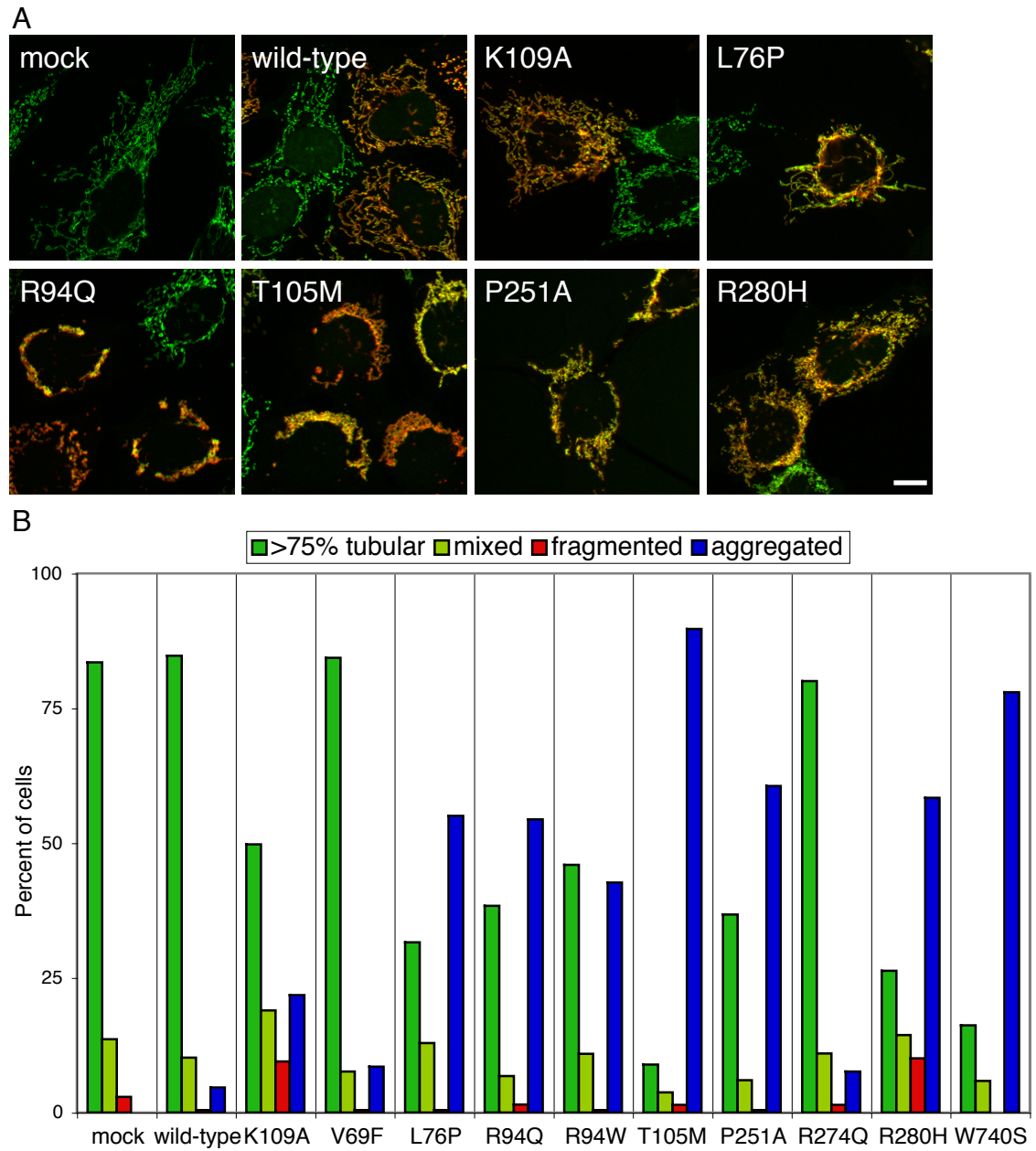
Supplementary figure 3. Quantification of retroviral expression levels. Double Mfn-null cells were infected at low multiplicity of infection with retrovirus expressing Mfn2-HA. Mfn2-HA expressing cells have a growth advantage compared to double Mfn-null cells and form the bulk of the population after several passages. Western blot analysis with an anti-Mfn2 antibody was used to compare expression in infected cells with

endogenous Mfn2 expression. The Mfn2 band in infected cells is higher due to the HA tag. The positions of molecular weight markers (in kDa) are indicated.

Supplementary figure 3-1



Supplementary figure 3-2



Chapter 4

Mitofusin 2 Disease Allele Causes Gait Defects and Axonopathy in Transgenic Mouse Model of CMT2A

Scott A. Detmer, Christine Vande Velde, Don W. Cleveland, David C. Chan

Christine Vande Velde, PhD, is a postdoctoral scholar in Don Cleveland's lab at the Ludwig Cancer Institute, University of California, San Diego. Christine instructed and assisted me in motor root dissections and performed the motor neuron measurements and imaging presented in figure 5 of this chapter.

Introduction

Mitochondria are essential and highly dynamic organelles. Mitochondria are actively transported within a cell to regions of energy demand by specific anterograde and retrograde motors (Chang et al., 2006; Pilling et al., 2006). Mitochondrial morphology is determined by balanced and opposing processes of fusion and fission. Disruption of either mitochondrial transport or morphology dynamics has been experimentally linked to neuronal dysfunction in *Drosophila* (Guo et al., 2005; Li et al., 2004; Stowers et al., 2002; Verstreken et al., 2005). In each case, a decrease in the number of mitochondria at synaptic regions results in synaptic dysfunction. Mutations in two mitochondrial fusion proteins, Mitofusin 2 and OPA1, cause human neuropathies Charcot-Marie-Tooth disease and dominant optic atrophy, respectively (Delettre et al., 2000; Zuchner et al., 2004).

Charcot-Marie-Tooth disease (CMT) is a common hereditary peripheral neuropathy characterized by loss of distal sensory and motor function (Young and Suter, 2003). CMT is progressive with variable age of onset, and most patients present clinically with loss of muscle mass in the feet and lower leg that cause gait impairments. There are two main classifications of CMT. The first, type 1, is due to myelination defects and is primarily caused by mutation of structural myelin proteins. Type 2 is caused by primary defects in axons. The most common form of the axonal class is CMT type 2A, caused by mutations in Mitofusin 2 (Zuchner et al., 2004).

Mitofusin are nuclearly encoded, mitochondrial integral outer membrane proteins that are required for mitochondrial fusion in yeast and mammals (Griffin et al., 2006).

Mitofusins have an N-terminal GTPase domain and two heptad-repeat domains, all of which face the cytoplasm. There are two mitofusin proteins in mammals, Mfn1 and Mfn2. Over forty mutations have been identified in Mitofusin 2 that cause dominantly inherited CMT type 2A (Chung et al., 2006; Engelfried et al., 2006; Kijima et al., 2005; Lawson et al., 2005; Verhoeven et al., 2006; Zuchner et al., 2006; Zuchner et al., 2004). The majority of these are missense point mutations and most occur within or adjacent to the GTPase domain. To date, Mfn2 CMT2A alleles have only been studied in cell culture. Overexpression of a majority of tested alleles results in mitochondrial aggregation as well as defects in mitochondrial transport in cultured dorsal root ganglion neurons (Baloh et al., 2007; Detmer and Chan, 2007). Some Mfn2 CMT2A alleles are functional for mitochondrial fusion, whereas others are not (Detmer and Chan, 2007).

In order to study the *in vivo* effects of an Mfn2 CMT2A allele, we generated transgenic mice expressing Mfn2 T105M under control of a motor neuron specific promoter. We confirmed motor neuron expression and find that animals homozygous for the transgene have hindlimb gait impairments, decreased hindlimb muscle mass and a decrease in motor neuron axons. Additionally, we find that mitochondrial morphology in neurons is both aggregated and irregularly distributed.

Results

Generation of Mfn2 T105M transgenic mouse

Charcot-Marie-Tooth Disease Type 2A (CMT2A) causes specific loss of long motor and sensory neurons due to mutations in Mitofusin 2 (Mfn2). To investigate the effect of an Mfn2 CMT2A allele in motor neurons, we generated transgenic mice expressing Mfn2 T105M 7xMyc under the control of the HB9 promoter. Mfn2 T105M has been found in three unrelated CMT2A families and has an early onset of foot and leg muscular atrophy and additional features of scoliosis and ataxia (Chung et al., 2006; Lawson et al., 2005; Zuchner et al., 2004). The Mfn2 T105M allele localizes normally to mitochondria and is non-functional for mitochondrial fusion (Detmer and Chan, 2007). Similar to other Mfn2 CMT2A alleles, Mfn2 T105M induces mitochondrial aggregation when overexpressed (Baloh et al., 2007; Detmer and Chan, 2007). Position T105 is in the middle of the GTPase G1 motif (103GxxxxGKS110) (Bourne et al., 1991).

HB9 is required embryonically for motor neuron identity determination and consolidation (Arber et al., 1999; Thaler et al., 1999). The HB9 promoter has been used as a reliable indicator of motor neuron cells as extensively detailed in HB9-EGFP transgenic mice (Wichterle et al., 2002). The transgenic construct we generated consists of the HB9 promoter driving expression Mfn2 T105M 7xMyc followed by an IRES and EGFP (Fig. 1A). We added the C-terminal Myc tag in order to label mitochondria in motor neurons by immunofluorescence. The IRES EGFP was included in order to label motor neurons and their processes with cytoplasmic EGFP.

Linearized transgene was injected into oocytes that were implanted into pseudopregnant surrogates. Founder animals were genotyped for the presence of the transgene and test mated to verify propagation of the transgene. Genotyping consisted of a PCR reaction spanning a small intron such that amplification from the genomic *Mfn2* locus results in a larger product than from the *Mfn2* transgene, which lacks introns (Fig. 1B). The reliability of this genotyping strategy was confirmed by agreement between genotyping results and embryonic protein lysates probed with Myc antibody (Fig. 1B).

We determined the genomic integration site for an interesting line of HB9-*Mfn2* T105M transgenic mice, hereafter referred to as Tg1. The transgene integrated line Tg1 in a non gene-coding region on chromosome 11 between genes *Rad51c* and *Ppm1e*. This integration site was confirmed using PCR oligos at both the 5' and 3' ends of the transgene (Fig. 1C). Identifying the transgene integration site allowed us to distinguish between heterozygous and homozygous Tg1 animals using PCR (Fig. 1C).

Hindlimb defect in Tg1/Tg1 animals

We noted that mice heterozygous for Tg1 were born with tails that were shorter than wild-type animals and had bony kinks or thickenings (Fig. 2A,B). When we mated heterozygous Tg1 animals, approximately one-fourth of the progeny had extremely short tails. We confirmed that the short-tailed animals were homozygous for the transgene using the PCR assay (Fig 1D). This tail phenotype allowed for visual genotyping of the Tg1 line.

Tg1 homozygous animals have hindlimb and gait defects, evident from birth (Fig. 2A). Young animals have hindpaws that appear limp due to a failure to dorsi-flex (Fig. 2D). When at rest, severely effected animals often fail to bring their hindpaws under their haunches and instead leave their hindlimbs extended behind their bodies. Tg1/Tg1 are active and can move effectively, though they use their hindlimbs in the extended trailing position in short push motions (Fig. 2E). In addition, Tg1/Tg1 animals commonly have hindpaws that are clenched and an apparent inability to spread their toes (Fig. 2F).

The severity of the hindlimb defect is variable between animals and is not absolute in all Tg1/Tg1 animals. Of 85 Tg1/Tg1 animals, 60% were bilaterally affected, 26% had only a single hindpaw with the defect and 14% had apparently normal hindpaws and gait. No hindpaw defects are observed in heterozygous animals, even at one year of age. Both Tg1/+ and Tg1/Tg1 animals live greater than 1 year and are fully fertile. Tg1/Tg1 have an approximate 15% reduction in body weight at weaning (P20). The hindpaw/gait defect does not appear to worsen with age and no defect was observed in the forelimbs. Tg1/Tg1 performed well on rotorod tests and could manage traversing a thin beam (data not shown). These surprising results are perhaps explained by their retention of sensory neurons that are important for determining foot placement.

The tail defects in the Tg1 animals are a consequence of the transgene and not the integration site. We generated compound heterozygotes with a second transgenic line of HB9 Mfn2 T105M animals (Tg2) that have normal tails. Tg1/+; Tg2/+ animals had intermediate tail defects: the tails of compound heterozygote animals were of intermediate length between Tg1/+ and Tg1/Tg1 animals (Supp. Fig. 1). Tg1/+; Tg2/+ had no hindlimb phenotype. This suggests that the transgene expression level is critical

for the observed phenotype and that only Tg1/Tg1 animals achieve this critical expression level. We do not know the basis of the tail defect in the Tg1 mice but it may be related to transient HB9 expression in tail mesoderm (H. Wichterle, personal communication).

Mfn2 T105M 7xMyc expression in motor neurons

We tested for motor neuron transgene expression in embryos and neonates. As a control, we examined day 12.5 HB9-EGFP embryos by cryosection. As expected, motor neurons are found in the ventral section of the developing spinal column and axons can be observed traveling into the body of the embryo (Fig. 3A). Similarly, in Tg1/Tg1 e12.5 embryos, we find ventral motor neuron EGFP signal. These sections were also stained using Myc immunofluorescence to identify mitochondria. Myc staining is confined within EGFP staining, consistent with our expectations (Fig. 3B). We note that in these cryosection images mitochondria have an aggregated appearance.

We next examined transgene expression in newborn animals (P0). P0 pups were transcardially perfused and their upper spinal cord dissected and cryosectioned. Spinal chord cross sections of HB9-EGFP control animals reveal motor neuron cell bodies in the ventral horns (Fig. 3C). Tg1/Tg1 pups had similar EGFP staining and Myc immunofluorescence was contained within EGFP-positive cell bodies (Fig. 3D). We note that in these samples mitochondria appear more tubular and distributed than in the e12.5 sections.

HB9 is expressed embryonically coincident with motor neuron formation (Arber et al., 1999; Thaler et al., 1999). To follow post-natal HB9 transgene expression, we made spinal cord lysates from P0, P2, P4, P6, P10 and P22 animals. We checked transgene expression using a Myc antibody and as a control for the HB9 promoter probed GFP expression in HB9-EGFP pups. Loads were normalized for protein level. Both GFP and Mfn2-Myc showed similar patterns of expression, with expression levels apparently dropping off during the first week after birth and undetectable in spinal cord lysates by three weeks of age. These data demonstrate Tg1 has similar expression pattern to HB9-EGFP, both in terms of motor neuron expression and expression timecourse.

We also examined the differences in transgene expression level in Tg1/+ and Tg1/Tg1 animals at P0 and P8. As expected, Tg1/Tg1 is expressed at levels approximately twice that of Tg1/+ as judged by Myc intensity in spinal cord lysates. These results are consistent with the expectation that the hindlimb phenotype correlates with transgene expression level.

Musculature defects in Tg1/Tg1 animals

Given the hindlimb specific defect in the Tg1/Tg1 animals, we investigated the musculature of the lower leg. Compared to wild-type and Tg/+ animals, Tg1/Tg1 animals have dramatically reduced anterior musculature of the lower leg that is readily visualized once the skin is removed. In contrast, the posterior calf muscle mass appear comparable across all genotypes. To quantify these observations, we dissected and weighed anterior and posterior muscles of the distal hindlimb. Muscles groups were

identified by their consistent distal tendon insertion site—the tendons were cut here, lifted away from the limb and severed at the proximal attachment site (Fig. 4A). This technique allowed for reproducible isolation of the same muscle in different animals despite differences in muscle size. We found that the masses of posterior calf muscles (as a fraction of animal body weight) were comparable in +/+, Tg/+ and Tg/Tg animals when assessed at P22 (Fig. 4B,C). In contrast, anterior muscles were comparable in +/+ and Tg/+, but dramatically less massive in Tg/Tg animals with affected hindlimbs (Fig. 4B,C). The loss of anterior musculature is responsible for the Tg/Tg hindlimb phenotype described above because the anterior muscles of Tg/Tg unaffected (normal) hindlimbs had variable, intermediate mass (Fig. 4C).

The loss of anterior muscles is consistent with the inability of affected homozygous animals to dorsiflex (Fig. 2D). Interestingly, weakness of the lower leg anterior peroneal muscle is a common symptom in CMT patients. CMT patients also have foot deformities, such as pes cavus and claw toes, due to weakness of foot muscles (Young and Suter, 2003). When the skin is removed from the hindfoot, there is obviously less musculature in affected Tg1/Tg1 animals compared to +/+ animals. However, these muscles are small and difficult to dissect so we were unable to quantify the differences.

Loss of motor neurons in adult animals

We directly investigated the possibility of motor neuron neuropathy in the Tg1/Tg1 animals by counting motor neuron axons. Motor neuron cell bodies reside in

the ventral horns of the spinal cord and send their axons down the spinal column. Bundles of axons exit the spinal column at junctions between the vertebrae and are called roots. For example, the bundle of axons that exits at the L5 vertebrae is called the L5 motor root. Motor roots of the lumbar spine innervate the hindlimbs. Since each motor neuron has one axon, and a particular motor root has a stereotypical number of axons, counting the number of axons in a specific motor root allows comparison of the number of intact motor neurons between different animals.

Six-week-old *+/+*, *Tg1/+* and *Tg1/Tg1* animals were transcardially perfused, and their L5 motor and sensory roots were dissected. Motor roots appeared smaller in *Tg1/Tg1* animals compared to *+/+* and *Tg1/+*. Roots were processed for plastic embedding and thin sections were stained with toluidine blue to identify myelin structures. (Fig. 5A). No defects in myelination are observed in *Tg1/+* or *Tg1/Tg1* animals.

There are ~40% fewer axons in both the L5 and L4 *Tg1/Tg1* motor roots compared to *+/+* and *Tg1/+* (Fig. 5B). We noted that there appeared to be a greater proportion of large caliber axons in the *Tg1/Tg1* root than in the other samples (Fig. 5A). We measured the diameter of all axons in the L5 motor root for several animals of each genotype (Fig. 5C). Wild-type and *Tg1/+* mice have a bimodal distribution of small and large diameter axons. In contrast, *Tg1/Tg1* animals have a relative decrease in small caliber axons and a relative increase in large caliber axons. We find the similar differences in axon diameter distributions in L4 motor roots (data not shown).

Mitochondrial aggregation and distribution defects in Tg1/Tg1 motor neurons

We investigated the morphology and distribution of mitochondria in Tg1/Tg1 motor neurons. In fibroblasts, overexpression of Mfn2 T105M causes perinuclear mitochondrial aggregation. For the wild-type control, we isolated motor neurons from HB9-EGFP embryos and infected them with lentiviral mito-dsRed. In this way, motor neurons were labeled with GFP, and a percentage of them had dsRed mitochondria. We found that mitochondria were concentrated in the motor neuron cell soma but also present throughout long axonal projections (Fig. 6A). Tg1/Tg1 motor neurons also expressed GFP and we labeled mitochondria in these cells with indirect immunofluorescence against Mfn2-Myc. In contrast to wild-type neurons, mitochondria in Tg1/Tg1 motor neurons appeared highly aggregated and largely confined to the cell soma. Mitochondria were poorly distributed in axons, and when present, appeared as small aggregates (Fig. 6A). We quantitated these differences in mitochondrial distribution and found that Tg1/+ had an intermediate phenotype between +/+ and Tg1/Tg1.

Discussion

We have generated a transgenic mouse that recapitulates some aspects of Charcot-Marie-Tooth Disease. Motor neuron expression of the CMT2A disease allele Mfn2 T105M resulted in a mouse with hindfoot and hindlimb musculature defects, gait impairment and axonopathy. Significantly, it is the longest motor neurons that are affected, as in CMT disease. Unlike CMT, these defects are not progressive—animals

exhibit the phenotype perinatally and do not noticeably worsen with age. This suggests that the axonopathy we observe occurs at a very young age, perhaps embryonically, and agrees with the expression profiling of the HB9 promoter which turns on early and fades in the first weeks after birth.

This is the first study to report the effect of Mfn2 CMT2A alleles in motor neurons *in vivo*. In cultured motor neurons expressing the Mfn2 T105M transgene we find aberrant mitochondria morphology and distribution, including predominant mitochondria aggregates present in the cell soma. This is very similar to the mitochondrial defect observed with other Mfn2 CMT2A alleles expressed in dorsal root ganglion neurons (Baloh et al., 2007). We propose that defects in mitochondrial morphology cause motor neuron dysfunction, and subsequently degeneration, analogous to the defects seen in flies or hippocampal neurons when mitochondrial dynamics are disrupted by mutation of Drp1 (Li et al., 2004; Verstreken et al., 2005).

There are several unanswered questions regarding the phenotype observed in these transgenic mice. First, why are the anterior muscles of the lower hindlimb affected whereas the posterior calf muscles are not? This feature is remarkably similar what is observed in CMT patients. Second, when during development does the observed 40% reduction in distal motor neurons occur? Do these motor neurons send out axons and then degenerate or are they never formed? Third, what is the significance of the increased representation of large diameter axons observed in Tg1/Tg1 motor neurons? Does this represent a compensatory mechanism for reduced axon numbers or is there a specific loss of small caliber axons? Reported nerve biopsy data from CMT2A patients is limited, but loss of large myelinated axons in sural has been observed in two early onset

patients, though large axons were preserved in late onset patients (Chung et al., 2006; Verhoeven et al., 2006). It is not clear how these findings relate to our observations in the Tg1/Tg1 motor roots.

The Tg1/Tg1 mice described here provide a mouse model for studying the effects of altered mitochondrial morphology in mammalian motor neurons and the consequences of early long motor neuron loss. These mice may also serve as a suitable host for re-innervation experiments using exogenous motor neurons.

Experimental Procedures

Generation of transgenic mice

Mfn2 T105M 7xMyc (Detmer and Chan, 2007) was cloned into an HB9-MCS-IRES-GFP vector provided by the Jessell lab and verified by restriction digest mapping and sequencing of the ligation junctions. The HB9-Mfn2 7xMyc-IRES-EGFP construct was linearized by XhoI digest, gel extracted, column purified, sterile filtered and delivered to Caltech animal facility for pro-nuclear injection. PCR genotyping for the transgene used the following oligos as depicted in Figure 1: A (GCGCCTCTCTGTGCTAGTTG) and B (GTCTGCAGTGAAGTGGCAAT).

The transgene insertion site in the Tg1 line was determined using a strategy described previously (Li et al., 1999). We cloned genomic sequence flanking the transgene by digesting Tg1 genomic DNA with EcoRI (site is present in 3' end of transgene), self-ligated this material and using it as a template for PCR with transgene GFP oligos. We confirmed the integration site with oligos as depicted in Figure 1: C

(TGGGGTGTGCTTTATTGACA), D (CTGCTTTCATGCACACACCT), E (CTGCTTTCATGCACACACCT) and F (GCCTTCTTGAGAACCTGTGC).

Cryosection and immunofluorescence

Midgestation e12.5 embryos were fixed in 4%PFA/PBS for two hours at 4 °C, washed in PBS, incubated in 30% sucrose/PBS and frozen in OCT. Embryos were cryosectioned at -20 °C, air dried and then subjected to Myc immunofluorescence using the 9E10 antibody and a Cy3-labeled secondary. EGFP signal was enhanced with an Alexa-488 conjugated anti-GFP antibody (Invitrogen).

Spinal cord lysates

The spinal cord between the lower neck and the lower rib cage was extruded with PBS and immediately dounce homogenized in 1XTBS/1%TX-100/1X Protease inhibitor cocktail (Roche). Cleared lysate was quantified with the BioRad Protein Assay kit and equivalent loads were analyzed by western blot.

Hindlimb muscle analysis

P22 animals were euthanized and the skin was removed from their hindlimbs. Calf and anterior muscles were dissecting by cutting the distal tendon, pulling the muscle away and cutting the proximal attachments. Muscles were weighed immediately following dissection.

Motor root dissection and staining

L4 and L5 motor roots were dissected from perfused six week old animals. Roots were further fixed, negatively stained with osmium and embedded in epon plastic for thin sectioning as described previously (Yamanaka et al., 2006). Thin sections were stained with toluidine blue. Bioquant software was used to count and individually measure axon diameters of motor roots.

Motor neuron cultures

Spinal columns were dissected from e12.5 embryos and dissociated using Papain protease (Worthington). Cultures were plated on coverslips treated with Matrigel (BD Biosciences) and processed for immunofluorescence 48 or 72 hours later. HB9-EGFP cultures were infected with lentivirus encoding mitochondrially-targeted dsRed. Tg1 cultures were probed with the anti-Myc antibody 9E10 and a Cy3 labeled secondary. EGFP signal in both cultures was enhanced using an Alexa-488 conjugated anti-GFP antibody (Invitrogen). Motor neurons were cultured in media as described previously (Wichterle et al., 2002).

Acknowledgements

We thank Tim Miller, John Griffin and members of the Chan lab for discussion, Tom Jessell for the HB9-IRES-EGFP cloning vector, and Diane Solis and Gwen Williams for mouse support. Pronuclear injections were performed at Caltech's mouse facilities.

References

- Arber, S., B. Han, M. Mendelsohn, M. Smith, T.M. Jessell, and S. Sockanathan. 1999. Requirement for the homeobox gene Hb9 in the consolidation of motor neuron identity. *Neuron*. 23:659-74.
- Baloh, R.H., R.E. Schmidt, A. Pestronk, and J. Milbrandt. 2007. Altered axonal mitochondrial transport in the pathogenesis of Charcot-Marie-Tooth disease from mitofusin 2 mutations. *J Neurosci*. 27:422-30.
- Bourne, H.R., D.A. Sanders, and F. McCormick. 1991. The GTPase superfamily: conserved structure and molecular mechanism. *Nature*. 349:117-27.
- Chang, D.T., A.S. Honick, and I.J. Reynolds. 2006. Mitochondrial trafficking to synapses in cultured primary cortical neurons. *J Neurosci*. 26:7035-45.
- Chung, K.W., S.B. Kim, K.D. Park, K.G. Choi, J.H. Lee, H.W. Eun, J.S. Suh, J.H. Hwang, W.K. Kim, B.C. Seo, S.H. Kim, I.H. Son, S.M. Kim, I.N. Sunwoo, and B.O. Choi. 2006. Early onset severe and late-onset mild Charcot-Marie-Tooth disease with mitofusin 2 (MFN2) mutations. *Brain*. 129:2103-18.
- Delettre, C., G. Lenaers, J.M. Griffoin, N. Gigarel, C. Lorenzo, P. Belenguer, L. Pelloquin, J. Grosgeorge, C. Turc-Carel, E. Perret, C. Astarie-Dequeker, L. Lasquelléc, B. Arnaud, B. Ducommun, J. Kaplan, and C.P. Hamel. 2000. Nuclear gene OPA1, encoding a mitochondrial dynamin-related protein, is mutated in dominant optic atrophy. *Nat Genet*. 26:207-10.
- Detmer, S.A., and D.C. Chan. 2007. Complementation between mouse Mfn1 and Mfn2 protects mitochondrial fusion defects caused by CMT2A disease mutations. *J Cell Biol*. 176:405-414.

- Engelfried, K., M. Vorgerd, M. Hagedorn, G. Haas, J. Gilles, J.T. Epplen, and M. Meins. 2006. Charcot-Marie-Tooth neuropathy type 2A: novel mutations in the mitofusin 2 gene (MFN2). *BMC Med Genet.* 7:53.
- Griffin, E.E., S.A. Detmer, and D.C. Chan. 2006. Molecular mechanism of mitochondrial membrane fusion. *Biochim Biophys Acta.* 1763:482-9.
- Guo, X., G.T. Macleod, A. Wellington, F. Hu, S. Panchumarthi, M. Schoenfield, L. Marin, M.P. Charlton, H.L. Atwood, and K.E. Zinsmaier. 2005. The GTPase dMiro is required for axonal transport of mitochondria to Drosophila synapses. *Neuron.* 47:379-93.
- Kijima, K., C. Numakura, H. Izumino, K. Umetsu, A. Nezu, T. Shiiki, M. Ogawa, Y. Ishizaki, T. Kitamura, Y. Shozawa, and K. Hayasaka. 2005. Mitochondrial GTPase mitofusin 2 mutation in Charcot-Marie-Tooth neuropathy type 2A. *Hum Genet.* 116:23-7.
- Lawson, V.H., B.V. Graham, and K.M. Flanigan. 2005. Clinical and electrophysiologic features of CMT2A with mutations in the mitofusin 2 gene. *Neurology.* 65:197-204.
- Li, J., H. Shen, K.L. Himmel, A.J. Dupuy, D.A. Largaespada, T. Nakamura, J.D. Shaughnessy, Jr., N.A. Jenkins, and N.G. Copeland. 1999. Leukaemia disease genes: large-scale cloning and pathway predictions. *Nat Genet.* 23:348-53.
- Li, Z., K. Okamoto, Y. Hayashi, and M. Sheng. 2004. The importance of dendritic mitochondria in the morphogenesis and plasticity of spines and synapses. *Cell.* 119:873-87.

- Pilling, A.D., D. Horiuchi, C.M. Lively, and W.M. Saxton. 2006. Kinesin-1 and Dynein are the primary motors for fast transport of mitochondria in *Drosophila* motor axons. *Mol Biol Cell*. 17:2057-68.
- Stowers, R.S., L.J. Megeath, J. Gorska-Andrzejak, I.A. Meinertzhagen, and T.L. Schwarz. 2002. Axonal transport of mitochondria to synapses depends on Milton, a novel *Drosophila* protein. *Neuron*. 36:1063-77.
- Thaler, J., K. Harrison, K. Sharma, K. Lettieri, J. Kehrl, and S.L. Pfaff. 1999. Active suppression of interneuron programs within developing motor neurons revealed by analysis of homeodomain factor HB9. *Neuron*. 23:675-87.
- Verhoeven, K., K.G. Claeys, S. Zuchner, J.M. Schroder, J. Weis, C. Ceuterick, A. Jordanova, E. Nelis, E. De Vriendt, M. Van Hul, P. Seeman, R. Mazanec, G.M. Saifi, K. Szigeti, P. Mancias, I.J. Butler, A. Kochanski, B. Ryniewicz, J. De Bleecker, P. Van den Bergh, C. Verellen, R. Van Coster, N. Goemans, M. Auer-Grumbach, W. Robberecht, V. Milic Rasic, Y. Nevo, I. Tournev, V. Guergueltcheva, F. Roelens, P. Vieregge, P. Vinci, M.T. Moreno, H.J. Christen, M.E. Shy, J.R. Lupski, J.M. Vance, P. De Jonghe, and V. Timmerman. 2006. MFN2 mutation distribution and genotype/phenotype correlation in Charcot-Marie-Tooth type 2. *Brain*. 129:2093-102.
- Verstreken, P., C.V. Ly, K.J. Venken, T.W. Koh, Y. Zhou, and H.J. Bellen. 2005. Synaptic mitochondria are critical for mobilization of reserve pool vesicles at *Drosophila* neuromuscular junctions. *Neuron*. 47:365-78.
- Wichterle, H., I. Lieberam, J.A. Porter, and T.M. Jessell. 2002. Directed differentiation of embryonic stem cells into motor neurons. *Cell*. 110:385-97.

- Yamanaka, K., T.M. Miller, M. McAlonis-Downes, S.J. Chun, and D.W. Cleveland. 2006. Progressive spinal axonal degeneration and slowness in ALS2-deficient mice. *Ann Neurol.* 60:95-104.
- Young, P., and U. Suter. 2003. The causes of Charcot-Marie-Tooth disease. *Cell Mol Life Sci.* 60:2547-60.
- Zuchner, S., P. De Jonghe, A. Jordanova, K.G. Claeys, V. Guergueltcheva, S. Cherninkova, S.R. Hamilton, G. Van Stavern, K.M. Krajewski, J. Stajich, I. Tournev, K. Verhoeven, C.T. Langerhorst, M. de Visser, F. Baas, T. Bird, V. Timmerman, M. Shy, and J.M. Vance. 2006. Axonal neuropathy with optic atrophy is caused by mutations in mitofusin 2. *Ann Neurol.* 59:276-81.
- Zuchner, S., I.V. Mersiyanova, M. Muglia, N. Bissar-Tadmouri, J. Rochelle, E.L. Dadali, M. Zappia, E. Nelis, A. Patitucci, J. Senderek, Y. Parman, O. Evgrafov, P.D. Jonghe, Y. Takahashi, S. Tsuji, M.A. Pericak-Vance, A. Quattrone, E. Battaloglu, A.V. Polyakov, V. Timmerman, J.M. Schroder, and J.M. Vance. 2004. Mutations in the mitochondrial GTPase mitofusin 2 cause Charcot-Marie-Tooth neuropathy type 2A. *Nat Genet.* 36:449-51.

Figure Legends

Figure 4-1. Generation of Mfn2 T105M transgenic mice. A. Schematic of transgene construct depicting motor neuron specific HB9 promoter, C-terminally tagged Mfn2 T105M-7xMyc, internal ribosome entry site (IRES) and EGFP. B. PCR scheme for detecting transgenic animals. Primers A and B were designed to produce a product of genomic Mfn2 product of 392bp and a transgene Mfn2 product of 159bp. e12.5 embryos from a mating between transgenic and wild-type (+/+) animals were genotyped (top panel); in transgenic DNA samples, the smaller product is favored over the longer endogenous product. Spinal column lysates from the same embryos were analyzed for Mfn2-Myc expression by western blot with a Myc antibody (bottom panel). C. The transgene integration in the Tg1 line is on Chromosome 11 between the Rad51c and Ppm1e genes; the transgene is depicted as a single dark arrow, though there are likely multiple tandem transgene insertions. The 5' transgene insertion site was confirmed with oligos CEF, where the wild-type product (EF) is 529bp and the Tg1 product (EC) is 279bp. The 3' integration site was confirmed with oligos DEF, where the Tg1 product (DF) is 800bp. Note the absence of wild-type product (EF) in Tg1/Tg1 samples and the absence of Tg1 product (EC, DF) in +/+ and Tg2 (second transgenic line) samples.

Figure 4-2. Tg1/Tg1 mouse phenotype. A and B. Tail defects in newborn (P0) (A) and P8 (B) +/+, Tg1/+ and Tg1/Tg1 animals: Tg1/+ animals have a shortened tail and Tg1/Tg1 animals have a very short tail. C and D. Compare hindpaw posture in P8 wild-type (C) and Tg1/Tg1 (D) animals (arrow). Tg1/Tg1 animal has limp hindpaws to due

failure to dorsiflex the hindfoot. E. Frame from video of P8 Tg1/Tg1 animal walking. Hindpaws are extended behind animal and used to push itself forward without retracting under the body in normal steps. F. Clenched hindpaw in adult Tg1/Tg1 animal, detailed in inset.

Figure 4-3. Transgene expression in motor neurons. A. Cryosection of Tg1/Tg1 spinal column showing GFP labeled motor neurons (green) and mitochondria labeled by anti-Myc immunofluorescence (red). Right panel is magnified image of indicated region. B. Spinal cord cryosection from P0 Tg1/Tg1 animals, stained as in A. C. Expression timecourse of HB9-Mfn2-Myc (top panels) and HB9-EGFP (bottom panels). Two spinal cord lysates were prepared from P0, P2, P4, P6, P10, and P22 Tg1/Tg1 and HB9-EGFP animals, normalized by protein concentration and analyzed by western blot using Myc (Tg1/Tg1) and GFP (HB9-EGFP) antibodies. In both cases, a β -actin antibody was used as a loading control. D. Comparison of Mfn2-Myc expression level in spinal cord lysates from Tg1/+ and Tg1/Tg1 animals at P0 and P8.

Figure 4-4. Hindlimb muscle mass. A. Schematic of hindlimb muscle dissection. Anterior (a) and posterior (p) muscle groups were identified and severed at the tendon sites indicated by the arrows. B. Images of dissected muscles from Tg1/+ and Tg1/Tg1 (bilaterally affected) animals. Posterior muscles (p) are of comparable size in both animals whereas anterior muscles (a) are severely atrophied in Tg1/Tg1 animals compared to Tg1/+. C. Quantitation of posterior and anterior muscle masses from +/+ (n

=2), Tg1/+ (n = 18), Tg1/Tg1 affected (n = 14) and Tg1/Tg1 unaffected (n = 8) hindlimbs; the error bars indicate standard deviations.

Figure 4-5. Loss of motor neurons in Tg1/Tg1 animals. A. Toluidine blue stained cross section of motor neuron L5 roots from the indicated genotypes. B. Quantitation of number of axons in L5 and L4 motor roots. Number (n) of roots counted for each genotype is indicated in chart. C. Distribution of motor neuron axon caliber in L5 roots. The total number of axons having diameters of 0 - 0.5, 0.5 - 1, 1 - 1.5 microns, etc. are indicated. Inset shows percent of axons of a given caliber relative to total axons for each genotype.

Figure 4-6. Altered mitochondrial distribution in Tg1/Tg1 motor neurons. A. Images of mitochondria in cultured motor neurons (MNs) derived from e12.5 mice. +/+ MNs were isolated HB9-EGFP mice and infected with lentiviral mito-dsRed. Tg1/Tg1 MNs express EGFP (from the transgene) and were stained by anti-Myc immunofluorescence to label mitochondrial Mfn2-Myc. Note that in +/+ MNs, mitochondria are distributed throughout the axon; in contrast, in Tg1/Tg1 MNs, mitochondria are poorly distributed. Tg1/Tg1 MNs also have aggregated mitochondria in the cell soma, but that is not conveyed in these images because overexposure was necessary to reveal axonal mitochondria. B. Quantitation of mitochondrial morphology and distribution in +/+ (n = 20), Tg1/Tg1 (n = 47) and Tg1/Tg1 (n = 65) motor neurons.

Supplementary figure 4-1. Transgene allelic series for tail phenotype. The tails of P22 animals of the indicated genotypes are shown. Note that the length of the Tg1/+; Tg2/+ tail is intermediate to the lengths of Tg1/+ and Tg1/Tg1 animal tails. The genotype of Tg1/+; Tg2/+ was confirmed by test mating.

Figure 4-1

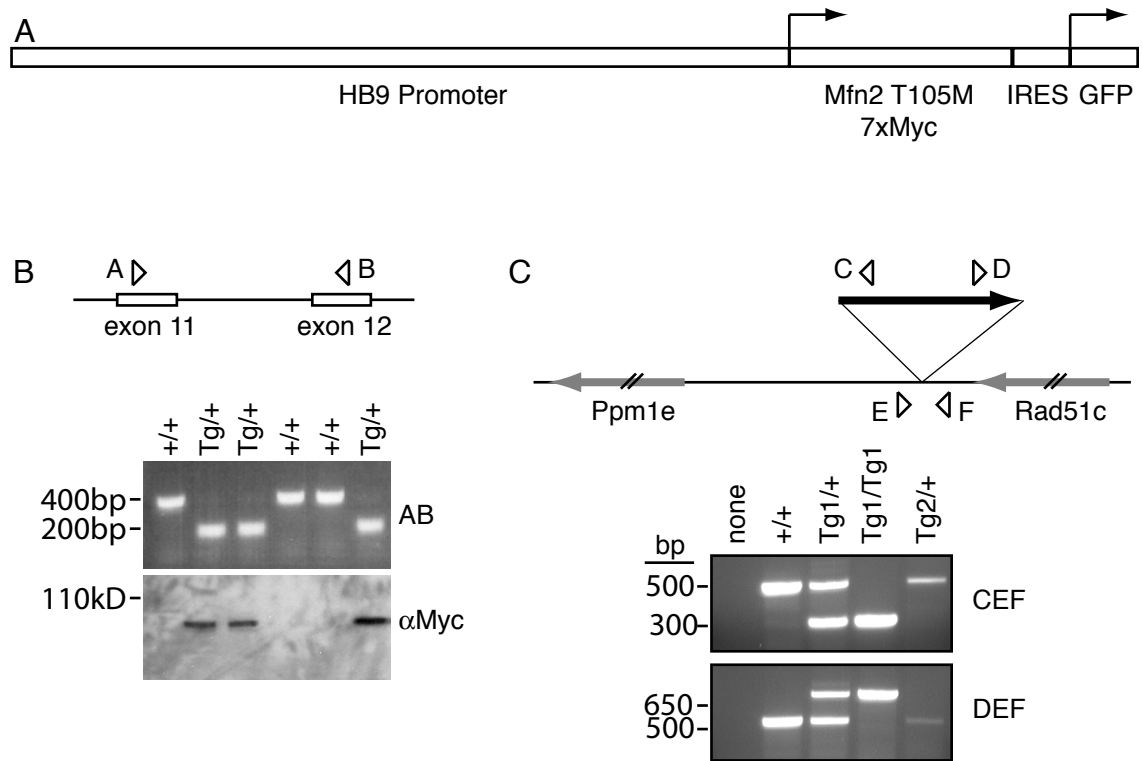


Figure 4-2

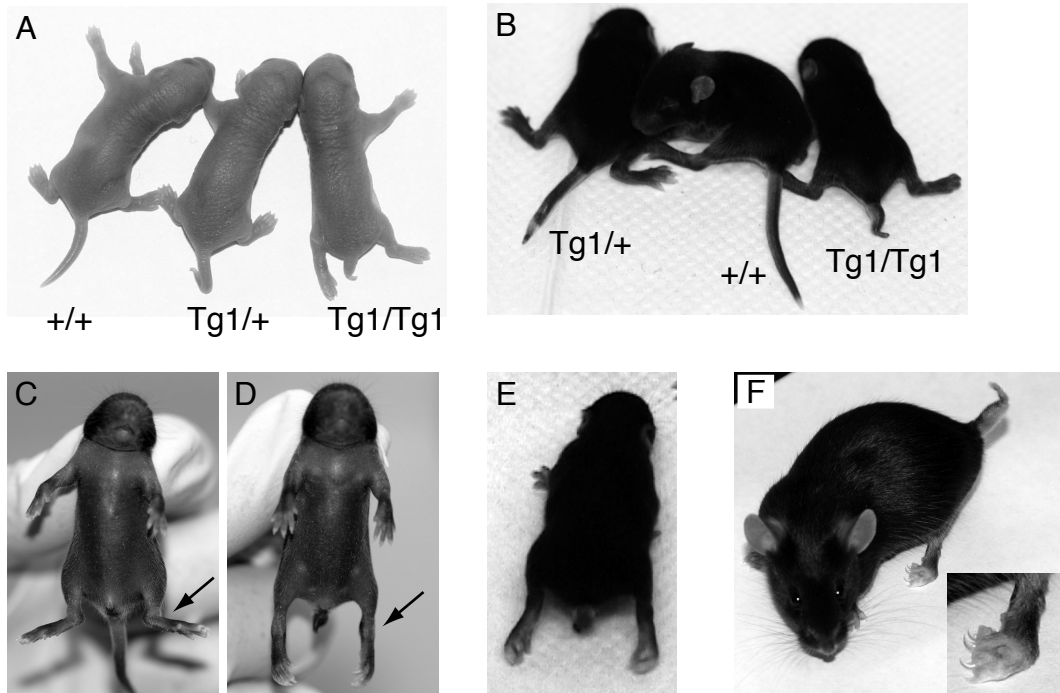


Figure 4-3

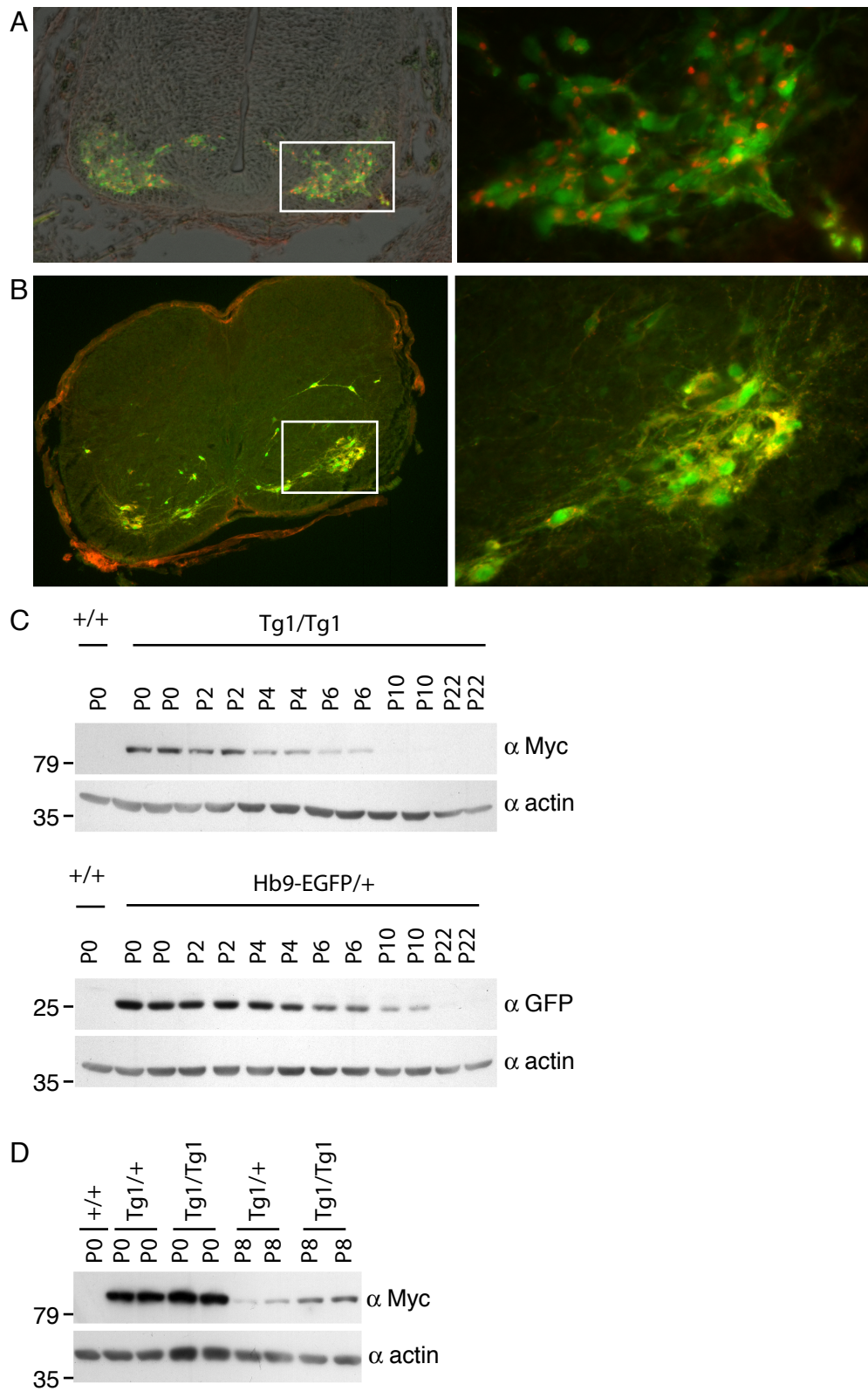


Figure 4-4

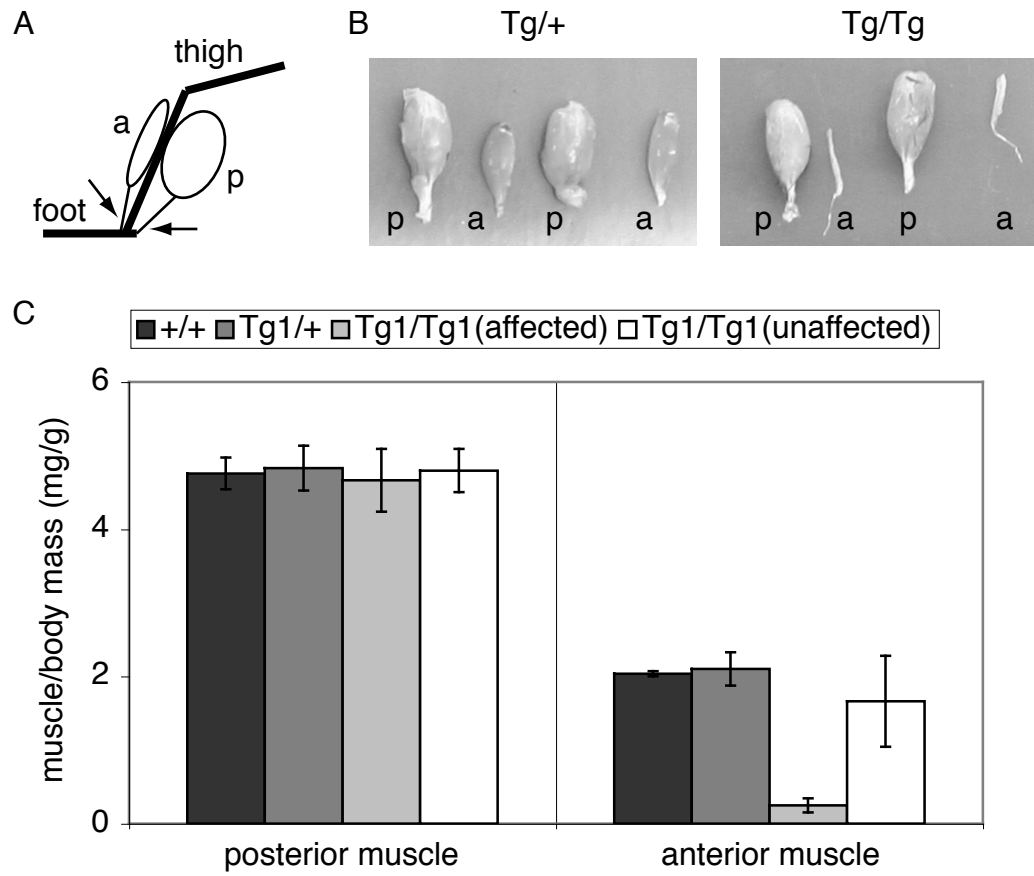


Figure 4-5

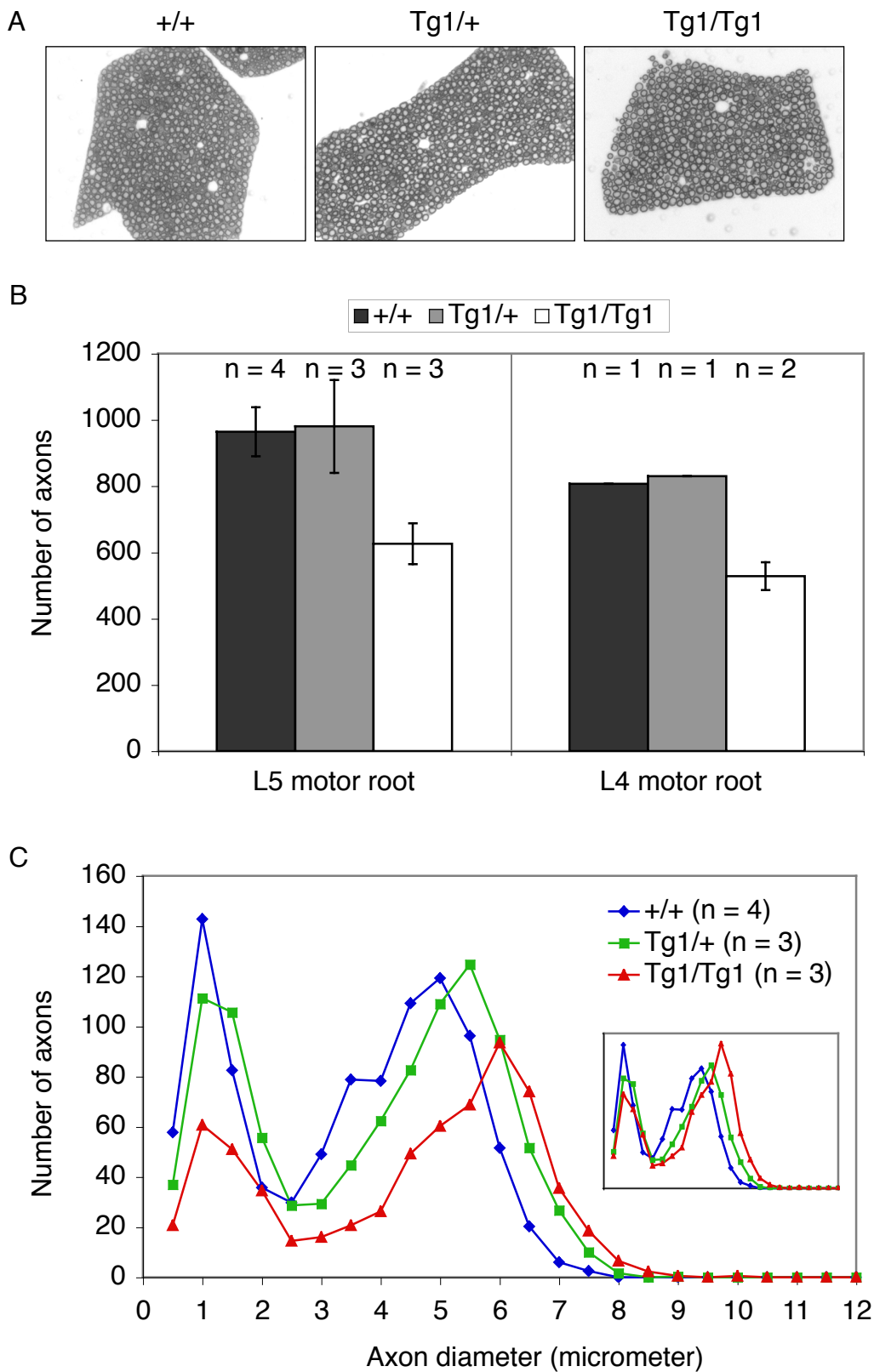
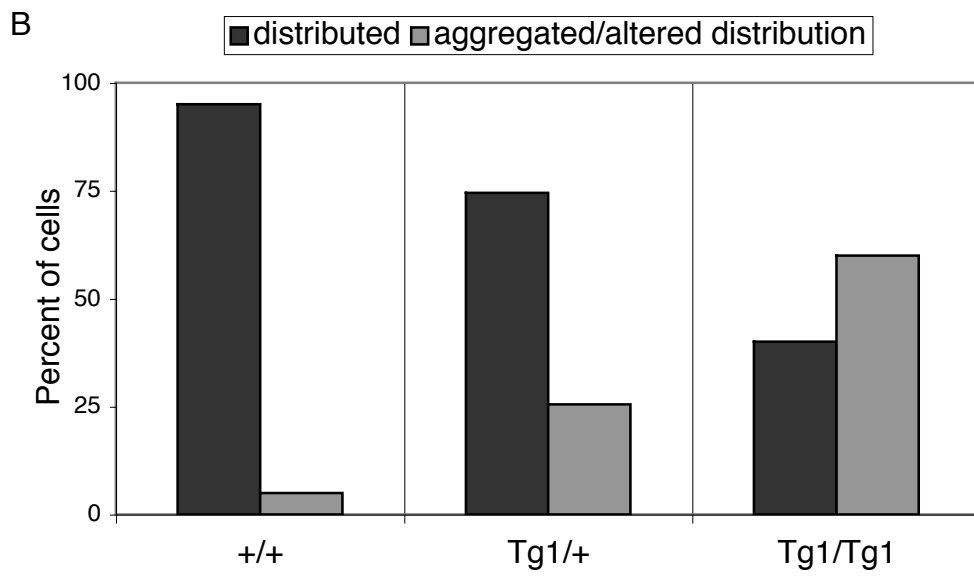
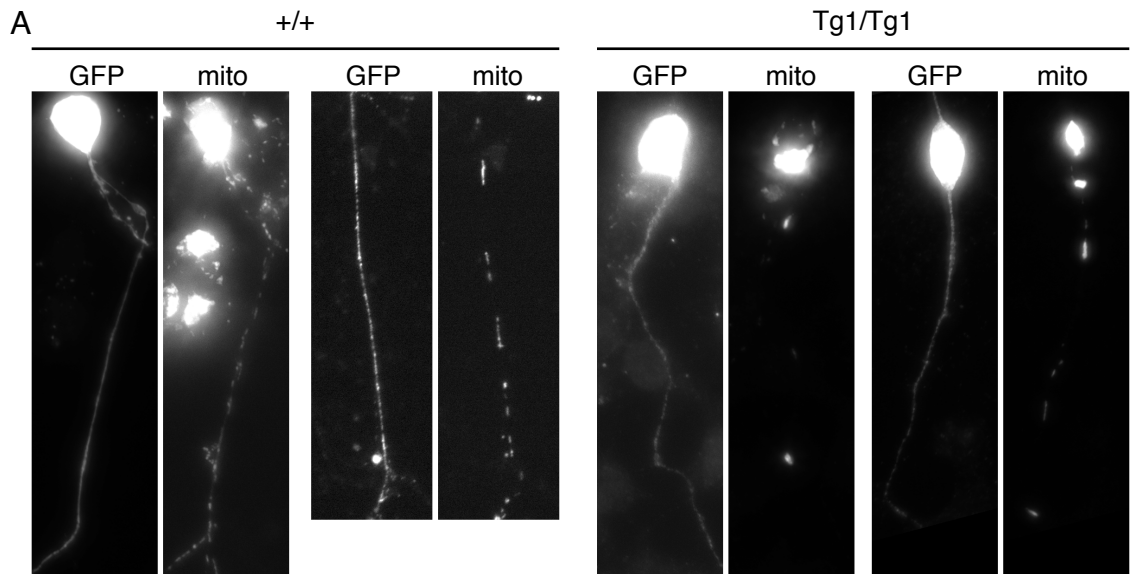
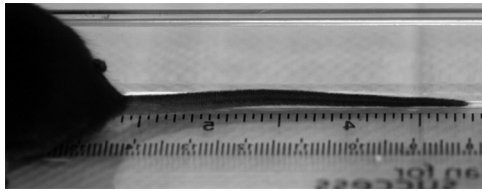


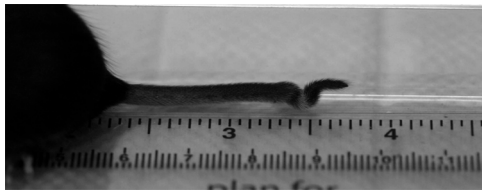
Figure 4-6



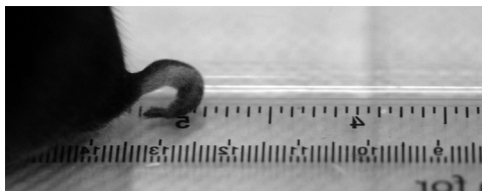
Supplementary figure 4-1



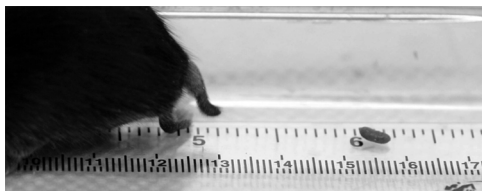
+/+



Tg1/+



Tg1/+; Tg2/+



Tg1/Tg1

Chapter 5

**Generation of Mitofusin 2 Knock-In Mouse Models of Charcot-Marie-Tooth
Disease Type 2A**

Scott A. Detmer and David C. Chan

Introduction

Mutations in the mitochondrial fusion factor Mitofusin 2 (Mfn2) cause axonal Charcot-Marie-Tooth Disease Type 2A (CMT2A) (Zuchner and Vance, 2005). CMT disease is a progressive neuropathy that selectively effects the longest motor and sensory neurons, causing muscle weakness and sensory loss in the feet and legs, which commonly advances to the hands and forearms with age (Young and Suter, 2003). The pathology in CMT is divided between primary defects in myelination (type 1) or in the axon proper (type 2). Type 1 and type 2 can be distinguished clinically by nerve conduction velocities and compound action potentials, or pathologically by nerve biopsy (Young and Suter, 2003).

Mfn2 CMT2A mutations are dominantly inherited. The majority of the 45 CMT2A mutations identified in Mfn2 are missense point mutations and most occur within or closely surrounding the GTPase domain (Chung et al., 2006; Engelfried et al., 2006; Kijima et al., 2005; Lawson et al., 2005; Verhoeven et al., 2006; Zuchner et al., 2004; Zuchner and Vance, 2005). A subset of these alleles have been characterized in cell culture overexpression studies and were found to be a mix of functional and non-functional alleles that commonly cause mitochondrial aggregation (Baloh et al., 2007; Detmer and Chan, 2007). Importantly, wild-type Mfn1, but not wild-type Mfn2, can functionally complement non-functional Mfn2 CMT2A alleles and this suggests that expression of Mfn1 may play a role in the cell type specificity of this disease (Detmer and Chan, 2007). Work in *Drosophila* demonstrates that normal mitochondrial

morphology and anterograde transport are required in neurons for proper synaptic function (Guo et al., 2005; Stowers et al., 2002; Verstreken et al., 2005).

The role of Mfn2 in CMT2A disease progression and pathology is unknown. For example, what effects do the Mfn2 alleles have on mitochondrial morphology and distribution in long motor and sensory neurons? What is the basis for the cell type specificity? In addition, there are limited treatment options for CMT2A, and, more broadly, for CMT disease and neuropathies in general. In an attempt to address some of these issues, we have generated knock-in mice for two Mfn2 CMT2A alleles. Characterization of these mice is now underway and here we present preliminary results. The key advantage of this approach over our transgenic mouse model of CMT2A (chapter 4) is that the mutant Mfn2 alleles are expressed from the endogenous promoter, thus ensuring normal expression level and tissue distribution. Heterozygous knock-in mice are genetically identical to CMT2A patients.

Results and Discussion

Generation of CMT2A knock-in mice

We generated knock-in mice for two Mfn2 CMT2A alleles, R94Q and L76P, by homologous recombination. Both R94Q and L76P are conserved between human and mouse Mfn2 and both occur in exon 4 of mouse Mfn2. The R94 position is the most commonly occurring CMT2A mutation reported and the L76P mutation has been

identified in two distinct probands. Previous analysis has identified R94Q as a loss-of-function mutation, whereas L76P is capable of promoting mitochondrial fusion (Detmer and Chan, 2007). When overexpressed in wild-type or Mfn-null fibroblasts, both alleles cause mitochondrial aggregation (Detmer and Chan, 2007).

Mfn2 L76P and Mfn2 R94Q were cloned into targeting vectors containing a loxP-flanked neomycin cassette for positive selection and tetanus toxin for negative selection. Cloning, homologous recombination, screening of embryonic stem (ES) cells and founder mice, and Cre-mediated recombination has been described previously for Mfn2 R94Q (Detmer and Chan, 2007). Since L76 is in the same exon as R94, generation of the L76P mouse was identical to R94Q, and is not detailed here.

ES cell differentiation to motor neurons

In vitro differentiation of mouse ES cells to motor neurons has been described (Wichterle et al., 2002). We used our ES cells in this differentiation assay to examine mitochondrial morphology in motor neurons heterozygous for Mfn2 L76P and Mfn2 R94Q. As a control for differentiation, we used HB9-EGFP ES cells that express EGFP when they have attained motor neuron identity. When mitochondria were stained with MitoTracker Red, we found no differences in mitochondrial morphology or distribution in motor neuron axonal processes between wild-type and Mfn2 L76P or Mfn2 R94Q heterozygous cells (data not shown). In all cases, mitochondria were short tubules and present throughout the axon. These results suggest that there is no gross defect in motor neuron mitochondrial morphology induced by these CMT2A alleles. This is not totally

unexpected given that CMT2A disease is progressive and selectively affects the longest neurons of the body. In this assay, differentiated motor neurons were only several days old and axonal processes were less than ~500 microns in length.

L76P and R94Q heterozygous mouse phenotypes

We observe no obvious phenotype in either L76P or the R94Q heterozygous animals, the directly relevant genotype to human disease. Even at one year of age, heterozygous animals are similarly sized and as active and coordinated as wild-type littermates when observed in their home cages and assessed by simple behavioral tests, including suspending by tail, traversing their home cage rim, ability to hang onto inverted cage top, and latency to paw flick in a hot plate assay (data not shown). In this regard, these Mfn2 CMT2A heterozygous animals are no different than the Mfn2 heterozygous knock-out mice, which are similarly asymptomatic.

The phenotype of the Mfn2 CMT2A heterozygous animals need to be examined more carefully for subtle or progressive defects by histology, for evidence of axonal degeneration (e.g., of motor and sensory roots, as in chapter 4), and by functional testing, for evidence of decreasing motor function with age (e.g., rotarod and gripstrength measurements). Lack of neuropathy in the CMT2A heterozygous animals may be due to differences between human and mouse anatomy and physiology. First, the longest neurons in mouse are roughly 4 centimeters, whereas in humans they can reach one meter in length. Second, age of onset is variable in CMT2A patients but is rarely documented

in patients less than 5 years of age; mice have only an approximate 2-year life span in laboratory facilities.

Mitofusin gene dosage effects in CMT2A animals

We sought to elicit a phenotype in the CMT2A animals by altering the ratio of mutant allele to total mitofusin levels. Wild-type animals have 2 copies of Mfn1 and 2 copies of Mfn2; heterozygous R94Q and L76P animals have 2 copies of Mfn1, 1 copy of wild-type Mfn2, and 1 copy of mutant Mfn2. Because Mfn1 can uniquely complement non-functional Mfn2 R94Q, we reasoned that altering the genomic ratios of Mfn1 and Mfn2 in CMT2A animals might cause more severe defects. Our lab has previously generated knock-out mice for Mfn1 and Mfn2 and found that mice fully lacking either mitofusin died as embryos, but that Mfn1 and Mfn2 null alleles could be carried in the heterozygous state without having an effect on the animal (Chen et al., 2003). We mated Mfn1 (+/-) and Mfn2 (+/-) animals with our CMT2A animals. We also mated our CMT2A animals with each other to generate homozygous and mixed genotypes (Table I).

This strategy did not elicit an animal phenotype in the case of Mfn2 L76P. We detected no behavioral pathology in Mfn2 L76P homozygous animals or in any of the genetic combinations tested (Table I). As above, closer examination may reveal histological or behavioral defects that distinguish these mice from simple Mfn2 L76P heterozygotes.

We did find defects in Mfn2 R94Q animals when no wild-type Mfn2 was present. Mfn2 R94Q homozygous (94Q/94Q) animals were born at expected ratios when R94Q

heterozygous parents were mated. At 5-6 days old, 94Q/94Q pups were obviously runted compared to wild-type and R94Q heterozygous littermates. This runting became more severe as animals developed and the majority of 94Q/94Q animals were dead by 2 weeks of age (Figure 1). Despite their small size, 94Q/94Q runts appeared grossly normal but had severe lack of overall musculature and had disproportionately smaller thymus and pancreas compared to littermates. 94Q/94Q runts appeared dehydrated but were found to have full stomachs when dissected. One 94Q/94Q animal lived to three weeks of age and had obvious movement defects—this animal would frequently trip and was generally lethargic. Younger 94Q/94Q animals exhibited frantic hindlimb flailing when suspended by the tail, whereas littermates would simply slowly stretch their hindlimbs. Similarly, animals that had one Mfn2 R94Q and one Mfn2 knock-out allele (94Q/ko) also suffered from severe runting. These animals commonly survived to 3 weeks of age, on average somewhat longer than 94Q/94Q animals. 94Q/ko animals also exhibited movement defects.

The physiological cause of runting and early death in 94Q/94Q and 94Q/ko animals remains to be determined. Analysis of potential neuropathy is an obvious starting point. In preliminary studies, we found no evidence for loss on motor neuron cell bodies in the spinal cord of 94Q/ko animals when stained with cresyl violet (data not shown). Histological analysis of thigh muscle fibers showed no alteration in COX activity and no aberrant trichrome staining, suggesting that, at least in muscle, there are not gross mitochondrial energetic defects (data not shown). A potential strategy to determine tissues involved in the 94Q/ko phenotype is to use the Mfn2 conditional allele (2C) (developed by H. Chen and D. Chan). For example, use of tissue-specific Cre

excision lines could be used with the 94Q/2C genotype to generate tissue-restricted 94Q/ko while the rest of the animal remains 94Q/2C.

It is significant that 94Q/94Q and 94Q/ko animals are born live. Mice lacking Mfn2 die in mid-gestation due to a placental defect (Chen et al., 2003). Mfn2 R94Q is non-functional for mitochondrial fusion when expressed alone, but can efficiently promote mitochondrial fusion in the presence of Mfn1 (Detmer and Chan, 2007). Thus, the birth of 94Q/94Q mice indicates that these non-functional alleles can bypass the placental defect of Mfn2-null embryos, likely by cooperating with Mfn1. In a similar situation, Mfn2 is required in Purkinje cells of the cerebellum and deletion of Mfn2 in these cells causes Purkinje cell death, cerebellar atrophy and severe movement defects in mice (H. Chen and D. Chan, manuscript in preparation). We found that Purkinje cells in 94Q/ko animals were present at normal density and were part of an apparently healthy, properly folded cerebellum (judged by calbindin and hemotoxylin/eosin staining, data not shown). Thus, as in the placental defect, Mfn2 R94Q has activity that is lacking in a null Mfn2 allele. Again, this activity is most likely due to complementation by Mfn1.

Mitochondrial morphology in CMT2A fibroblasts

Overexpression of C-terminally Myc tagged Mfn2 L76P or Mfn2 R94Q causes mitochondrial aggregation (Detmer and Chan, 2007). We generated mouse embryonic fibroblasts (MEFs) that are heterozygous or homozygous for Mfn2 L76P or Mfn2 R94Q to evaluate the mitochondrial morphology in cells expressing endogenous levels of Mfn2 CMT2A alleles. We found that 76P/+, 94Q/+ and 94Q/94Q MEFs had wild-type

mitochondrial morphology distributions and essentially no mitochondrial aggregation (Figure 2). 76P/76P MEFs also had normal mitochondrial morphology distributions plus aggregated mitochondria in approximately 10% of cells (Figure 2). Notably, Mfn2 L76P was one of the few CMT2A alleles that induced mitochondrial aggregation even when over-expressed at low levels (approximately fourfold endogenous levels) (Detmer and Chan, 2007). Though we realize that a morphology found in MEFs may not be relevant in other cell types, these results motivate investigation of mitochondrial morphology and distribution in neurons of Mfn2 L76P homozygous animals. For example, electron microscopy can be used to examine mitochondria in axonal cross-sections or specifically at distal synaptic junctions. Additionally, we will monitor the Mfn2 L76P homozygous animals as they age for any emerging phenotypes that may be related to aggregated mitochondria.

Assessing mitochondrial fusion competency of endogenous Mfn2 L76P and R94Q alleles

We previously determined that Mfn2 L76P was functional for mitochondria fusion and Mfn2 R94Q was non-functional for mitochondrial fusion by expressing Myc-tagged recombinant constructs in Mfn-null cells and assaying for mitochondrial fusion in the PEG fusion assay (Detmer and Chan, 2007). To unequivocally determine the fusion capability of these alleles, we want to test endogenously expressed Mfn2 L76P and R94Q in the mitochondrial fusion assay, thereby alleviating any concerns of expression level or epitope tag effecting fusion activity. To generate cell lines containing only mutant Mfn2 (and no wild-type Mfn1 or Mfn2), we mated the CMT2A knock-in mice with mice that

have conditional Mfn1 and Mfn2 alleles (1C and 2C) (developed by H. Chen and D. Chan). These conditional Mfn alleles can be deleted from the genome by Cre recombinase. We have generated the following CMT2A MEF cell lines: C1/C1; C2/76P and C1/C1; C2/94Q, and the following control MEF lines: C1/C1; C2/2 and C1/C1; C2/C2. The plan is to transiently transfect these cells with Cre-GFP, FACS sort for GFP-expressing cells, confirm excision of conditional alleles in the sorted cells, and test all cell lines in the mitochondrial fusion assay.

Perspectives

We have generated Mfn2 L76P and Mfn2 R94Q knock-in mice in an attempt to model the progressive peripheral axonal neuropathy CMT2A. Despite not having an obvious neuropathy phenotype as heterozygous mutants, these animals should prove useful to the CMT and mitochondrial morphology research communities. First, these animals await a full neurological evaluation and may well exhibit histological neuropathy that has not been detected functionally. We will continue to age and analyze the heterozygotes. If defects are detected, these animals could potentially be used for designing therapeutic interventions for CMT and other neuropathies. For example, it would be interesting to test if neuronal expression of Mfn1 could rescue defects in Mfn2 R94Q animals, as we hypothesized (Detmer and Chan, 2007). Second, the severe phenotype found in the 94Q/94Q and 94Q/ko animals provides an animal reagent for defining critical contributions of Mfn2 in developing mammals. These animals also provide *in vivo* evidence for complementation between Mfn1 and fusion-defective Mfn2.

Finally, some of these animals (e.g., 76P/76P) may provide means to assess the effects of altered mitochondrial morphologies (e.g. aggregation) *in vivo*, either by electron microscopy or time-lapse visualization of mitochondria in living tissue.

References

- Baloh, R.H., R.E. Schmidt, A. Pestronk, and J. Milbrandt. 2007. Altered axonal mitochondrial transport in the pathogenesis of Charcot-Marie-Tooth disease from mitofusin 2 mutations. *J Neurosci.* 27:422-30.
- Chen, H., S.A. Detmer, A.J. Ewald, E.E. Griffin, S.E. Fraser, and D.C. Chan. 2003. Mitofusins Mfn1 and Mfn2 coordinately regulate mitochondrial fusion and are essential for embryonic development. *J Cell Biol.* 160:189-200.
- Chung, K.W., S.B. Kim, K.D. Park, K.G. Choi, J.H. Lee, H.W. Eun, J.S. Suh, J.H. Hwang, W.K. Kim, B.C. Seo, S.H. Kim, I.H. Son, S.M. Kim, I.N. Sunwoo, and B.O. Choi. 2006. Early onset severe and late-onset mild Charcot-Marie-Tooth disease with mitofusin 2 (MFN2) mutations. *Brain.* 129:2103-18.
- Detmer, S.A., and D.C. Chan. 2007. Complementation between mouse Mfn1 and Mfn2 protects mitochondrial fusion defects caused by CMT2A disease mutations. *J Cell Biol.* 176:405-414.
- Engelfried, K., M. Vorgerd, M. Hagedorn, G. Haas, J. Gilles, J.T. Epplen, and M. Meins. 2006. Charcot-Marie-Tooth neuropathy type 2A: novel mutations in the mitofusin 2 gene (MFN2). *BMC Med Genet.* 7:53.
- Guo, X., G.T. Macleod, A. Wellington, F. Hu, S. Panchumarthi, M. Schoenfield, L. Marin, M.P. Charlton, H.L. Atwood, and K.E. Zinsmaier. 2005. The GTPase dMiro is required for axonal transport of mitochondria to Drosophila synapses. *Neuron.* 47:379-93.

- Kijima, K., C. Numakura, H. Izumino, K. Umetsu, A. Nezu, T. Shiiki, M. Ogawa, Y. Ishizaki, T. Kitamura, Y. Shozawa, and K. Hayasaka. 2005. Mitochondrial GTPase mitofusin 2 mutation in Charcot-Marie-Tooth neuropathy type 2A. *Hum Genet.* 116:23-7.
- Lawson, V.H., B.V. Graham, and K.M. Flanigan. 2005. Clinical and electrophysiologic features of CMT2A with mutations in the mitofusin 2 gene. *Neurology.* 65:197-204.
- Stowers, R.S., L.J. Megeath, J. Gorska-Andrzejak, I.A. Meinertzhagen, and T.L. Schwarz. 2002. Axonal transport of mitochondria to synapses depends on milton, a novel Drosophila protein. *Neuron.* 36:1063-77.
- Verhoeven, K., K.G. Claeys, S. Zuchner, J.M. Schroder, J. Weis, C. Ceuterick, A. Jordanova, E. Nelis, E. De Vriendt, M. Van Hul, P. Seeman, R. Mazanec, G.M. Saifi, K. Szigeti, P. Mancias, I.J. Butler, A. Kochanski, B. Ryniewicz, J. De Bleecker, P. Van den Bergh, C. Verellen, R. Van Coster, N. Goemans, M. Auer-Grumbach, W. Robberecht, V. Milic Rasic, Y. Nevo, I. Tournev, V. Guerguelcheva, F. Roelens, P. Vieregge, P. Vinci, M.T. Moreno, H.J. Christen, M.E. Shy, J.R. Lupski, J.M. Vance, P. De Jonghe, and V. Timmerman. 2006. MFN2 mutation distribution and genotype/phenotype correlation in Charcot-Marie-Tooth type 2. *Brain.* 129:2093-102.
- Verstreken, P., C.V. Ly, K.J. Venken, T.W. Koh, Y. Zhou, and H.J. Bellen. 2005. Synaptic mitochondria are critical for mobilization of reserve pool vesicles at Drosophila neuromuscular junctions. *Neuron.* 47:365-78.

- Wichterle, H., I. Lieberam, J.A. Porter, and T.M. Jessell. 2002. Directed differentiation of embryonic stem cells into motor neurons. *Cell*. 110:385-97.
- Young, P., and U. Suter. 2003. The causes of Charcot-Marie-Tooth disease. *Cell Mol Life Sci*. 60:2547-60.
- Zuchner, S., I.V. Mersiyanova, M. Muglia, N. Bissar-Tadmouri, J. Rochelle, E.L. Dadali, M. Zappia, E. Nelis, A. Patitucci, J. Senderek, Y. Parman, O. Evgrafov, P.D. Jonghe, Y. Takahashi, S. Tsuji, M.A. Pericak-Vance, A. Quattrone, E. Battaloglu, A.V. Polyakov, V. Timmerman, J.M. Schroder, and J.M. Vance. 2004. Mutations in the mitochondrial GTPase mitofusin 2 cause Charcot-Marie-Tooth neuropathy type 2A. *Nat Genet*. 36:449-51.
- Zuchner, S., and J.M. Vance. 2005. Emerging pathways for hereditary axonopathies. *J Mol Med*. 83:935-43.

Figure Legends

Figure 5-1. 94Q/94Q animals have runted phenotype. 12-day-old pups from a mating of heterozygous 94Q mice. The mouse on the left, 94Q/94Q, is dramatically smaller than its normally sized littermate, +/+ or 94Q/+.

Figure 5-2. Mitochondrial morphologies in CMT2A MEFs. Quantitation of mitochondrial morphology in MEFs of the indicated genotypes. For each genotype, greater than 150 cells from three independently derived cell lines were scored between passages 5 and 8. The large standard deviation error bars reflect variability that is commonly observed in early passage, independent cell lines; however, all cell lines clearly have predominantly tubular mitochondrial morphologies. Mitochondrial aggregation was scored independent of morphology in the cell lines listed and is tabulated below the chart; aggregation in 94Q/94Q cell lines was not scored directly, but it was noted that aggregation occurred rarely (less than 5% of cells).

Table 5-1

genotype		N*	Phenotype (maximum age**)
Mfn1	Mfn2		
+/+	76P/+	many	none detected (14 months)
+/+	76P/76P	>15	none detected (13 months)
+/+	76P/ko***	7	none detected (5 months)
+/ko	76P/+	9	none detected (8 months)
+/ko	76P/76P	3	none detected (5 months)
+/ko	76P/ko	3	none detected (3 months)
+/+	94Q/+	many	none detected (14 months)
+/+	94Q/94Q	>10	severe runting, movement defects, die at ~P14
+/+	94Q/ko	>10	severe runting, movement defects, die at ~P20
+/ko	94Q/+	5	none detected (3 months)
+/+	76P/94Q	3	none detected (13 months)

*total number of animals generated

**age of oldest animals attained of given genotype

***ko: knock-out(null) allele

Figure 5-1

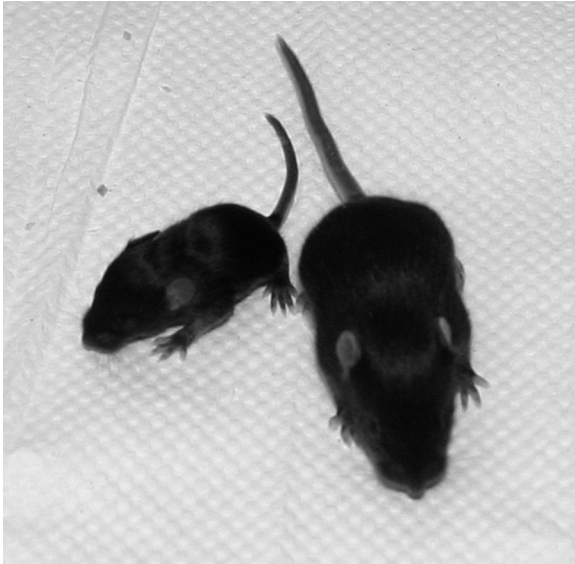
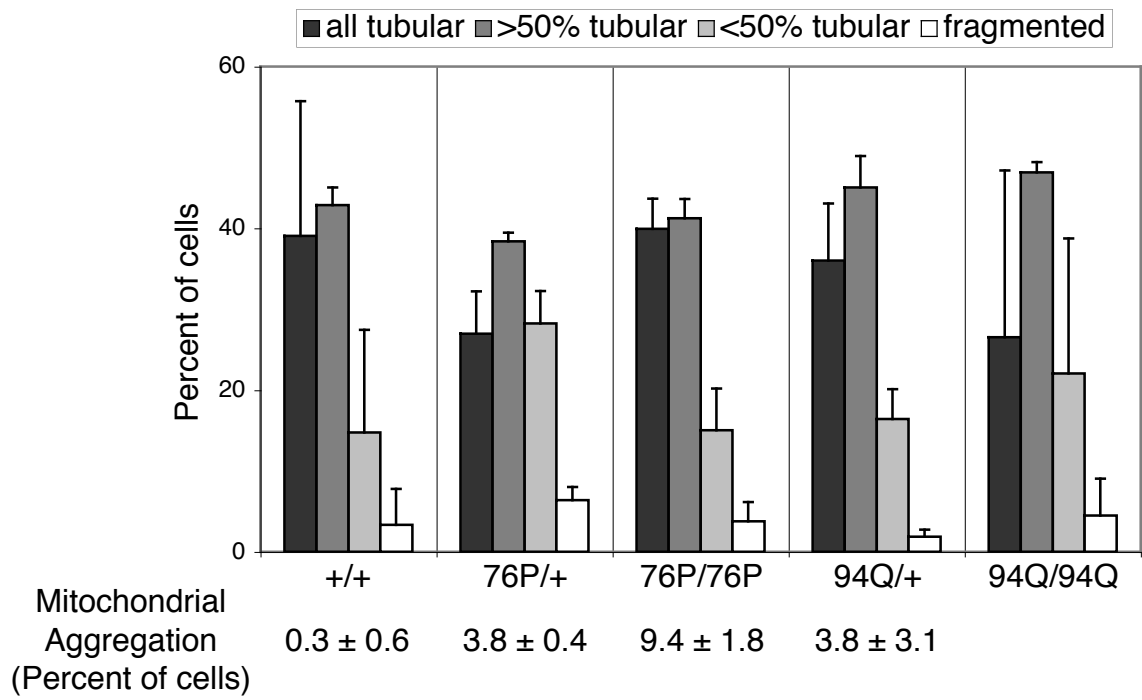


Figure 5-2



Chapter 6

Future Directions

Though a great deal of progress has been made since the identification of the first mitochondrial fusion factor ten years ago, the field of molecular mitochondrial dynamics is still in its infancy (Hales and Fuller, 1997). Key avenues of research for the future include identification of additional mitochondrial morphology factors, mechanistic studies of known factors and construction of relevant animal models of mitochondrial diseases to learn about *in vivo* mitochondrial dynamics and disease progression.

Mammalian mitochondrial fusion

Mitochondrial fusion is most completely understood in yeast due to the identification of essential factors by genetic screens. The study of mitochondrial fusion in mammals has been guided by homology to proteins in the yeast system and thus largely confined to study of Mitofusins and OPA1. Other yeast mitochondrial fusion proteins such as Ugo1 have no obvious mammalian homologs. However, in both yeast and mammals the precise molecular mechanisms of fusion remains a mystery. A priority for a more complete understanding of mammalian mitochondrial fusion is the identification of additional fusion factors. Because even a reduction in mitochondrial

fusion is sufficient to alter mitochondrial morphology, expression knock-down approaches are amenable to identifying putative fusion factors. Genome-scale RNAi visual screens for multiple cell types are now available (Echeverri and Perrimon, 2006; Root et al., 2006) and may prove useful for identifying morphology factors, as visual screens of knock-out yeast libraries have been (Altmann and Westermann, 2005; Dimmer et al., 2002). A second approach to discover additional mitochondrial morphology factors is to identify proteins that interact with known fusion factors. Several recent reports have identified proteins that co-immunoprecipitate with Mitofusin 2 and are putatively implicated in maintaining mitochondrial morphology (Eura et al., 2006; Hajek et al., 2006; Nakamura et al., 2006). An alternative unbiased and more sensitive approach using multidimensional protein identification technology (MudPIT) has been successfully used to identify yeast mitochondrial morphology factors (Graumann et al., 2004; Griffin et al., 2005). This approach has recently been employed to identify Mitofusin interacting proteins (Z. Song and D. C. Chan, unpublished results). It is likely that identification of additional fusion factors will also contribute to the discovery of mechanisms regulating mitochondrial dynamics, which are currently unknown.

A bottleneck in characterizing putative factors is validating their role in mitochondrial fusion. Mitochondrial morphology studies are not always straightforward because overexpression of mitochondrial proteins can cause mitochondrial aggregation independent of their normal function. Similarly, RNAi knock-down experiments are difficult to interpret in the absence of an antibody to determine the extent of expression inhibition, a common situation when initially characterizing novel proteins. Further complicating matters, mitochondrial morphology is very sensitive to the expression level

of some proteins. For example, overexpression of the fusion factor OPA1 causes mitochondrial fragmentation, which, taken alone, would suggest that it is involved in mitochondrial fission (Chen et al., 2005). Additionally, current mitochondrial fusion assays are only semiquantitative, and it is difficult to characterize incremental defects in mitochondrial fusion. Thus, characterization of novel factors would benefit from a mammalian *in vitro* mitochondrial fusion assay in which the reaction timecourse and cytoplasmic variables could be tightly controlled. In yeast, such an assay has clarified the role of Mgm1 and Fzo1 in inner and outer-membrane fusion (Meeusen et al., 2006; Meeusen et al., 2004). Potentially even more advantageous would be development of an *in vitro* lipid reconstitution system, as has benefited the study of SNARE proteins (Weber et al., 1998). A challenge to establishing such a system will be recreating the unique lipid composition of mitochondrial membranes, which may be required for the fusion reaction (discussed in chapter 1).

Molecular mechanism of Mitofusin function

The finding that Mitofusin 1 heptad-repeat 2 mediates *trans* mitochondrial tethering was the first mechanistic description of Mitofusin function in mitochondrial fusion (Koshiba et al., 2004). It is not clear how such tethered structures progress to mitochondrial fusion, or indeed if Mitofusins are involved in this transition, but any structural rearrangements are very likely to depend on the GTPase domain (chapter 2). Biochemical and structural characterizations will be important in determining additional features of Mitofusin function. My attempts at *in vitro* reconstitution of Mitofusin 1 N-

and C-terminal interactions were largely thwarted by solubility issues with bacterially expressed protein fragments. Though refolded Mitofusin fragments appeared to interact directly by elution profile shifts in size-exclusion chromatography, I could not demonstrate GTP binding or GTPase activity in various GTPase domain constructs of Mfn1, either in the presence or absence of C-terminal fragments (S. A. Detmer and D. C. Chan, unpublished observations). Insect or mammalian cell expression systems may allow recovery of soluble Mitofusin domain fragments that would be amenable to enzymatic and structural studies. Other groups have reported GTPase activity for Mitofusin proteins but these studies were based on crudely purified full-length molecules and, in the absence of GTPase-defective mutants, difficult to interpret (Ishihara et al., 2004; Neuspiel et al., 2005).

Yeast have a single Mitofusin that functions as an oligomer (Griffin and Chan, 2006). Mammals have two closely related mitofusins, Mfn1 and Mfn2, which form both homooligomers and heterooligomers (Mfn1/Mfn1, Mfn2/Mfn2, Mfn1/Mfn2) (Chen et al., 2003). Each of these *trans* oligomers can promote mitochondrial fusion, but it is not clear if there are functional distinctions between them (Chen et al., 2005). Our observation that wildtype Mfn1, but not Mfn2, can complement non-functional Mfn2 Charcot-Marie-Tooth disease mutations demonstrates functional differences between Mfn2/Mfn2 and Mfn1/Mfn2 oligomers (chapter 3). Construction of chimeric Mfn1/2 molecules could be used to uncover the sequence requirements of this unique complementation. Again, an *in vitro* mitochondrial fusion assay may provide a quantitative way to assess different functional activities of the three Mitofusin oligomers.

Animal models of mitochondrial diseases

Mitochondrial dysfunction is the basis of several hereditary and spontaneous diseases, including mental illness, metabolic diseases, neuropathies and ageing (Lin and Beal, 2006). These diseases can be caused by mutations in mitochondrial DNA, oxidative phosphorylation proteins or mitochondrial morphology proteins, such as OPA1, Mfn2 and GDAP1 (discussed in chapter 1) (Delettre et al., 2000; Niemann et al., 2005; Zuchner et al., 2004). In general, these diseases are progressive in nature, manifest as modest physical limitations, and generally do not grossly compromise life expectancy. These reasons have made it difficult to generate mouse models of mitochondrial disorders because the most useful animal phenotype is one that is mechanistically relevant to the disease state and (1) not so severe that the animals cannot develop into adults and propagate and (2) not so mild that phenotypes only appear at late age.

A clear success in modeling mtDNA mutations is the proofreading-deficient mtDNA polymerase PolgA mouse that has a dramatic premature ageing phenotype coincident with accumulating mtDNA mutations and deletions (Trifunovic et al., 2004). Attempts to model CMT disease have been more difficult. Our transgenic Mfn2 T105M and homozygous Mfn2 R94Q knock-in animals have more severe phenotypes than are found with the disease (chapter 5). In other situations, CMT models have effects that are too mild. For example, mouse models of Mtmr2 mutations in CMT4B1 result in animals with only very subtle defects that manifest at late age and can only be scored by histological criteria (Bolino et al., 2004; Bonneick et al., 2005). This is likely a similar situation to our heterozygous Mfn2 knock-in animals (chapter 5). Future studies with

theses apparently asymptomatic animals should try to elicit phenotypes. For example, if low levels of neuropathy or slightly compromised motor function are present, conditions of heavy or continual exercise may unveil relevant phenotypic defects. Alternatively, animals could be reared under conditions that demand greater mitochondrial function, for example, at slightly reduced temperatures or with low levels of dietary oxidative phosphorylation uncouplers.

References

- Altmann, K., and B. Westermann. 2005. Role of essential genes in mitochondrial morphogenesis in *Saccharomyces cerevisiae*. *Mol Biol Cell*. 16:5410-7.
- Bolino, A., A. Bolis, S.C. Previtali, G. Dina, S. Bussini, G. Dati, S. Amadio, U. Del Carro, D.D. Mruk, M.L. Feltri, C.Y. Cheng, A. Quattrini, and L. Wrabetz. 2004. Disruption of *Mtmr2* produces CMT4B1-like neuropathy with myelin unfolding and impaired spermatogenesis. *J Cell Biol*. 167:711-21.
- Bonneick, S., M. Boentert, P. Berger, S. Atanasoski, N. Mantei, C. Wessig, K.V. Toyka, P. Young, and U. Suter. 2005. An animal model for Charcot-Marie-Tooth disease type 4B1. *Hum Mol Genet*. 14:3685-95.
- Chen, H., A. Chomyn, and D.C. Chan. 2005. Disruption of fusion results in mitochondrial heterogeneity and dysfunction. *J Biol Chem*. 280:26185-92.
- Chen, H., S.A. Detmer, A.J. Ewald, E.E. Griffin, S.E. Fraser, and D.C. Chan. 2003. Mitofusins Mfn1 and Mfn2 coordinately regulate mitochondrial fusion and are essential for embryonic development. *J Cell Biol*. 160:189-200.
- Delettre, C., G. Lenaers, J.M. Griffoin, N. Gigarel, C. Lorenzo, P. Belenguer, L. Pelloquin, J. Grosgeorge, C. Turc-Carel, E. Perret, C. Astarie-Dequeker, L. Lasquelléc, B. Arnaud, B. Ducommun, J. Kaplan, and C.P. Hamel. 2000. Nuclear gene OPA1, encoding a mitochondrial dynamin-related protein, is mutated in dominant optic atrophy. *Nat Genet*. 26:207-10.

- Dimmer, K.S., S. Fritz, F. Fuchs, M. Messerschmitt, N. Weinbach, W. Neupert, and B. Westermann. 2002. Genetic basis of mitochondrial function and morphology in *Saccharomyces cerevisiae*. *Mol Biol Cell*. 13:847-53.
- Echeverri, C.J., and N. Perrimon. 2006. High-throughput RNAi screening in cultured cells: a user's guide. *Nat Rev Genet*. 7:373-84.
- Eura, Y., N. Ishihara, T. Oka, and K. Mihara. 2006. Identification of a novel protein that regulates mitochondrial fusion by modulating mitofusin (Mfn) protein function. *J Cell Sci*. 119:4913-25.
- Graumann, J., L.A. Dunipace, J.H. Seol, W.H. McDonald, J.R. Yates, 3rd, B.J. Wold, and R.J. Deshaies. 2004. Applicability of tandem affinity purification MudPIT to pathway proteomics in yeast. *Mol Cell Proteomics*. 3:226-37.
- Griffin, E.E., and D.C. Chan. 2006. Domain interactions within Fzo1 oligomers are essential for mitochondrial fusion. *J Biol Chem*. 281:16599-606.
- Griffin, E.E., J. Graumann, and D.C. Chan. 2005. The WD40 protein Caf4p is a component of the mitochondrial fission machinery and recruits Dnm1p to mitochondria. *J Cell Biol*. 170:237-48.
- Hajek, P., A. Chomyn, and G. Attardi. 2006. Identification of a novel mitochondrial complex containing mitofusin 2 and stomatin-like protein 2. *J Biol Chem*.
- Hales, K.G., and M.T. Fuller. 1997. Developmentally regulated mitochondrial fusion mediated by a conserved, novel, predicted GTPase. *Cell*. 90:121-9.
- Ishihara, N., Y. Eura, and K. Mihara. 2004. Mitofusin 1 and 2 play distinct roles in mitochondrial fusion reactions via GTPase activity. *J Cell Sci*. 117:6535-46.

- Koshiba, T., S.A. Detmer, J.T. Kaiser, H. Chen, J.M. McCaffery, and D.C. Chan. 2004. Structural basis of mitochondrial tethering by mitofusin complexes. *Science*. 305:858-62.
- Lin, M.T., and M.F. Beal. 2006. Mitochondrial dysfunction and oxidative stress in neurodegenerative diseases. *Nature*. 443:787-95.
- Meeusen, S., R. DeVay, J. Block, A. Cassidy-Stone, S. Wayson, J.M. McCaffery, and J. Nunnari. 2006. Mitochondrial inner-membrane fusion and crista maintenance requires the dynamin-related GTPase Mgm1. *Cell*. 127:383-95.
- Meeusen, S., J.M. McCaffery, and J. Nunnari. 2004. Mitochondrial fusion intermediates revealed in vitro. *Science*. 305:1747-52.
- Nakamura, N., Y. Kimura, M. Tokuda, S. Honda, and S. Hirose. 2006. MARCH-V is a novel mitofusin 2- and Drp1-binding protein able to change mitochondrial morphology. *EMBO Rep*. 7:1019-22.
- Neuspiel, M., R. Zunino, S. Gangaraju, P. Rippstein, and H. McBride. 2005. Activated mitofusin 2 signals mitochondrial fusion, interferes with Bax activation, and reduces susceptibility to radical induced depolarization. *J Biol Chem*. 280:25060-70.
- Niemann, A., M. Ruegg, V. La Padula, A. Schenone, and U. Suter. 2005. Ganglioside-induced differentiation associated protein 1 is a regulator of the mitochondrial network: new implications for Charcot-Marie-Tooth disease. *J Cell Biol*. 170:1067-78.

- Root, D.E., N. Hacohen, W.C. Hahn, E.S. Lander, and D.M. Sabatini. 2006. Genome-scale loss-of-function screening with a lentiviral RNAi library. *Nat Methods*. 3:715-9.
- Trifunovic, A., A. Wredenberg, M. Falkenberg, J.N. Spelbrink, A.T. Rovio, C.E. Bruder, Y.M. Bohlooly, S. Gidlof, A. Oldfors, R. Wibom, J. Tornell, H.T. Jacobs, and N.G. Larsson. 2004. Premature ageing in mice expressing defective mitochondrial DNA polymerase. *Nature*. 429:417-23.
- Weber, T., B.V. Zemelman, J.A. McNew, B. Westermann, M. Gmachl, F. Parlati, T.H. Sollner, and J.E. Rothman. 1998. SNAREpins: minimal machinery for membrane fusion. *Cell*. 92:759-72.
- Zuchner, S., I.V. Mersiyanova, M. Muglia, N. Bissar-Tadmouri, J. Rochelle, E.L. Dadali, M. Zappia, E. Nelis, A. Patitucci, J. Senderek, Y. Parman, O. Evgrafov, P.D. Jonghe, Y. Takahashi, S. Tsuji, M.A. Pericak-Vance, A. Quattrone, E. Battaloglu, A.V. Polyakov, V. Timmerman, J.M. Schroder, and J.M. Vance. 2004. Mutations in the mitochondrial GTPase mitofusin 2 cause Charcot-Marie-Tooth neuropathy type 2A. *Nat Genet*. 36:449-51.